Assessing the Paleoceanographic Potential

of the Coral *Montipora venosa*

at Fanning Atoll, Central Equatorial Pacific

A thesis presented to the Faculty

of the University at Albany, State University of New York

in partial fulfillment of the requirements

for the degree of

Master of Science

College of Arts and Sciences

Department of Earth and Atmospheric Sciences

Alexa Stolorow
2006

Abstract

As interest in global climate change increases, so does the need for better and more extensive climate proxies. The central equatorial Pacific has been established as the region with the largest ENSO-related sea surface temperature (SST) and precipitation (PPT) anomalies, which are known to impact global interannual climate variability. Of the coral-based paleo-reconstructions of ENSO and lower frequency phenomena, the coral genus *Porites* has been most commonly utilized. However, due to questions of biological artifacts in corals, in order to more fully understand coral-based reconstruction, different coral genera need to be analyzed.

In this study, oxygen ($\delta^{18}O$) and carbon ($\delta^{13}C$) isotopic time series as well as Sr/Ca time series, were generated from a colony of the massive hermatypic coral *Montipora venosa*, a genus not previously studied. This coral core was recovered from Fanning Island (3º 52'N, 159º 20'W) in the central equatorial Pacific, in the heart of the important Niño 3.4 region. The *Montipora venosa* core FI4 is compared to the previously unpublished $\delta^{18}O$ data from a *Porites spp.* core FI5 taken at the same location. While core FI4 *M. venosa* spans 111yr (1997-1887, 662mm), the FI5 *Porites* core only spans 75 yr (1997-1922, 1260mm). Thus, with a shorter core, FI4 *M. venosa* provides a longer record.

Core FI5 *Porites* contains an undetermined deviation towards increased $\delta^{18}O$ values from 1945-1955, which is not recorded in core FI4 *Montipora venosa*. Results indicate that this deviation is not common among other central equatorial Pacific *Porites* records, and thus supports the need for a multi-core replication strategy.

There has been a suggestion by Cane et al. (1997) that the pattern of 20th century SST changes across the Pacific may be due to an increase in the west to east temperature gradient. However, comparison of the *M.venosa* core FI4 $\delta^{18}O$ time series with $\delta^{18}O$ time series from Maiana (1ºN, 173ºE) and Urvina Bay (0º 24.5'S, 91º 14'W) indicates there has been no change in SST gradient across the Pacific during the studied time period (1997-1887), assuming that $\delta^{18}O$ is primarily affected by temperature.

Coral data from several locations throughout the Pacific Ocean show a shift in 1976 towards lighter $\delta^{18}O$ values, which is often interpreted as a trend towards warmers SSTs. However, it is not clear how much of this trend is real and how much might be attributable to biological effects. The results of this study indicate that the magnitude of the shift varies not only by location, but also by coral genus. Again, this substantiates the need for a replication strategy.

Acknowledgements

First and foremost, I would like to thank my advisor, Dr. Braddock K. Linsley, for allowing me to be a part of the ongoing research here in the Stable Isotope lab even before I was a graduate student. Thank you for giving me the opportunity to work on this “accidental” coral, which has turned out to be a very interesting and fruitful project. In addition to this, I would also like to thank him for amazing trip to Fiji and Tonga, despite all the craziness.

I would also like to give a very big thank you to Stephen Howe, who has helped me more than I can say. Thank you for taking the time to teach me about the mass spectrometer and allowing me work in the lab. His support and advice helped me see this project to an end.

Thank you to Drs. Rob Dunbar and Andrea Grottoli for letting me use the FI5 *Porites* data, which was a big part of this paper. And thank you to my other committee member, Dr. John Arnason.

Thank you to my family for supporting me through everything, and thank you to Jimmy for always believing in me – you keep me going. And last but not least, thank you to Lynn Hughes and Sharon Baumgartner for being my office moms.

TABLE OF CONTENTS

Page

LIST OF TABLES

LIST OF FIGURES

Page

Introduction and Objectives of This Study

As greenhouse gas concentrations continue to increase in the atmosphere and the controversy of potential global warming is upon us, it is evermore crucial to evaluate the range of natural variability in tropical environments. The tropical ocean-atmosphere system is a major governing factor of Earth's climate system and exerts a strong influence on global climate variability (Philander, 1990; Cole et al., 1993; Boiseau et al., 1998; Draschba et al., 2000; Alexander et al., 2002). It is well documented that the El Niño/Southern Oscillation (ENSO), which is a tropical Pacific phenomenon, is a major source of interannual (2-7 yrs) variability worldwide (e.g., Philander, 1990; Diaz and Kiladis, 1992; Picaut et al., 1997; Rimbu et al., 2003). The fundamental dynamic features of ENSO – changes in upwelling and wind patterns, precipitation, thermocline depth, sea surface temperature (SST) and sea surface salinity (SSS) anomalies – produce distinct compositional and thermal changes in the surface waters of the tropical Pacific. At present, instrumental records of these ocean properties from the tropical Pacific are sparse and generally do not span more than 75 years. Proxy records such as stable isotopic time-series generated from massive hermatypic coral skeletons are extremely important for paleoclimatological research because they have the potential to supplement and extend instrumental records to pre-industrial times, thus giving scientists the ability to assess natural climate variability.

Scleractinian coral skeletons are well suited to document both low (>10yrs) and high (<10 yrs) frequency climate signals. Their stable isotopic skeletal chemistry can record fluctuations in oceanic and atmospheric conditions in a relatively direct and predictable manner, especially in ENSO-dominated regions of the tropics (Cole et al., 1992). By incorporating chemical oceanographic tracers into their aragonite skeletons, coral skeletal chemistry can reflect environmental conditions such as SST, SSS, nutrient levels, precipitation, river runoff and changes in the isotopic composition of surrounding seawater (e.g., Cole and Fairbanks, 1990; Shen et al., 1992; Cole et al., 1993; Linsley et al., 1994; Druffel, 1997; Gagan et al., 2000; Lough, 2004, among many others).

Scleractinian corals can grow continuously at rates of 2-20 mm per year and can live for several hundred years (Druffel, 1997), making multi-century records possible locally. Long (at least multi-decadal) records are a main goal of current paleoclimatological research, and in this respect, corals are vital to the science (Lough and Barnes, 1997). Coral skeletons, depending on sampling technique, can yield high temporal resolution geochemical time-series with at least near-monthly to seasonal resolution. This is achievable due to high skeletal extension rates. In addition, corals have fairly dense skeletons resistant to bioturbation, which is a hindrance when analyzing sediment cores (Druffel, 1997). Many massive corals can generate distinct growth bands that have been proven to be annual (e.g.; Knutson et al., 1972; Lough and Barnes, 1997; Draschba et al., 2000; Watanabe et al., 2003). These bands, couplets of low and high density, are a useful tool for producing a chronology and can be counted much like tree rings (Lough and Barnes, 1997).

At present, the genus *Porites* is the coral most commonly used to reconstruct tropical phenomena such as ENSO (e.g., Gagan et al., 1994; Boiseau et al., 1998; Cole et al., 2000; Linsley et al., 2000; Charles et al., 2003 among others). *Porites* has the advantage of wide geographic extent, high growth rates of ~10-20mm/yr, and deposition of continuous skeletal records 100 to 500 years in length. However, identified and/or proposed potential problems with utilizing *Porites* colonies include: fish grazing (Linsley et al., 1999), boring by marine organisms, diagenetic overprinting of primary geochemical signals (Müller et al., 2001; Müller et al., 2004), and skeletal growth-related artifacts, which has lead to some uncertainty in the interpretation of lower frequency (>10yrs) modes of variability in *Porites* geochemical series. However, it is important to clarify that *Porites* is not the only coral genus subject to these complications. To date, published single colony *Porites* records in the ENSO critical region of the central and western equatorial Pacific extend back to only the 1850's, demonstrating the need to develop other potential coral archives in this region.

Here I present oxygen ($\delta^{18}O$) and carbon ($\delta^{13}C$) isotopic data, and Sr/Ca data, generated from a core of the massive hermatypic coral *Montipora venosa* (a genus not previously studied) from Fanning Island (3º52'N, 159º20'W) in the Niño 3.4 region of the central equatorial Pacific. The coral core analyzed is 650mm in length and is interpreted to span 111 yr (1997-1887). *M. venosa* typically grows at rates of 5-7mm/yr, therefore generating records that may be twice as long as *Porites* in a core of the same length. Comparison of the *M. venosa* record to a *Porites* $\delta^{18}O$ record cored ~4m away demonstrates that the slower growth of *M. venosa* does not affect the reconstruction of seasonal, interannual or decadal/interdecadal oceanographic variability in either time or amplitude.

Background

1. *Coral Biology*

Massive hermatypic, or reef-building corals are generally found at water depths of <40m and water temperatures between 16ºC and 32ºC. Corals can grow continuously at rates of ~2-20mm/yr via the secretion of an aragonite skeleton (e.g., Highsmith, 1979; Druffel, 1997; Linsley et al., 1999; Gagan et al., 2000; Lough and Barnes, 2000). Due to their continuous skeletal accretion throughout the year, corals potentially contain uninterrupted records of the chemical and physical characteristics of the ambient seawater (Druffel, 1997).

The aragonite is secreted by the polyps of the coral, which occupy an inner cavity surrounded by an outer wall (Fig. 1). A single polyp consists of three tissue layers: the ectoderm, the mesogloea and the endoderm. Certain parts of the ectoderm are in direct contact with the skeleton through the submembrane space – a very thin layer between the tissue and skeleton.

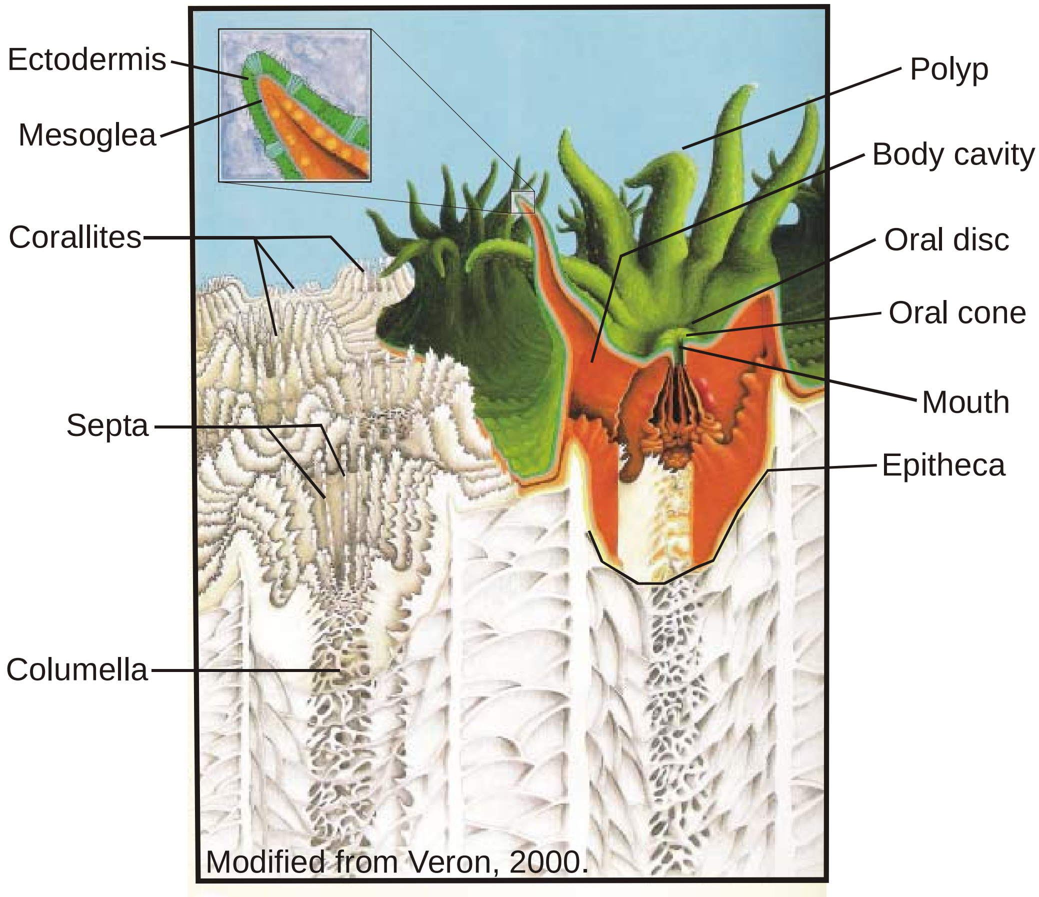

Fig. 1 Diagram of the general coral structure showing the polyp and internal skeletal structure.

Symbiotic dinoflagellate algae, called zooxanthellae, are found within the endoderm of most hermatypic corals (Druffel, 1997). Zooxanthellae in coral skeletons facilitate the precipitation of calcium carbonate ($CaCO_3$) skeleton by using the carbon dioxide (CO_2) produced in this reaction:

$$Ca^{2+} + 2HCO^{-}_3 \rightarrow \underset{\text{(aragonite)}}{CaCO_3\downarrow} + H_2O + CO_2$$

Carbon dioxide dissolves $CaCO_3$, therefore, for skeleton-building purposes it is advantageous for the coral to host an organism that keeps CO_2 levels in the water to a minimum. This is one of the reasons why corals with symbiotic algae are able to accrete their aragonite skeletons at such rapid rates (see Druffel, 1997 for review).

As the coral polyp grows upward, each new layer creates a skeletal cup called the epitheca (Fig 1). The epitheca appears to be the layer in which the density growth bands are formed. Annual density bands are primary skeletal characteristics of the coral that consist of one high density and one low density portion per year: a couplet that exhibits growth rate variations as a function of the seasons (see Druffel, 1997 for review). These bands are perceptible in an x-ray positive of a thin (~7-10mm) slab of the core, which is cut along the maximum growth axis. Annual density banding in many cases allows the generation of a chronology, especially in environments with significant seasonal variability (Cole et al., 1992; Gagan et al., 2000). The variations in annual density bands are representative of fluctuations in both the rate of calcification (mass addition) and the rate of growth (length addition) (see Druffel, 1997 for review).

Unusually dense growth bands have been associated with abnormally slow growth periods and minor growth discontinuities (Dunbar et al., 1994). Minor growth discontinuities and longer periods of nondeposition of the skeleton may be related to anomalously warm or cold events, possibly an effect of ENSO in the Niño 3.4 region (Druffel, 1997; Dunbar et al., 1994). When density bands are poorly defined or locally absent, $\delta^{18}O$ and $\delta^{13}C$ stable isotopic records can help resolve the annual chronology (e.g.; Gagan et al., 2000).

***2.** Oxygen Isotopic Analysis and Temperature Calibration*

For massive corals, skeletal extension rate is thought to be dependent on SST of the ambient seawater. Most favorable growing conditions occur within an SST range of 20-26ºC (see Druffel, 1997 for review). Coral skeletal $\delta^{18}O$ is primarily influenced by SST at the time of aragonite accretion (Cole and Fairbanks, 1990). Secondary factors affecting coral skeletal $\delta^{18}O$ values include the oxygen isotopic composition of seawater ($\delta^{18}O_{SW}$), sea surface salinity (SSS), biological "vital effects" and kinetic isotope effects (KIE), variation in the amount of time being sampled due to errors in chronological assumptions, variability in ocean circulation patterns and the current climate conditions (Cole and Fairbanks, 1990; Heikoop et al., 2000; Rimbu et al., 2002). When comparing $\delta^{18}O$ of two or more corals from the same site, the differences between them should be a result of KIE due to the fact that the environmental conditions were the same (Heikoop et al., 2000). However, these differences have also been attributed to "vital effects" (Linsley et al., 2004, among others).

In the tropical ocean, variations in the oxygen isotopic composition of the surface waters result from changes in evaporation ($\delta^{18}O$ enrichment), precipitation ($\delta^{18}O$ depletion) and meteoric water input from terrestrial runoff. Changes in the $\delta^{18}O_{SW}$ of the equatorial Pacific have been shown to reflect the intense precipitation and SSS anomalies that are often associated with the zonal migration of the Western Pacific Warm Pool (WPWP) as related to ENSO (Cole et al., 1992; Picaut and Delcroix, 1995; Picaut et al., 1996; Picaut et al., 1997; Picaut et al., 2001).

It is known that the $\delta^{18}O$ of coral skeletal aragonite varies inversely with SST at a rate of -0.17‰ to -0.21‰ for every 1ºC increase in water temperature. This relationship between $\delta^{18}O$ of coral skeletal aragonite and SST was first determined by Epstein et al. (1953) and later investigated by Weber and Woodhead (1970, 1972). The oxygen isotopic ratio ($^{18}O/^{16}O$) of seawater is near ~0‰ (Gagan et al., 2000). However, the precipitation of coralline aragonite takes place at rates faster than the establishment of isotopic equilibrium within the corals' calcioblast, resulting in skeletal $\delta^{18}O$ values around –4 to –5‰ (see Druffel, 1997 for review; Gagan et al., 2000). However, this disequilibrium offset may not always be constant within a coral colony or even individual polyps, according to Land et al. (1975) and McConnaughey (1989). For instance, the disequilibrium offset would not remain constant if some parts of the colony were growing faster than other parts.

3. *Carbon Isotopic Analysis*

Corals are heterotrophs, which means that they cannot synthesize their own food and are therefore dependent on an organic source of nutrition. There are two main organic sources from which corals obtain their food – photosynthesis, whereby carbon is fixed by symbiotic zooxanthellae, and heterotrophy, or zooplankton grazing. These two mechanisms of carbon acquisition have been shown to have opposite effects on the coral skeletal $\delta^{13}C$ values. As the rate of photosynthesis increases, so does skeletal $\delta^{13}C$ values. However, due to the more negative $\delta^{13}C$ values of zooplankton, increased ingestion tends to result in a coral skeleton more depleted in $\delta^{13}C$ (Grottoli, 2000).

The $\delta^{13}C$ signal in coral skeletal isotopic records is more difficult to decipher than that of $\delta^{18}O$ because of complicated biological processes which can cause strong isotopic fractionation (McConnaughey, 1989; Cole et al., 1992). The environmental forcing mechanisms on coral skeletal $\delta^{13}C$ include the isotopic composition of the ambient seawater, photosynthetic modulation of the coral's internal dissolved inorganic carbon (DIC) isotopic composition, kinetic isotope effects (KIE) associated with the coral's growth and calicification rate, the availablility of nutrients in the water, photosynthesis and the level of heterotophic activity, and colony topography (Cole et al., 1992; Grottoli, 2000; Heikoop et al., 2000). The carbon isotopic composition of a zooxanthellate, or hermatypic, coral involves three factors: an equilibrium constituent, a kinetic isotopic depletion, and photosynthetic isotopic enrichment (Heikoop et al., 2000).

As KIE tend to mask the $\delta^{13}C$ metabolic signals related to light availability, photosynthesis and respiration, it is often difficult to distinguish correlations between $\delta^{13}C$ and environmental variables (Heikoop et al., 2000). KIE variation can be minimized if the coral is sampled along the maximum growth axis. The magnitude of kinetic fractionation is affected by linear growth rate, skeletal density, and calcification rate (Heikoop et al., 2000). If these kinetic effects are resolved, information on depth, water clarity and insolation may be deduced. If the corals precipitated their aragonite skeleton under similar environmental conditions, KIE should theoretically be minimized.

The rate at which photosynthesis takes place is dependent upon the amount of incoming solar radiation. It has been shown that photosynthesis and coral skeletal $\delta^{13}C$ are positively correlated, meaning that as photosynthetic activity increases due to higher solar radiation the coral skeleton becomes enriched in the heavy isotope (or $\delta^{13}C$ increases) (McConnoughey, 1989; Grottoli, 2000; Heikoop et al., 2000). This is because photosynthetic zooxanthellae (living symbiotically with the coral) preferentially take up the lighter ^{12}C isotope from the internal DIC pool, leaving the heavier ^{13}C isotope available to the coral for calcification (Heikoop et al., 2000). That is why hermatypic corals generally have higher skeletal $\delta^{13}C$ values than ahermatypic (or non-symbiotic) corals (Grottoli, 2000, among others). Therefore, the variations of $\delta^{13}C$ in the coral isotopic record should to some extent be a proxy for changes in incoming solar radiation, which should vary seasonally at most sites.

Evaluating $\delta^{13}C$ in corals may help us understand the long-term variability in seasonal cloud cover (incoming solar radiation) and upwelling patterns. It is crucial to understand coral $\delta^{13}C$ in order to have a more complete picture of tropical climate variability and how it affects the climate worldwide (Grottoli, 2000). $\delta^{13}C$ records in *Porites* corals at the same sites are not perfectly reproducible, therefore indicating potential problems with interpretation of $\delta^{13}C$.

4. Sr/Ca analysis

The Sr/Ca ratio in corals appears to be a promising paleothermometer (e.g., Beck et al., 1992; Marshall and McCulloch, 2002). Like the use of $\delta^{18}O$ of coral skeletons, a Sr/Ca coral geochemical proxy for SST has important implications for climate reconstruction as well as understanding the causes of past climate fluctuations. By analyzing both the Sr/Ca molar ratios and $\delta^{18}O$ in coralline aragonite from the same samples, the potential exists to deconvolve both the $\delta^{18}O$ of seawater and the sea surface salinity (SSS) signals. Each of these significant climatic parameters are generally limited to the last several decades in instrumental records, therefore having a way to reconstruct their past variations would be extremely valuable to paleoclimatologic studies.

Sr in the skeletons of marine carbonates has been studied since the early 1960's, and the subsequent analyses have shown the relationship between skeletal Sr incorporation and SST to be inconsistent and contradictory (Weber, 1973 and references therein). According to Sun et al. (2005), some of this disparity is due to the inconsistency of the concentration of Sr in seawater and not the Sr/Ca ratio or Ca content of seawater.

Sr incorporation into coral skeletal aragonite is such that Sr^{2+} and Ca^{2+} ions in the ambient seawater are absorbed through the living tissue layer into centers of calcification and become incorporated into the skeleton. Marshall and McCulloch (2002) assumed that Sr/Ca in seawater is constant on scales of at least 100,000 years due to the long residence times (10^6) of Sr^{2+} and Ca^{2+} in seawater. Therefore, uptake into the skeleton should theoretically be directly proportional to concentration of these ions in surrounding seawater (Weber, 1973). In addition to their respective ionic concentrations in seawater, Sr/Ca is affected by the Sr/Ca distribution coefficient between aragonite and seawater.

This distribution coefficient is a function of the temperature of the seawater in which the coral is living (Beck et al., 1992). Another controlling factor of coral skeletal Sr/Ca is the possible kinetic effect, such as calcification rate, which conceivably could generate inaccuracies of up to 2-4ºC (Weber, 1973; Cohen et al., 2001; Marshal and McCulloch, 2002). According to both Weber (1973) and Cohen et al. (2001), slower-growing corals have higher Sr/Ca than those of faster-growing corals.

An important assumption made about using Sr/Ca as a paleothermometer has been that the substitution of Sr for Ca during the formation of aragonite is strictly temperature dependent (Cohen et al., 2001; Allison et al., 2005). There are two points that affect this thermal relationship and could possibly complicate the seemingly simple Sr/Ca-SST connection. The first is the aforementioned influence of calcification and growth rate. Several studies have found that there is significant variation of Sr/Ca-SST calibration equations within a single coral species, as well as down core within a single coral colony, suggesting a depth dependence (Weber, 1973 and references therein; Cohen et al., 2001). This is indirectly related to growth rate because some corals extend more rapidly as they approach the sea surface due to more available sunlight. The second is the possibility that Sr is not just substituted for Ca in aragonite, but instead exists in a different mineral phase such as strontianite, which would drastically complicate the Sr/Ca paleothermometer. No other Sr-bearing phase has been identified in field-collected corals to date (Allison et al., 2005).

5. *Oceanography of the Central Equatorial Pacific as Related to ENSO*

It has been established that the central equatorial Pacific is where ENSO typically originates (McPhaden and Picaut, 1990; Graham and Barnett, 1995; Picaut and Delcroix, 1995; Picaut et al., 1996; Barnston et al., 1997; Picaut et al., 1997; Picaut et al., 2001). SST of this region of the Pacific Ocean is generally between 26º-30ºC, averaging around 28ºC, which is the threshold temperature required to maintain organized atmospheric convection, which in turn is related to ENSO. An oceanic convergence zone (barrier layer) has been discovered on the eastern edge of the WPWP and has been termed the Eastern Pacific Warm Pool Convergence Zone (EWPCZ) (See Fig. 15 in Picaut et al., 2001). Colder, more saline water from the eastern Pacific flows westward almost continuously (on the surface) with the South Equatorial Current (SEC) until just past the dateline where it converges with the eastward-flowing surface jets of warm, fresh water from the WPWP. At this point, the cold saline water is subducted under the warm, fresh pool and just above the thermocline, forming a barrier layer and a zonal salinity/density front (McPhaden and Picaut, 1990; Taft and Kessler, 1991; Chiswell et al., 1995; Picaut et al., 1996; Picaut et al., 1997; Picuat et al., 2001). The WPWP migrates meriodionally on interannual timescales associated with the SO, or warm and cold phases of ENSO. During La Niña (cool phase), the barrier layer, as well as Ekman divergence, help to drive the trade winds, thus perpetuating the convergence zone and salinity front. Upwelling in the eastern Pacific is strong, and the SSTs are cool. During this phase of the SO, sea level pressure (SLP) is high in the eastern Pacific and low in the western Pacific. As the SO changes phase, SLP switches to low in the eastern Pacific and high in the western Pacific. These pressure changes are in part driven by interannual SST variations in the tropical Pacific, which are caused by surface wind fluctuations associated with the SLP changes, so the ENSO system is a feedback loop. Concurrently, the trade winds weaken, causing the eastern Pacific upwelling to subside, allowing warm surface waters of the western Pacific to flow eastward, warming the central and eastern Pacific (Philander, 1990; Taft and Kessler, 1991; Diaz and Kiladis, 1992). This east-west movement of the EWPCZ has been found to migrate in phase with the SO, mainly as a result of zonal advection of ocean currents (McPhaden and Picaut, 1990; Picaut et al., 1996; Picaut et al., 1997; Delcroix and Picaut, 1998; Picaut et al., 2001). The warm, fresh water of the WPWP is displaced eastward with the changing SLP (high to low in the eastern Pacific), affecting the region (~5ºN-5ºS, 160ºE-140ºW), and effectively bringing with it the atmospheric convection associated with warmer SSTs and heavy rains of an El Niño event.

The prevailing ENSO theory is the delayed action oscillator (DAO) (Battisti, 1988; Suarez and Schopf, 1988; Battisti and Hearst, 1989, among many others), wherein Kelvin and Rossby waves, inherent in ocean dynamics, travel eastward and westward, respectively, as a result of equatorial wind-stress. These wave signals have a profound impact in the variation of equatorial Pacific SST. The DAO theory suggests wind-stress anomalies in the central Pacific and equatorial SST pattern are strongly coupled. The trade winds appear to be the crucial feedback of the coupled ocean-atmosphere system, as they reinforce the meridional SST gradient across the Pacific basin, but at the same time, the SST contrast between the eastern and western Pacific reinforces the winds. However, this positive feedback alone would lead to a kind of "locking" of the ENSO system into an everlasting warm or cold phase. Thus, the trade winds feedback process working in conjunction with the Kelvin and Rossby wave oscillator will produce the interannual variations in SLP, SST, rainfall and SSS seen in the ENSO system. The center of action for the whole system appears to be the central equatorial Pacific, and this signal has a global effect (McPhaden and Picaut, 1990; Graham and Barnett, 1995; Picaut and Delcroix, 1995; Picaut et al., 1996; Barnston et al., 1997; Picaut et al., 1997; Picaut et al., 2001).

6. *Quasi-biennial Oscillation*

It is also recognized that there is a biennial component related to ENSO, called the Quasi-biennial Oscillation (QBO), which was originally discovered in equatorial stratospheric wind records (Naujokat, 1986; Rasmusson et al., 1990; Gray et al., 1992; Baldwin et al., 2001). The QBO is potentially an important pacemaker of ENSO variability (Rasmusson et al., 1990; Gray et al., 1992). According to Rasmusson et al. (1990) and Baldwin et al. (2001) the QBO is a dominant aspect of interannual global stratospheric variability. Gray et al. (1992) have also discovered through empirical analysis that the QBO plays a statistically significant role in forcing the ENSO phenomenon. Analysis of the QBO suggests that the oscillation appears to reflect basic interannual features of ENSO (Rasmusson et al., 1990; Gray et al., 1992; Baldwin et al., 2001). Studies by Baldwin et al. (2001) indicate that the QBO signal is pronounced in tropical Pacific temperature records. The QBO appears to modulate the timing of ENSO warm El Niño events if the WPWP is carrying sufficient heat energy. Modulation of ENSO events by the QBO is most likely due to tropical Pacific circulation and SLP anomalies that are a result of QBO forcings on equatorial deep convection (Gray et al., 1992). Wallace and Chang (1982) and Van Loon and Labitzke (1987) believe ENSO and QBO signals are difficult to disconnect because the phases of the two phenomena tend to coincide. As per Gray et al. (1992), the direct correlation between ENSO and the QBO "being weak and inconsistent should not be interpreted as a lack of a physical phenomena," rather it appears to be a statistical weakness.

Study Site

Fanning Atoll (British name), locally known as Tabuaeran Island, is part of the Line Islands and belongs to the island nation of Kiribati. Fanning Island lies just north of the equator at 3º52'N latitude and 159º20'W longitude (Fig. 2). This region of the central equatorial Pacific Ocean is believed to have a sizeable influence on global climate due to ENSO and the seasonal movement of the Intertropical Convergence Zone (ITCZ), and is therefore an important site for paleoclimatological research. Fanning Island is a geologically typical atoll – an island and reef surrounding a lagoon (Fig.3). Fanning has three channels (North Pass, Rapa Pass, and English Harbor), although only one (English Harbor) is accessible to large sailing vessels. Tidal flow both in and out of the lagoon occurs along the three channels – 90% at English Harbor on the west side and 10% combined through North Pass and Rapa Pass on the northern and eastern sides, respectively.

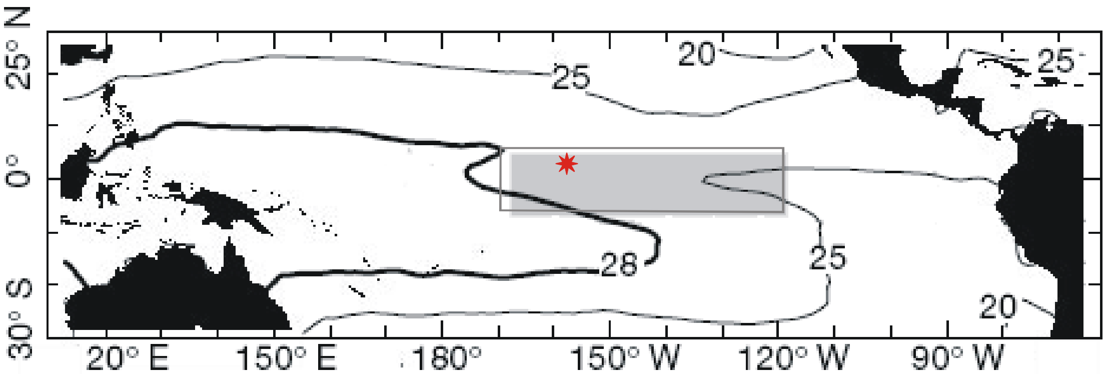

Modified from Urban et al., 2000

Fig. 2 Map of central equatorial Pacific showing the location of Fanning Island (3°52'N, 159°20'W), as denoted by the red star. The outlined area defines the Nino 3.4 region, and the shaded area represents the region used for the central Pacific rainfall index. Also shown on the map is the Western Pacific Warm Pool, outlined by the 28°C isotherm.

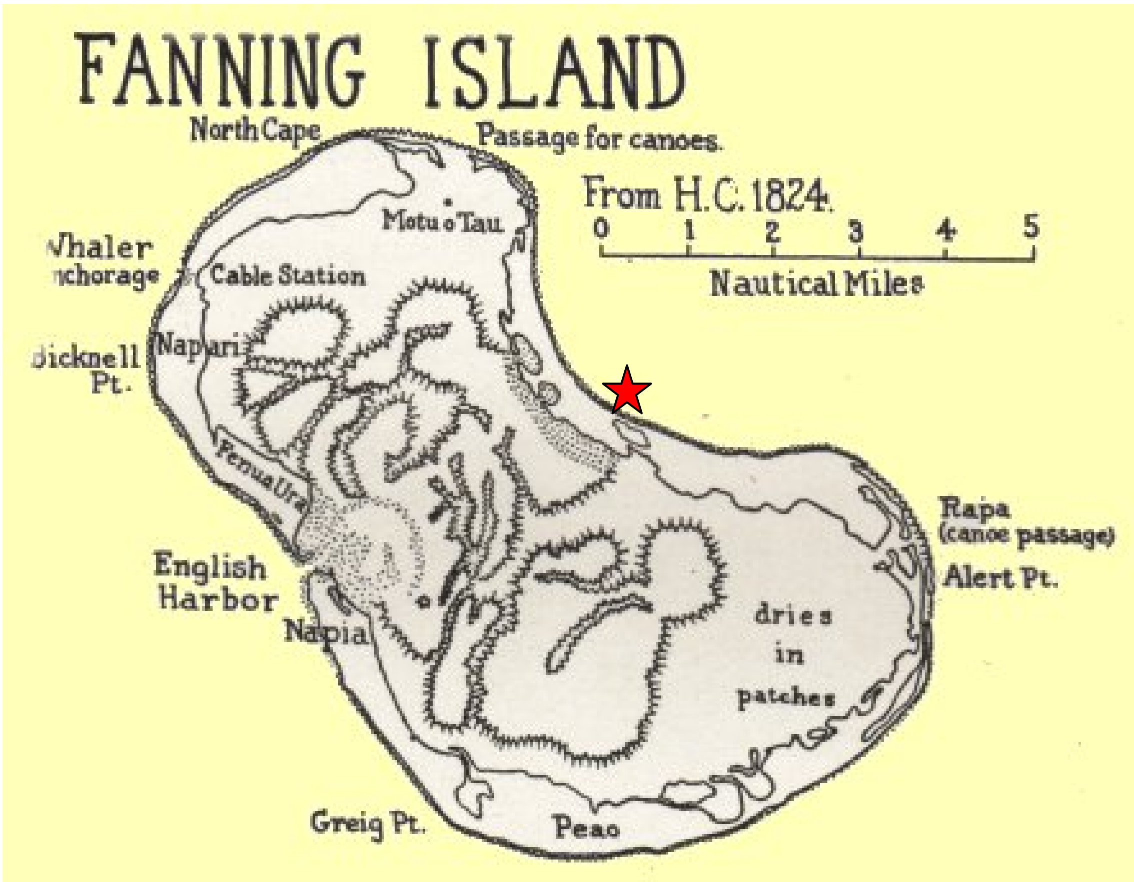

Figure 3. Old British navigational map of Fanning (Tabuaeran) Island showing the three channels – North Pass, Rapa Pass and English Harbor. The red star indicates the approximate location of the coral cores FI4 and FI5 (FI5 previously analyzed by R. Dunbar, pers. comm.). http://www.janeresture.com/kiribati_line/fanning.htm

Maximum water depth in the lagoon is ~18m. Inside the lagoon, average water temperature is approximately 28ºC, with very little fluctuation and no observed gradient with depth (Chave et al., 1970). Outside the lagoon, average water temperature is 27.6ºC (NCEP OI SST 1970-2003). Average air temperature at the island is 28.6ºC, ranging from 22.8ºC – 33.3ºC. Salinity in the lagoon is variable, ranging from 34.56-35.28 psu with an average of 34.92 psu (Chave et al., 1970). There is a slight gradient in salinity with depth, increasing at a rate of 0.0286 psu/10m. The relatively low salinity in the lagoon is related to ITCZ precipitation. Rainfall on the island occurs every month and there is no consistent month of maximum or minimum precipitation (PPT), however the PPT peak most often occurs between May and August. The average monthly rainfall from 1922-2005 at Fanning Island is ~164.03mm (n=498) (COADS and NOAA precipitation indices)(Fig.4). Fanning Island is influenced by seasonal latitudinal shifts of equatorial ocean currents. From approximately May to July, Fanning Atoll lies in the path of the westward-flowing SEC, and from approximately November to January lies in the path of the eastward-flowing North Equatorial Countercurrent (NECC). The source waters of the SEC are cool, upwelled waters from the west coast of South America and equatorial upwelling that supplies the current with nutrient-rich, pCO_2-rich (~435ppm), oxygen-undersaturated water (Taft and Kessler, 1991; Chiswell et al., 1995; Archer et al., 1997; Hönisch et al., 2004). The NECC consists of warm water that is depleted in nutrients and has a pCO_2 that is in equilibrium with the atmospheric concentrations (~350ppm) (Taft and Kessler, 1991; Chiswell et al, 1995; Archer et al., 1997; Hönisch et al., 2004).

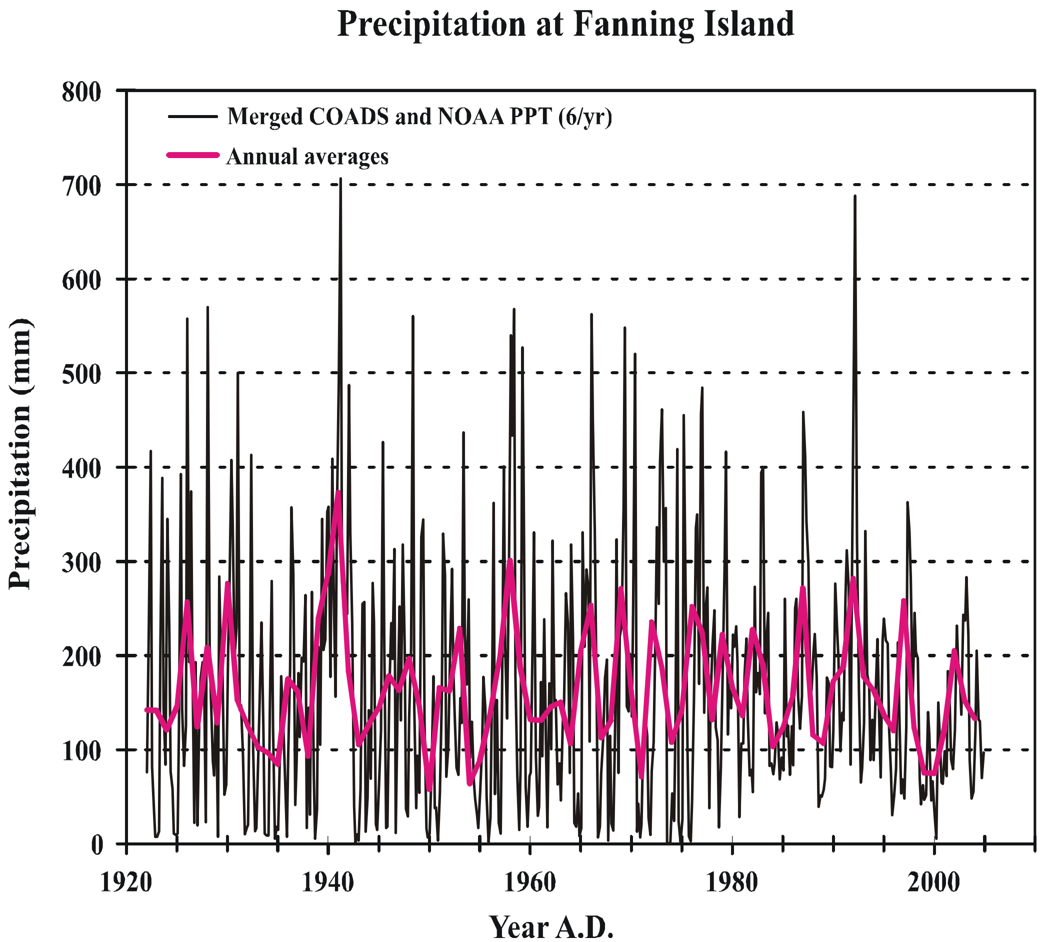

Figure. 4 Merged COADS (Comprehensive Ocean-Atmosphere Data Set) and NOAA NCEP CPC (National Oceanographic and Atmospheric Administration, National Centers for Environmental Protection, Climate Prediction Center) precipitation indices for the period 1922-2005. COADS data is from the old British Cable and Wireless Station at Fanning Island and is rain gauge measurements, while NOAA data is from satellite measurements. The average monthly precipitation (mm) between 1922 and 2005 at Fanning Island is 164.03mm (n=498).

The Line Islands lie within the ITCZ (Figure 5), the most prominent zone of high rainfall in the Pacific Ocean, and are also subjected to high trade wind activity. SST at Fanning Island has been found to vary at interannual timescales as a function of the eastern Pacific cool tongue and phase of ENSO. The cool tongue extends westward during stronger SEC, moderated by El Niño and La Niña events and by the strength of the trade winds. During an average Northern Hemisphere summer, the cool tongue extends far westward and the trade winds are intense. The ITCZ is located at its northernmost position near 10ºN. However, during El Niño events, the cool tongue remains retracted to the east as a result of the substantial relaxation of the trade winds. Concurrently, the heat-laden waters of the WPWP extend eastward past the Dateline. The cool phase of ENSO, or La Niña, is characterized by westward extension of the eastern Pacific cool tongue along with stonger SEC and more intense trade winds. The anomalously cool waters along the equator extend all the way past the Line Islands (Fu et al., 1986; Philander, 1990; Diaz and Kiladis, 1992; Diaz and Pulwarty, 1992; Enfield, 1992; Haug et al, 2001; Serra and Houze, 2002; Horii and Hanawa, 2004; McGauley, 2004). Coral records from this region can be extremely informative in the reconstruction of these ENSO-forced movements, as well as the associated climate impacts (Cole et al., 1992, 1993; Evans et al., 1999; Urban et al., 2000; Cobb et al., 2001, 2003; Grottoli et al., 2003). Due to the fact that Fanning Island lies right in the middle of the region affected by these phenomena, corals from this location may provide records of east-west variability associated with ENSO and migrations of the EWPCZ, as well as the north-south variability due to the seasonal ITCZ shifts.

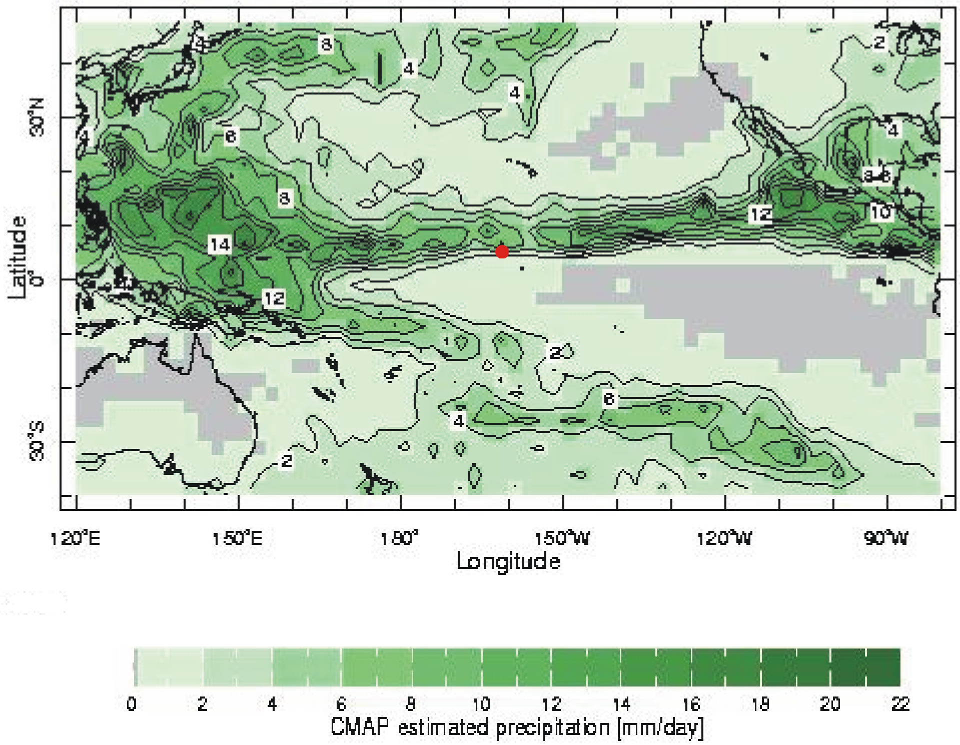

Figure 5. Map of the Intertropical Convergence Zone (ITCZ) – an area of rainfall maximum in the northern hemisphere tropical Pacific. Fanning Island, approximate location of the red dot, lies within the ITCZ and experience heavy seasonal rainfall. http://ingrid.ldeo.columbia.edu/SOURCES/.NOAA/.NCEP/.CPC/.Merged_Analysis/.monthly/.v0312/.ver2/.prcp_est/figview.

Studying climate events in the Nino 3.4 region is key to understanding these changes in the ENSO system because it is an area where the Pacific SST anomalies tend to have the strongest influence on global climate (Philander, 1990; Cole et al., 1992; Diaz and Kiladis, 1992; Barnston et al., 1997; Lough and Barnes, 1997; Kaplan et al., 1998; Urban et al., 2000; Cobb et al., 2001, 2003).

Materials and Methods

1. *Core Extraction And Sample Preparation*

In October, 1997 coral cores were collected from the eastern side of Fanning Island (3º52’N, 159º20’W) in 3 meters of water using SCUBA. The core sampled in this study was collected from a colony of *Montipora venosa*. The core is 765mm in length but the paleoclimatologically useful sections total about 100mm shorter overall and span approximately 111 years (1887 – 1997). It is designated FI4.

The core was split in half lengthwise using a tile saw and cleaned in an ultrasonic washer to remove sea salt and coral dust. Slabs ~7mm thick were then cut from one of the two halves of the core and again cleaned in an ultrasonic washer to remove saw-cuttings (Figure 6).

The slabs were x-rayed and x-ray positives were generated (Figure 7). This revealed density growth bands and individual corallite growth patterns. Samples for geochemical analysis were collected every 1mm with a low-speed diamond-bit drill following a corallite path (~2mm wide) mapped on the core slabs (Fig. 6) guided by the x-ray positives (Fig. 7). After each sample was drilled, the powdered coral skeleton was collected on a square of scientific weighing paper and tapped into a small centrifuge tube with proper labeling.

Core FI5, from a *Porites* colony, was drilled at the same location (Fig. 3) and previously unpublished oxygen isotope data is presented in this thesis (R. Dunbar, pers. comm.).

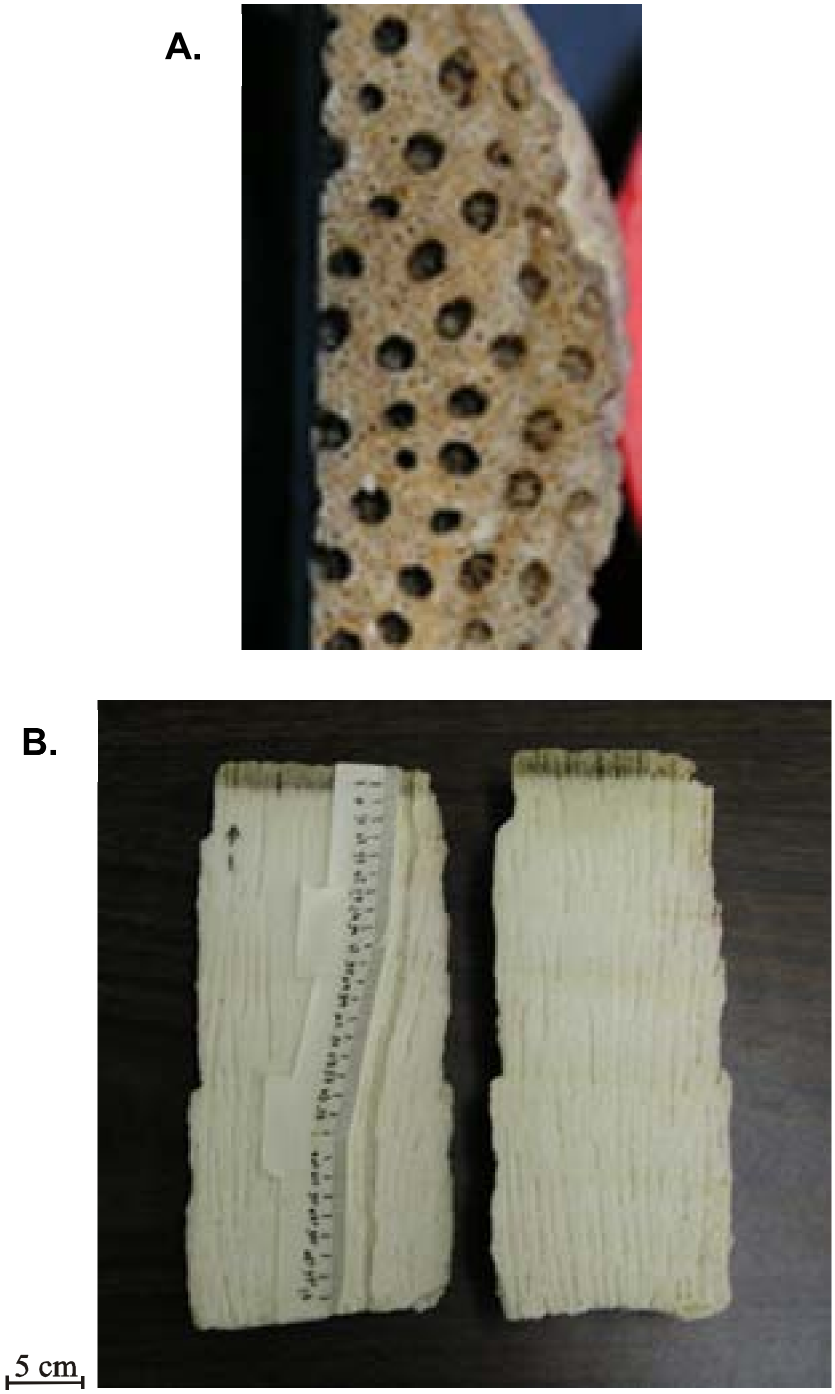

Figure 6. Top section of *Montipora venosa* core FI4 showing (A) corallite geometry and (B) corallite growth pattern (uppermost tissue layer appears as brownish band; sampling track adjacent to location).

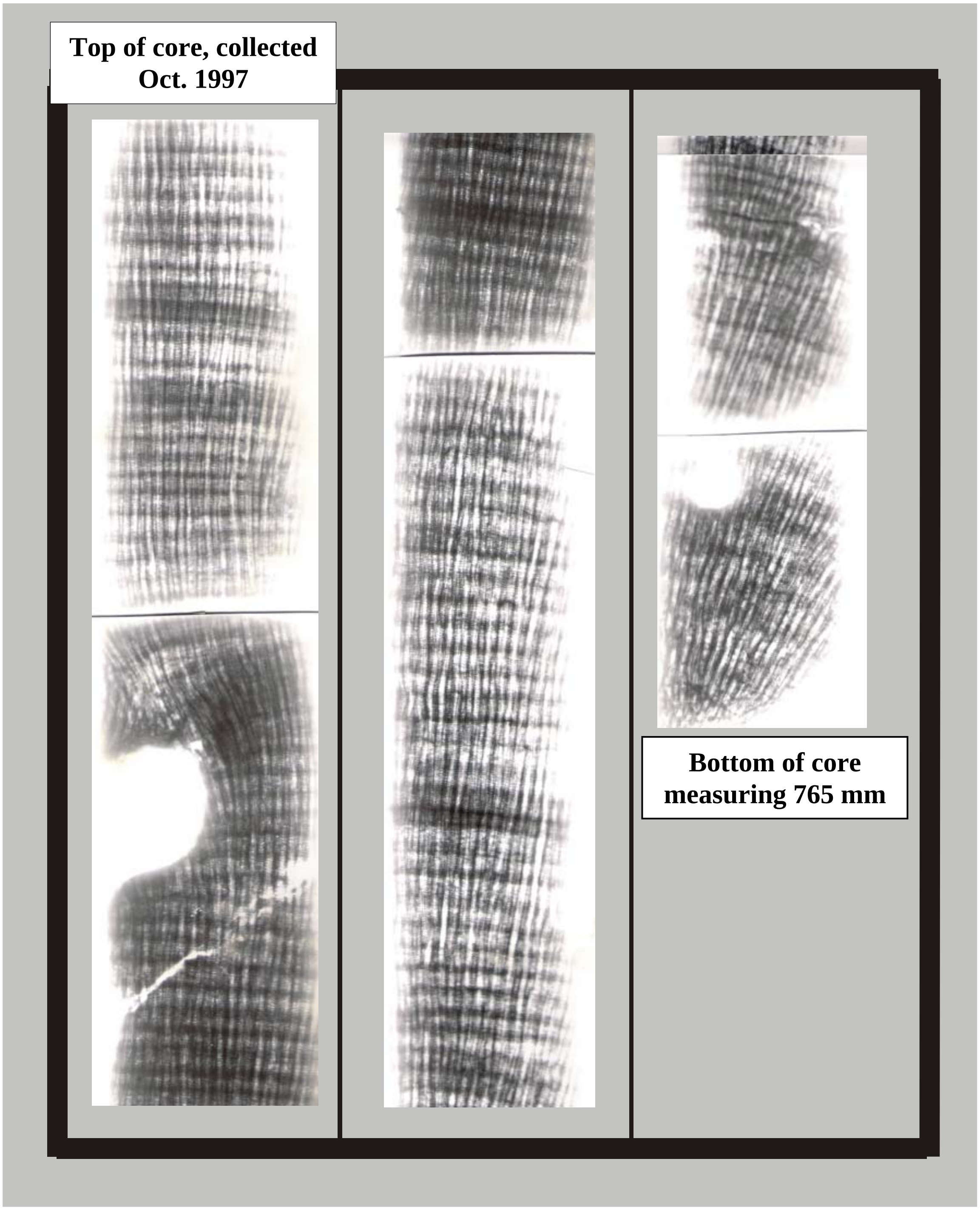

Figure 7. X-radiograph positives of core FI4 *Montipora venosa*.

2. *Carbon and Oxygen Isotope Analysis*

Carbon and oxygen isotope analyses were carried out using a Micromass Optima gas-source triple collector mass spectrometer in the Stable Isotope Laboratory at the University at Albany, State University of New York. Approximately 100-150µg of each sample was dissolved in 100% H_3PO_4 (phosphoric acid) at 90ºC in individual v-vials in a MultiPrep automated sample preparation device. A total of 765 samples were analyzed, with 10% analyzed as replicates to test precision. The average differences for $\delta^{13}C$ and $\delta^{18}O$ values for 103 replicate pairs were 0.092‰ and 0.081‰, respectively. The average $\delta^{13}C$ and $\delta^{18}O$ (standard deviation) values for 144 samples of NBS-19 standard were 1.952‰ (0.018‰) and –2.202‰ (0.028‰), respectively. All data are presented as per mil (‰) deviations relative to international standard Vienna Peedee belemnite (VPDB).

3. *Sr/Ca Analysis*

Sr/Ca analysis was performed at Columbia University's Lamont-Doherty Earth Observatory using a 33-detector Jobin-Yvon Panorama ICP-AES (33 detector) (inductively coupled plasma-atomic emission spectrophotometer) with autosampler attachment for sub-ppb concentration determination. A total of 230 samples were run: 147 samples at mm-scale back through 1970 A.D., and 83 composite samples as yearly averages from 1969 back through 1887 using the chronology as discussed in section 4. The yearly averages were made by taking the raw depth-age data and sorting the samples into batches of individual years. An equal aliquot was then taken from each sample within a given year and mixed evenly to create one annually-averaged sample. This mix was then put into a new small vial and labeled with the year. The samples used here were the same as those used for $\delta^{13}C$ and $\delta^{18}O$ analysis. Each annually-averaged sample consisted of ~100-150μg powdered coral skeletal aragonite.

To prepare the samples for the ICP-AES, ~50-90μg of the individual mm-scale and annually-averaged samples were deposited into vials and vigorously injected with 2.5mL of 2% HNO_3 (nitric acid). The samples were left to dissolve and mix for 6-10 hrs, after which time they were loaded into the ICP-AES for analysis. Replicate error for Sr/Ca analysis on ICP-AES is less than 0.2% RSD.

The Sr/Ca data was then adjusted with a sample size correction after noticing that the concentration of Ca affected the Sr/Ca values generated by the Jobin-Yvon Panorama ICP-AES.

***4.** Chronology*

The chronology was first roughly derived from the annual growth bands as seen on the x-radiograph positives (Figure 7) and the regular annual cycle of the $\delta^{13}C$ record (see Figure 12 in later chapter). The well-defined annual cycle in the $\delta^{13}C$ record is most likely due to seasonal changes in respiration and photosynthesis. After producing a loose chronology from the carbon isotopic record, a few definite, corresponding data points, or "tie-points", were chosen from both the $\delta^{13}C$ and the $\delta^{18}O$ records and tied to the Kaplan Niño 3.4 SST anomaly series – a record of SST anomalies (SSTa) closely correlated with ENSO events in a region (5ºS-5ºN, 170º-120ºW) of the central equatorial Pacific (Kaplan et al., 1998) (Figure 8). The next step was to interpolate manually calendar ages for the rest of the data set, picking one to three points per year. The specific points were entered into a computer program, Arand software package (P. Howell, personal communication), that linearly interpolates ages between the age control "tie points" at a chosen step of 6 points per year, corresponding to the average growth rate of the coral (Figure 9). The final $\delta^{18}O$ and $\delta^{13}C$ series extends from 1887 to 1997. Instrumental data sets used for correlation and analysis were run through the same computer program, also at 6 points per year, so that the data sets could then be compared at the same resolution.

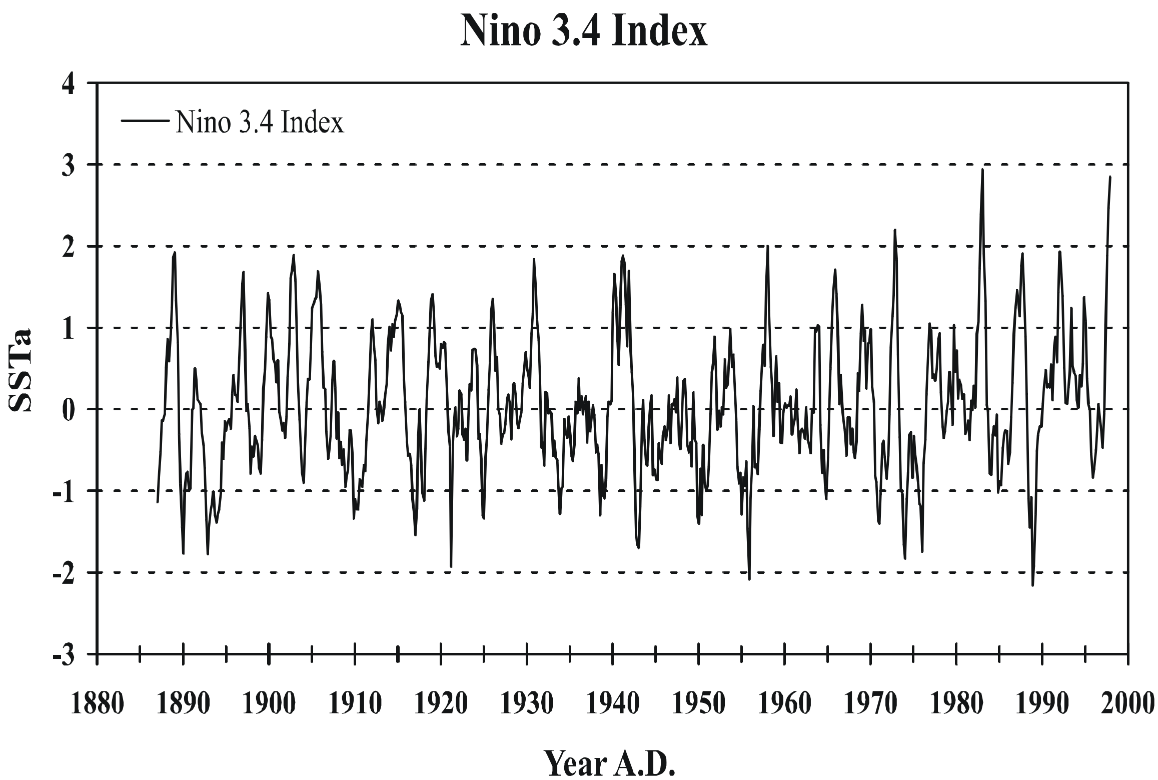

Figure 8. The Niño 3.4 Index (Kaplan et al., 1998) is a record of anomalous SSTs (SSTa) related to ENSO events in a region of the central equatorial Pacific (5ºS-5ºN, 170º-120ºW) that is part of the region of rainfall maximum, as shown in Figure 2.

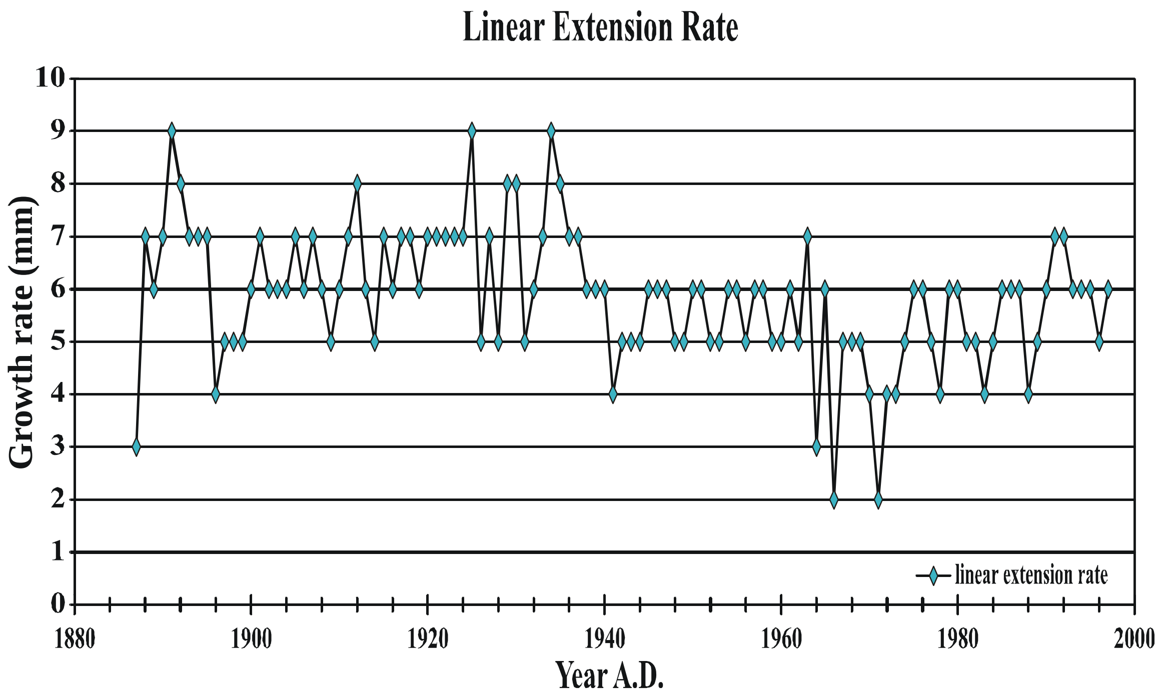

Figure 9. Linear extension rate is a measure of the number of millimeters the coral grew each year. It is not the same as calcification rate. The average linear extension rate of core FI4 *Montipora venosa* is 6mm/yr, yielding an approximate bimonthly resolution for geochemical analyses of samples collected on a mm scale from the core.

5. *Singular Spectrum Analysis*

Singular spectrum analysis (SSA) was carried out on FI4 $\delta^{18}O$ as well as the CAC SST data. SSA is a fully non-parametric technique based on a principle components analysis designed to deconstruct the prominent frequencies, called RCs (reconstructed components), from time series data (Vautard and Ghil, 1989, Vautard et al., 1992). The separation of time series data by frequency domain is useful for studying interannual variations of ENSO, as well as decadal or lower frequency changes in ENSO or any climatological parameter.

Results

1. *δ^{18}O and δ^{13}C time series, Sr/Ca analysis*

Listed in the Appendix are all the “raw”, or original δ^{18}O, δ^{13}C, and Sr/Ca data. Figure 10 shows the raw δ^{18}O and δ^{13}C data plotted by depth, while the δ^{18}O time series at 6 points per year is shown in Figure 11. The lowermost 115 samples were not used in this study due to a tilting in the growth axis, as seen in figure 7 of the coral skeletal x-radiograph positive as well as Figure 10 of the raw data. The average δ^{18}O value for the studied time period (1887-1997 A.D.; 111yr; n=662) is -4.56‰. The minimum (maximum) δ^{18}O value for the same period is –5.40‰ (-3.91‰) in 1915 and 1918, respectively. There is no well-defined annual cycle in δ^{18}O at this site and the maximum and minimum δ^{18}O values do not occur at the same time every year. There is, however, a pronounced interannual cycle.

The δ^{13}C time series at 6 points per year is shown in Figure 12. The average δ^{13}C value for the studied time period (1887-1997 A.D.; 111yr; n=662) is –0.14‰. The minimum (maximum) δ^{13}C value for the same time period is –1.64‰ (0.82‰) in 1992 and 1898, respectively. The carbon data do have a consistent annual cycle at this site that was used in conjunction with interannual variations in δ^{18}O for construction of the chronology.

The results of the Sr/Ca analysis are shown in Figure 13. The Sr/Ca data are plotted at the same scale as the isotope data so that the youngest 30 years would have mm-scale resolution for the purpose of comparing it to SST. In this figure, the Sr/Ca data is not in time series form and shows individual analyses of the age model (see Appendix).

The average Sr/Ca value for the studied time period (1887-1997 A.D.; n=231) is 9.21mmol/mol.

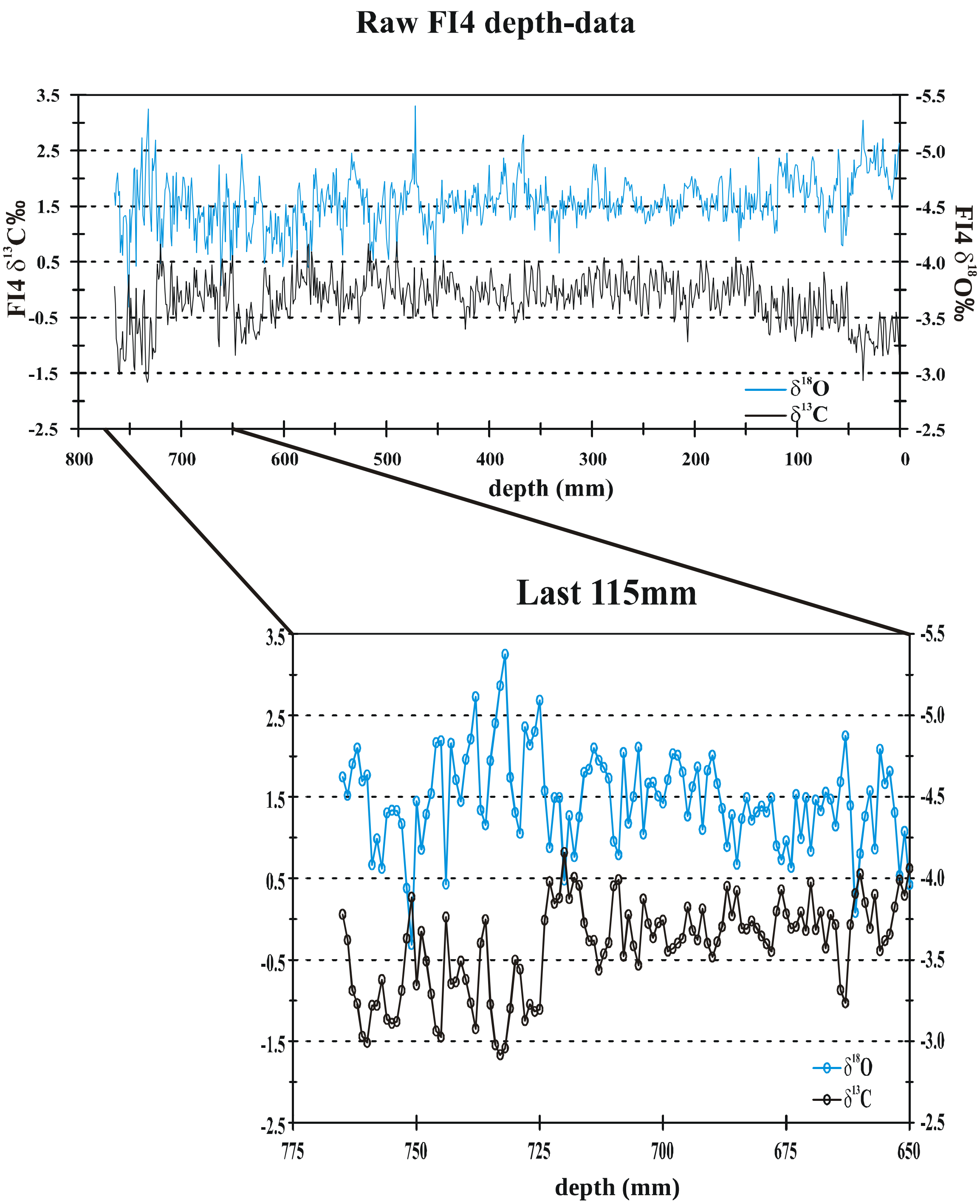

Figure 10. Raw FI4 $\delta^{18}O$ and $\delta^{13}C$ data plotted versus depth in core. The expanded plot depicts data from the deepest 115mm of the core, which were not used in this study due to a tilting of the maximum growth axis in the core, which could have caused the disequilibrium offset to change. Therefore, since the values were not reflective of the rest of the data set, they were not incorporated into a chronology.

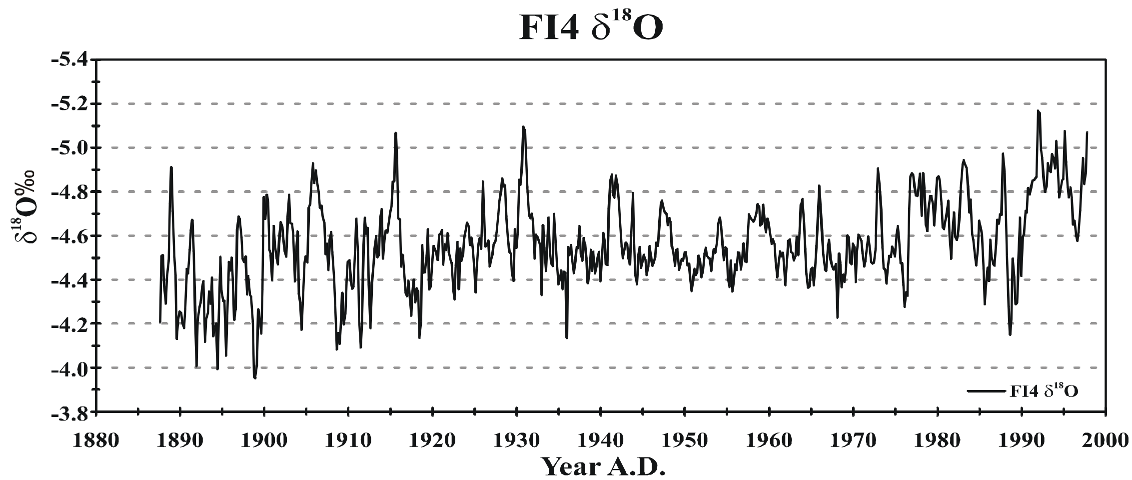

Figure 11. Fanning Island *Montipora venosa* δ^{18}O time series. Average δ^{18}O value for the period 1887-1997 A.D. is -4.56‰. Note that the δ^{18}O values of the y-axis are plotted in reverse order.

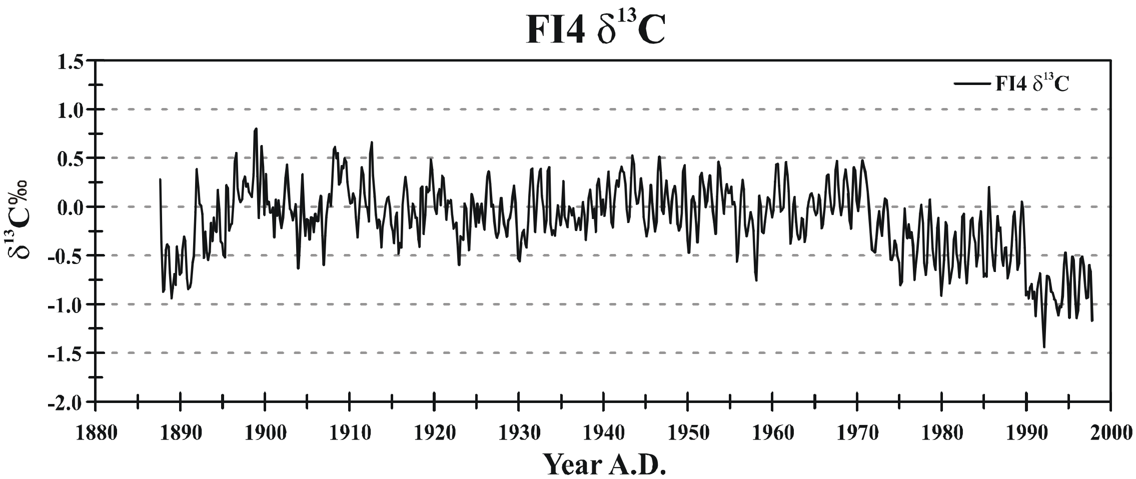

Figure 12. Fanning Island *Montipora venosa* δ^{13}C time series. Average δ^{13}C value for the period 1887-1997 A.D. is -0.14‰.

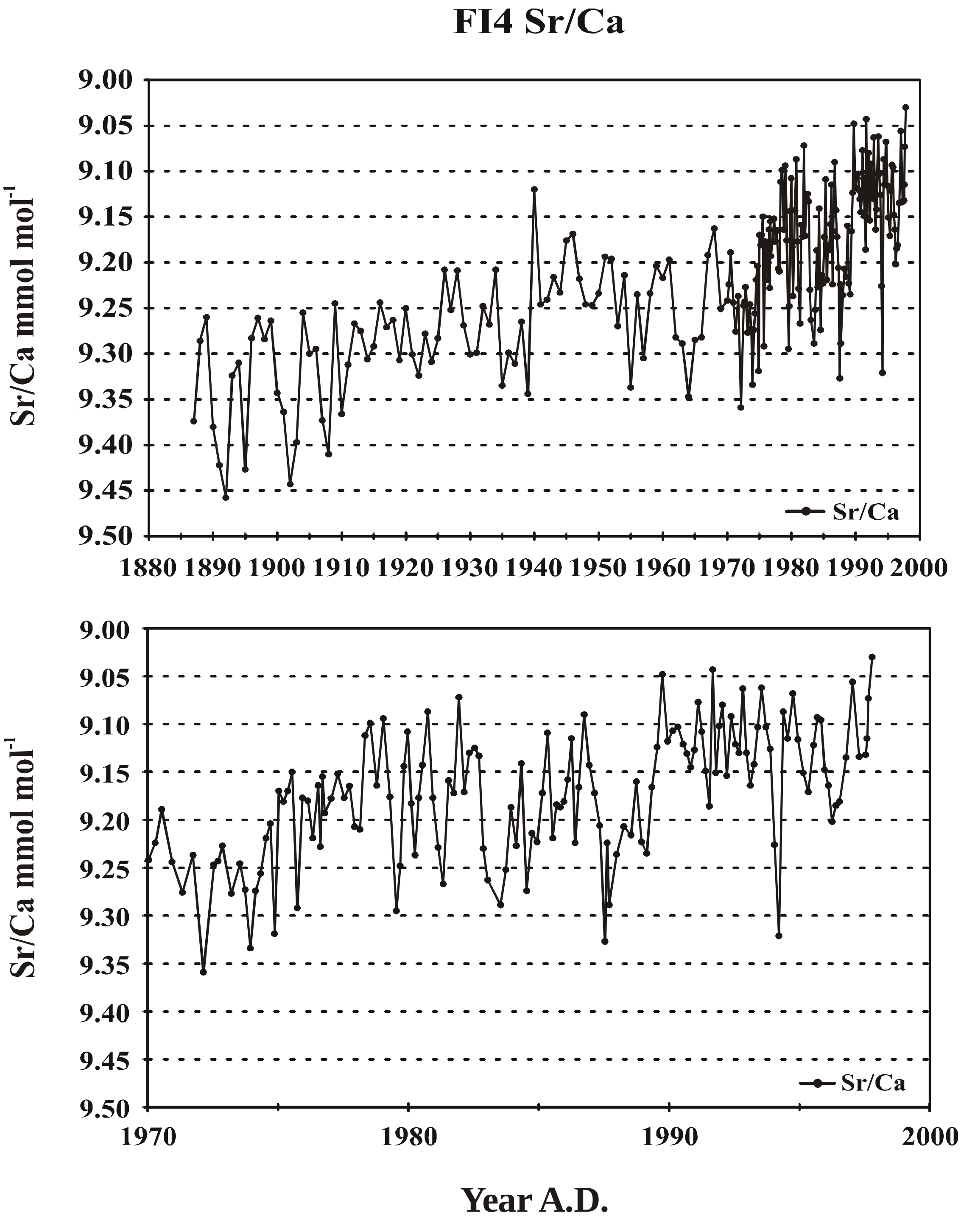

Figure 13. (Top) FI4 Sr/Ca data for the length of the core, which is on mm-resolution samples to 1970 and on annually averaged older samples below. (Bottom) FI4 Sr/Ca data for the top 30 years, sampled at mm-scale resolution for calibration with temperature.

2. *δ^{18}O and Sr/Ca compared to instrumental records*

2a*. Temperature Calibration*

The SST data set used for calibration in this study was obtained from the National Centers for Environmental Protection Optimum Interpolation Sea Surface Temperature (NCEP OI SST) (Reynolds and Smith, 1994) in a 2º x 2º grid around Fanning Island using both shipboard and satellite data. The SST data is weekly data for the period 1970-2003 A.D. (n=200 at 6/yr)(Figure 14). The average temperature during that time was 27.6ºC. The SST data set was interpolated to 6 measurements per year for the purposes of calibration with FI4 δ^{18}O, which also has 6 points per year. A least squares regression between the two data sets over the time period 1970-1997 A.D. had an r-value of 0.56 (Table 1). The same regression was performed again, comparing annual average values from the two data sets, and had an r-value of 0.75 (Table 1). The slopes of the two regression equations are also different, most likely due to the fact that FI4 has no annual cycle and generating annual averages removes more extreme values. Figure 15 shows FI4 δ^{18}O plotted against SST of both 6/yr and annual average resolution.

A least squares regression of annually averaged Sr/Ca and SST for the time period 1970-1997 A.D. resulted in an r-value of 0.77 (see Table 1 for regression equation). Figure 16 shows the difference between ~bimonthly Sr/Ca and annual average Sr/Ca against SST for *M. venosa*.

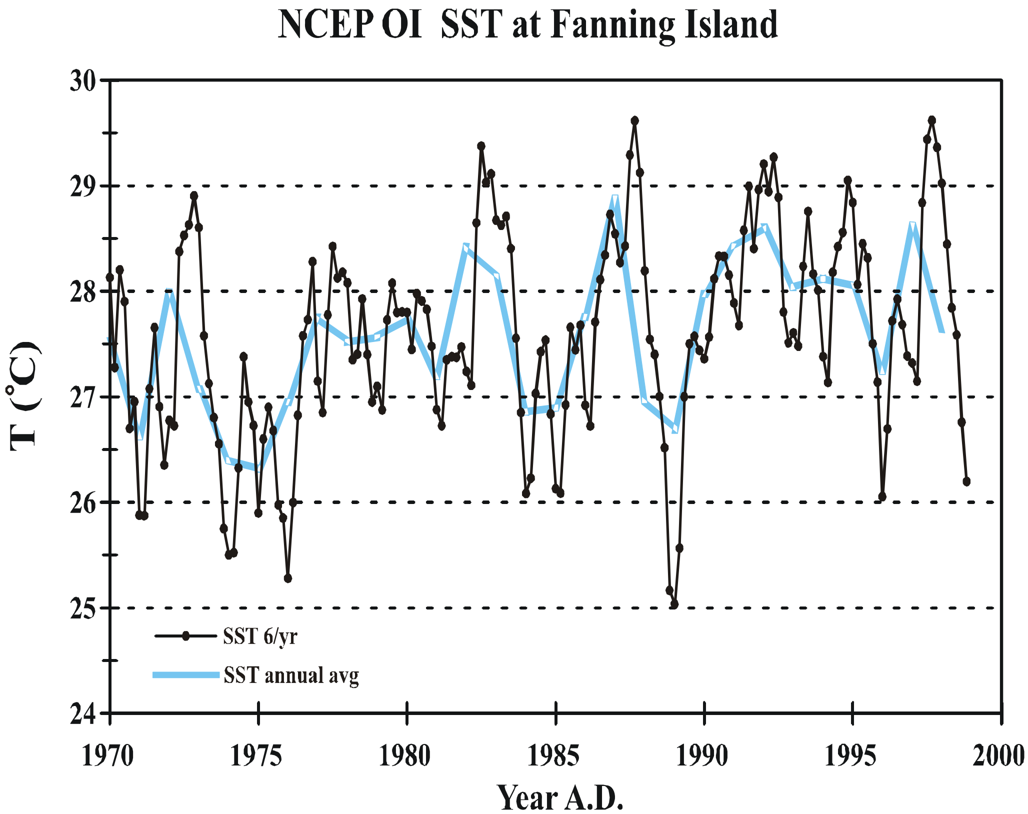

Figure 14. NCEP OI SST (Reynolds and Smith, 1994) is a blend of shipboard and satellite measurements in a 2º x 2º grid around Fanning Island from 1970-2003, using the data from 1970-1997 for this study. Annual averages (orange) are plotted at the beginning of the year. The average temperature during this time is 27.6ºC (n=200).

Table I. Least Squares Regression Equations for the Temperature Calibration of $\delta^{18}O$ and Sr/Ca in *Montipora venosa* Core FI4 for the period 1970-1997

Data Set Used	Equation	r-value
FI4 $\delta^{18}O$ 6/yr	$\delta^{18}O = -0.11 * T (ºC) – 1.59$	0.56
FI4 $\delta^{18}O$ ann avg	$\delta^{18}O = -0.17 * T (ºC) + 0.08$	0.75
FI4 Sr/Ca ann avg	Sr/Ca = -0.062 * T (ºC) + 10.91	0.77

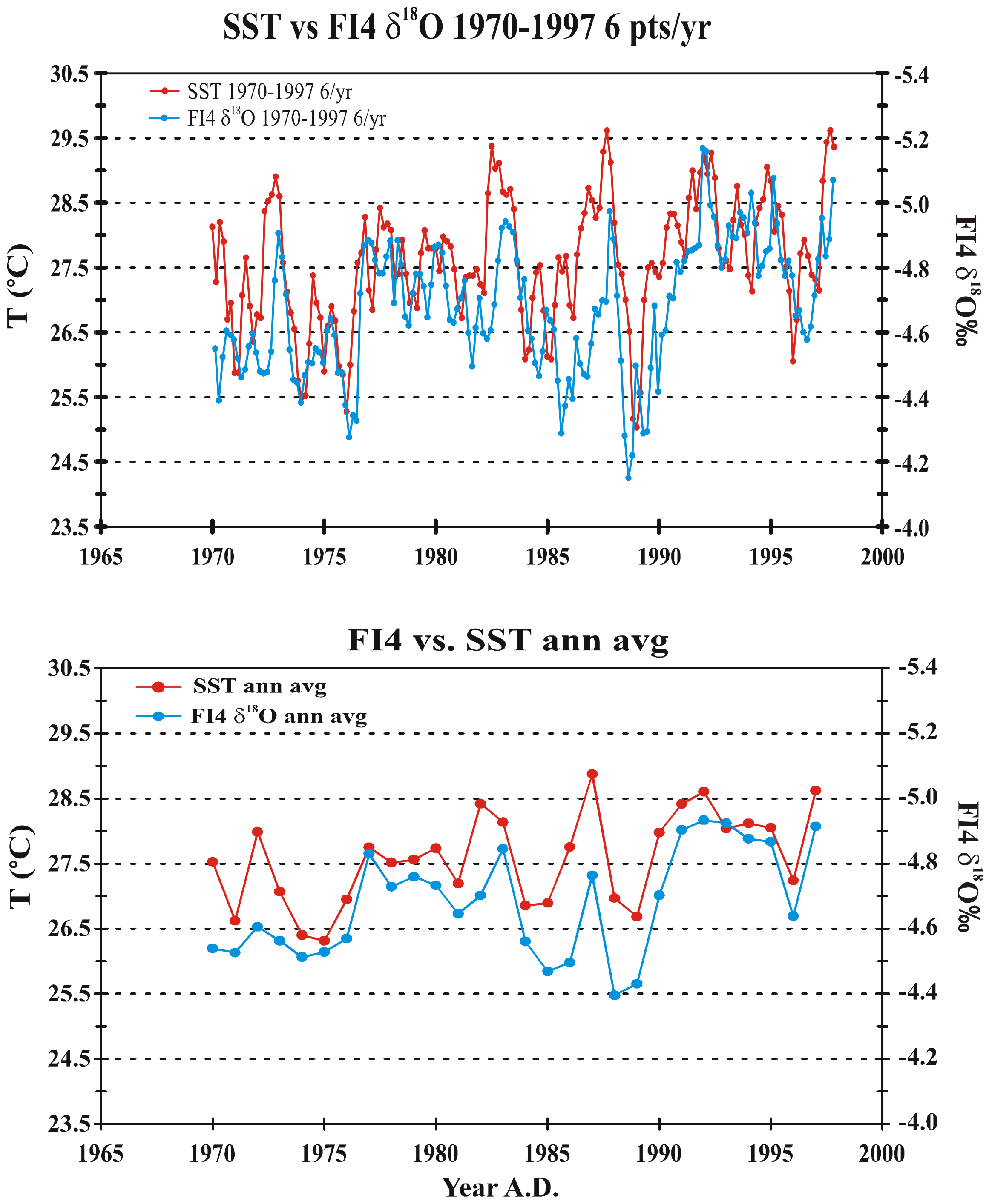

Figure 15. (Top) NCEP OI SST 1970-1997 plotted with FI4 $\delta^{18}O$ at bimonthly resolution. The r-value between the two data sets is 0.56, as shown in Table 1. (Bottom) Same data sets at annual average resolution, r-value is 0.75 (Table 1).

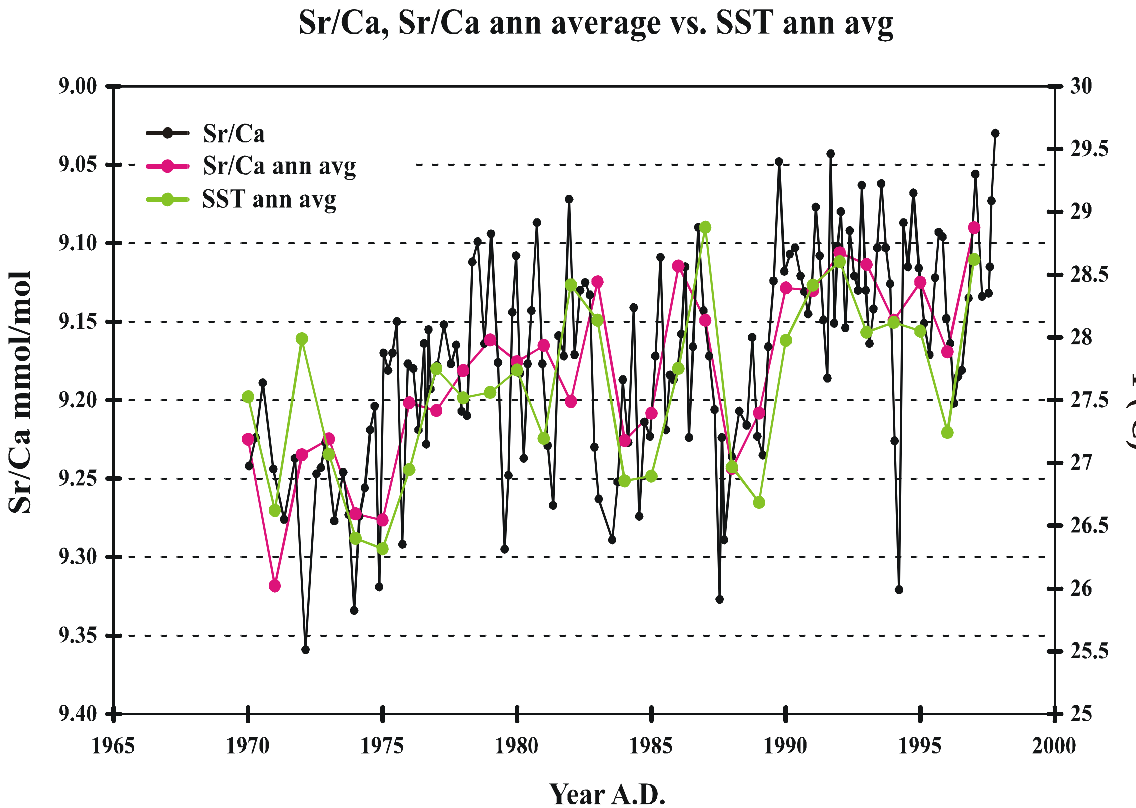

Figure 16. Sr/Ca at mm-scale (~bimonthly) resolution shown in black and annual average Sr/Ca in magenta, plotted with annual average SST in lime green. The r-value between the annual average data sets is 0.77 (Table 1).

2b. *Niño 3.4 Index*

The Niño 3.4 Index (Kaplan et al., 1998) is a record of anomalous SST (SSTa) related to ENSO events in a region (5ºS-5ºN, 170º-120ºW) of the central equatorial Pacific (Figure 2 and Figure 8). The Niño 3.4 data set was interpolated from 12 to 6 measurements per year to allow correlation with FI4 $\delta^{18}O$ (Figure 17). Although the Niño 3.4 data set covers the period 1856-1997 A.D., only the data from the period 1887-1997 common to both the Niño 3.4 and FI4 $\delta^{18}O$ data sets were used. A least squares regression between the two data sets for the common time period resulted in an r-value of 0.56 for the 6/yr series and 0.57 for the annual average series (Table 2).

2c. *Southern Oscillation Index*

The Southern Oscillation Index (SOI) is a measure of the SLP difference across the Pacific Ocean between Darwin, Australia and Tahiti. The instrumental record of SOI spans 1882-1996. The Southern Oscillation is driven in part by tropical Pacific SST variations, which are forced by surface wind fluctuations. The Southern Oscillation is a coupled ocean-atmosphere interaction.

The SOI was also interpolated to 6 points per year. A least squares regression between the SOI and FI4 $\delta^{18}O$ over the common time period 1887-1997 had in an r-value of 0.29 when compared at bimonthly resolution, while comparison of annual averages yielded an r-value of 0.45 (Table 2).

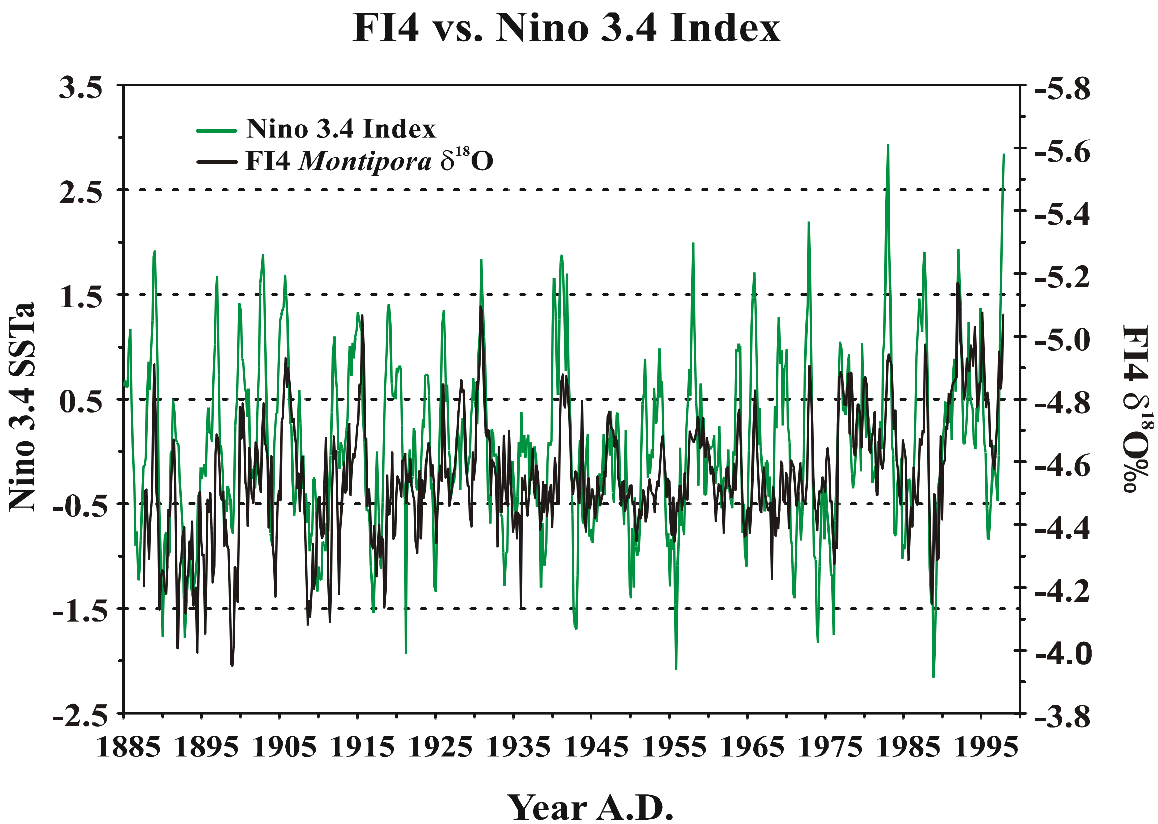

Figure 17. Nino 3.4 Index of SSTa in the central Pacific region of (5ºS-5ºN, 170º-120ºW) from 1856-1997 plotted with FI4 $\delta^{18}O$.

Table II. Least Squares Regression Equations Between *Montipora venosa* Core FI4 $\delta^{18}O$ and Instrumental Indices Niño 3.4 and SOI for the period 1887-1997

Data Sets Used	Equation	r-value
FI4 $\delta^{18}O$/Niño 3.4 (6/yr)	$\delta^{18}O = -0.13 * T (^{o}C) - 4.55$	0.56
FI4 $\delta^{18}O$/Niño 3.4 (1/yr)	$\delta^{18}O = -0.15 * T (^{o}C) - 4.55$	0.57
FI4 $\delta^{18}O$/SOI (6/yr)	$\delta^{18}O = 0.005 * SLP - 4.6$	0.29
FI4 $\delta^{18}O$/SOI (1/yr)	$\delta^{18}O = 0.01 * SLP - 4.6$	0.45

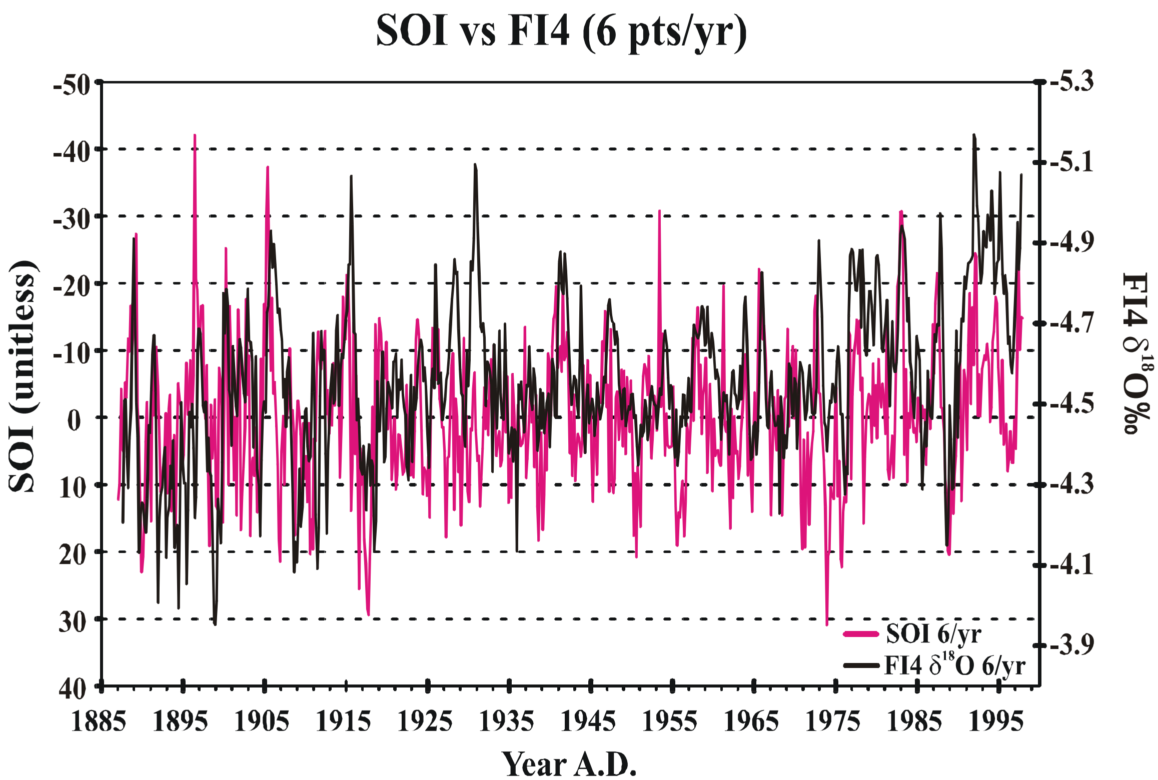

Figure 18. SOI (1882-1996) plotted with FI4 $\delta^{18}O$.

2d. *Precipitation*

Two precipitation (PPT) data sets were used in this study. The first is the Comprehensive Ocean-Atmosphere Data Set (COADS) which contains monthly data from Fanning Island spanning 1922-1980. The second is the National Oceanographic and Atmospheric Administration, National Centers for Environmental Protection, Climate Prediction Center (NOAA NCEP CPC) data set, containing average daily precipitation for the period 1979-2005. The NOAA data set was converted to average monthly mm-values by multiplying each daily value within the year by the appropriate number of days in the corresponding month. Both the NOAA and COADS PPT data were interpolated to 6 points per year to match the FI4 time series data. The two PPT data sets were then merged, using the full COADS set from 1922 through 1980, and the NOAA set from 1981 on. Figure 19 shows the area of overlap between the two data sets. The average monthly PPT value prior to interpolation to 6 pts/yr is 163.35mm (n=997), and the average bimonthly value is 164.03mm (n=498). Figure 20 shows the similarities between PPT, FI4 $\delta^{18}O$ and SST at Fanning Island. All three data sets have striking similarities showing higher SST and rainfall and lower $\delta^{18}O$ during El Niño events and the opposite during La Niña events.

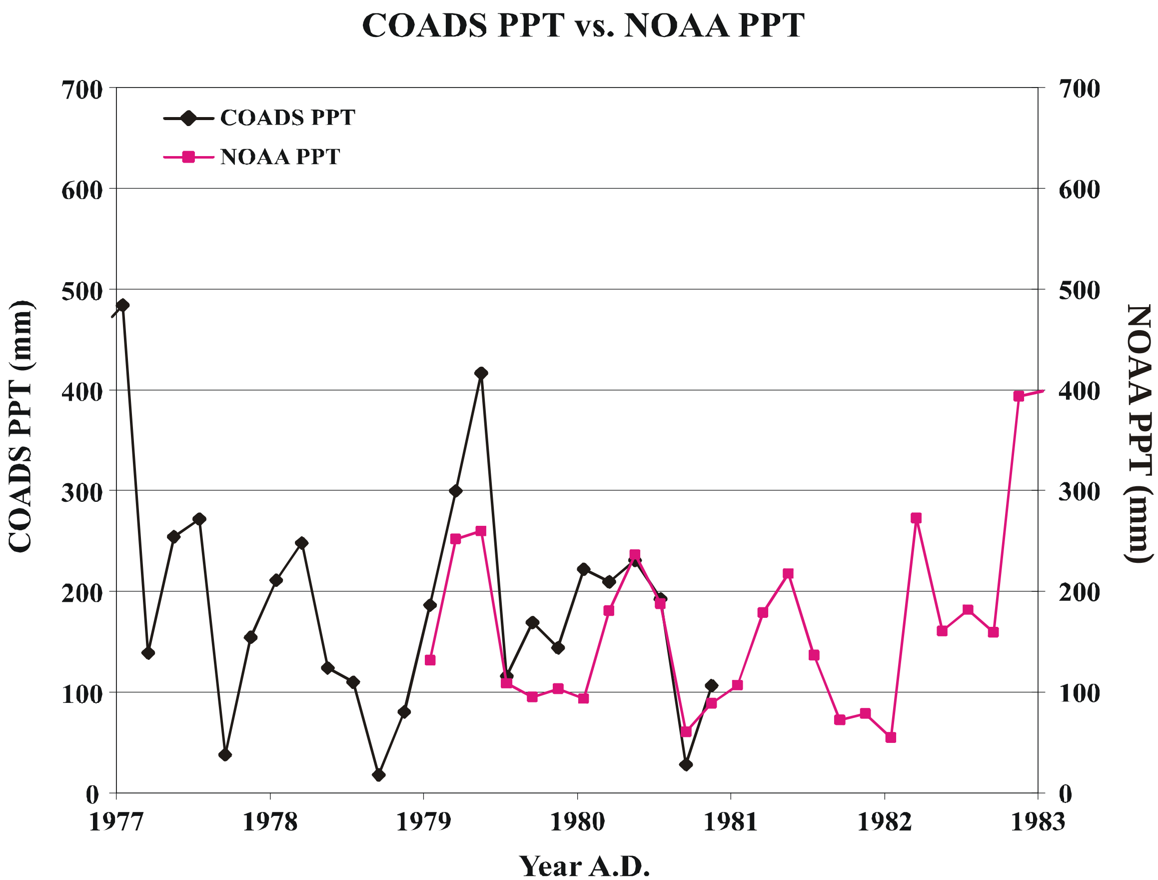

Figure 19. Overlap between COADS (1922-1981) and NOAA (1979-2005) PPT data sets. The data sets were merged using the full COADS set and stacking it with the NOAA data set starting in 1981, resulting in a full PPT data set spanning from 1922-2005, as shown in Figure 4.

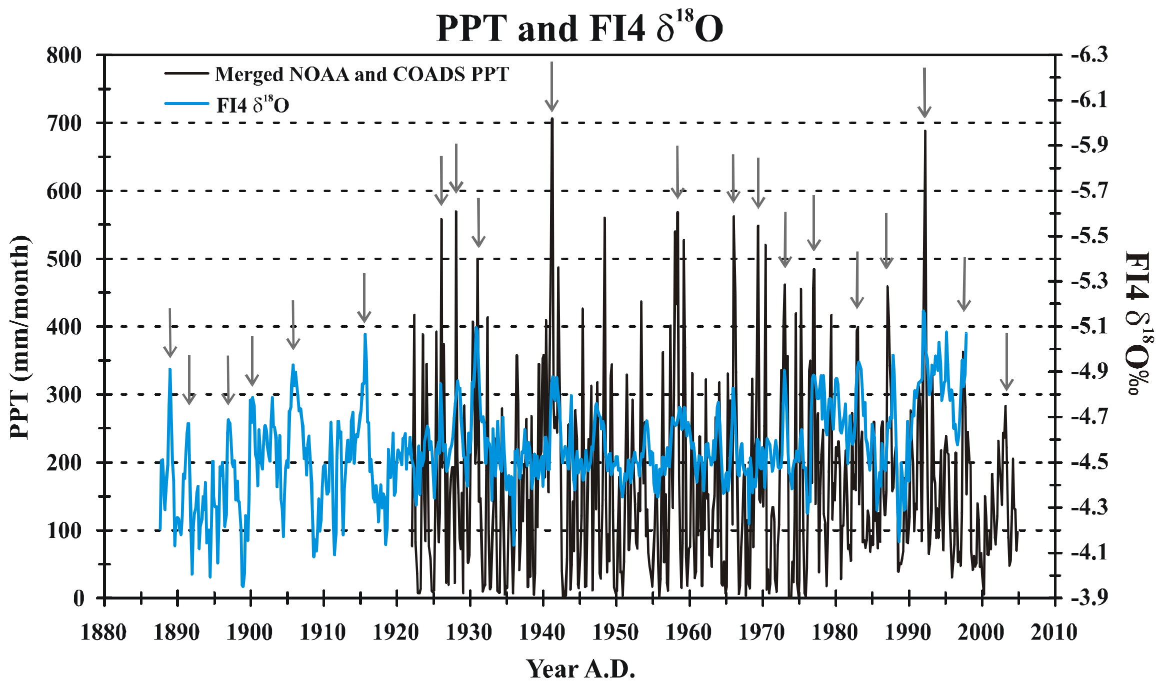

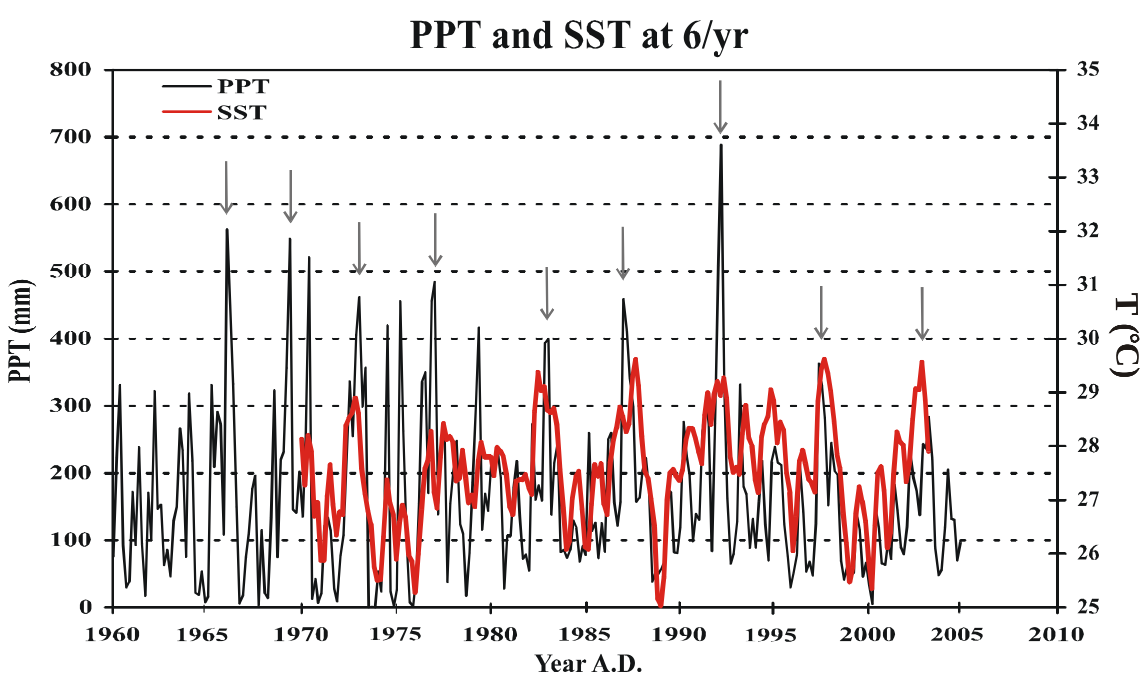

Figure 20. (Top) FI4 $\delta^{18}O$ plotted with merged PPT data. (Bottom) SST plotted with PPT. Gray arrows on both plots indicate ENSO events.

***3.** FI4 Montipora venosa $\delta^{18}O$ vs. FI5 Porites $\delta^{18}O$*

Montipora venosa and *Porites* corals have different growth patterns and average growth rates (for ex; at Fanning 6mm/yr vs. 16.5mm/yr for FI4 and FI5, respectively), yet both can potentially be used for paleoclimatic reconstruction. In this study, the useable length of the *M. venosa* coral is 650mm, yielding a time series record spanning 111 years, while the *Porites* coral is 1260mm long, yet only covers a time span of 75 years (1922-1997). The average FI5 *Porites* $\delta^{18}O$ value (n=1260) is –4.78‰. The minimum (maximum) $\delta^{18}O$ value for the same period is -5.67‰ (-3.57‰) in 1997 and 1950, respectively. The mean is 0.22‰ lower than that of the *M. venosa* data, and the total range between minimum and maximum $\delta^{18}O$ values is significantly larger. Figures 21 and 22 show the two $\delta^{18}O$ time series and demonstrate that despite differences in growth rate and sampling resolution, the slower growth of *M. venosa* does not limit the reconstruction of interannual oceanographic variability. However, there are some significant differences in the $\delta^{18}O$ values between the two records. In particular, an increase in $\delta^{18}O$ in the Fanning *Porites* record from 1950-1951 is not recorded in the Fanning *Montipora* or in *Porites* $\delta^{18}O$ records from Tarawa (1º3'N, 172ºE) (Cole et al., 1993), Palmyra (5º52'N, 162ºW) (Cobb et al., 2001) and Maiana (1ºN, 173ºE) (Urban et al., 2000) (Figure 23). There is also a *Porites* core from inside the lagoon at Fanning Island (FL6), which does not show this anomaly either (R. Dunbar, pers. comm.). This difference suggests an unexplained anomaly in the FI5 *Porites* record and supports the need for a multi-core replication strategy. There is also a pronounced trend toward markedly lower $\delta^{18}O$ values in the *Porites* data after 1955.

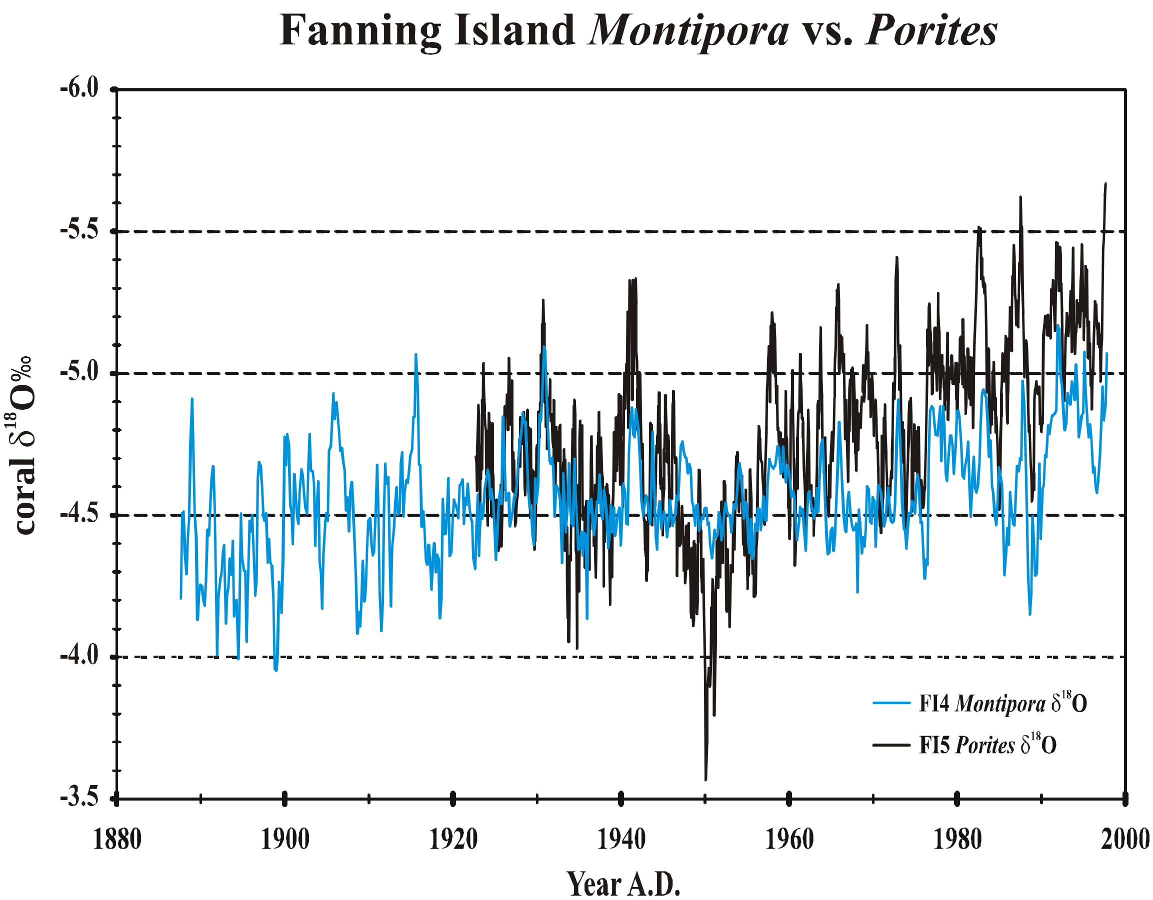

Figure 21. δ^{18}O time series of coral cores FI4 (*Montipora venosa*; bimonthly) and FI5 (*Porites*; monthly) from Fanning Island, cored ~4m apart. This figure demonstrates how both corals record ENSO events and oceanographic climate variations with similar magnitude and timing despite the difference in sample resolution. Note the unexplained deviation from the mean in FI5 in 1950 and 1951. *Porites* time series data is from R. Dunbar (personal communication).

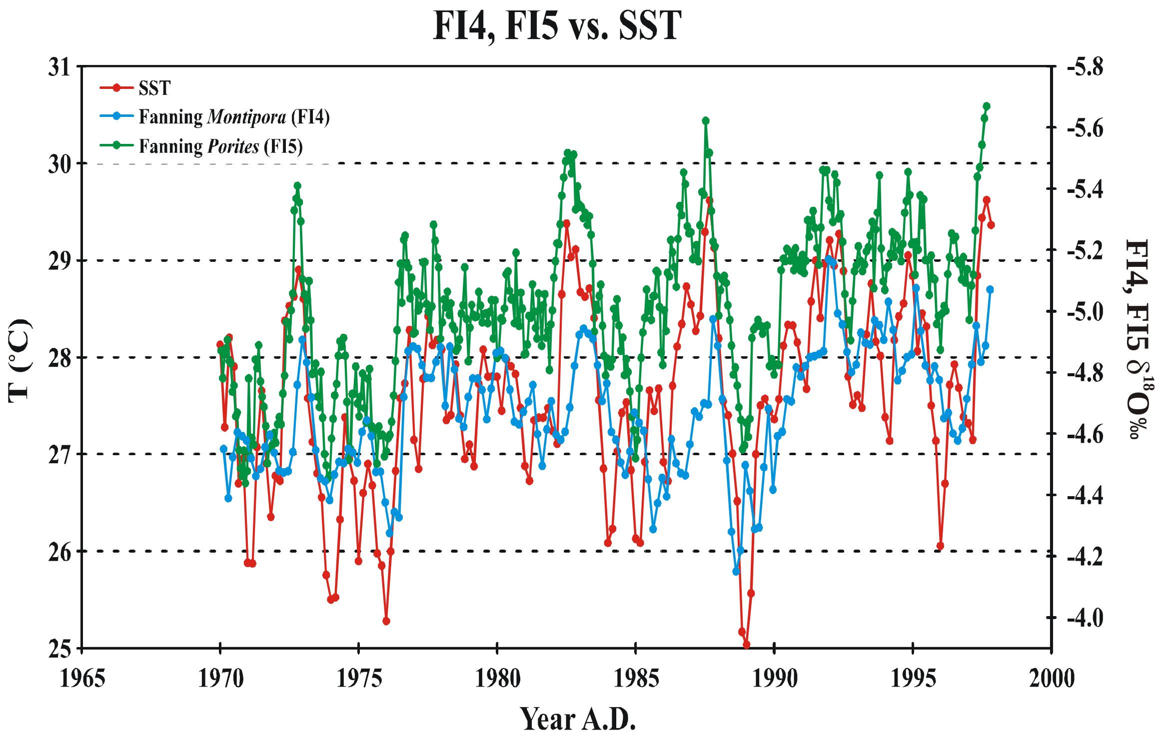

Figure 22. A plot of both the Fanning Island cores – FI4 *Montipora venosa* and FI5 *Porites* vs. NCEP OI SST in a 2 x 2 grid (3.5ºN, 158ºW) around Fanning Island. FI5 is shown at 12 points per year to further emphasize that the resolution difference between the two time series does not affect the paleoclimatological merit of the *M. venosa* data set. Note that the graph is not to correlative scale due to the fact that the FI4 and FI5 cores are plotted on the same PDB scale.

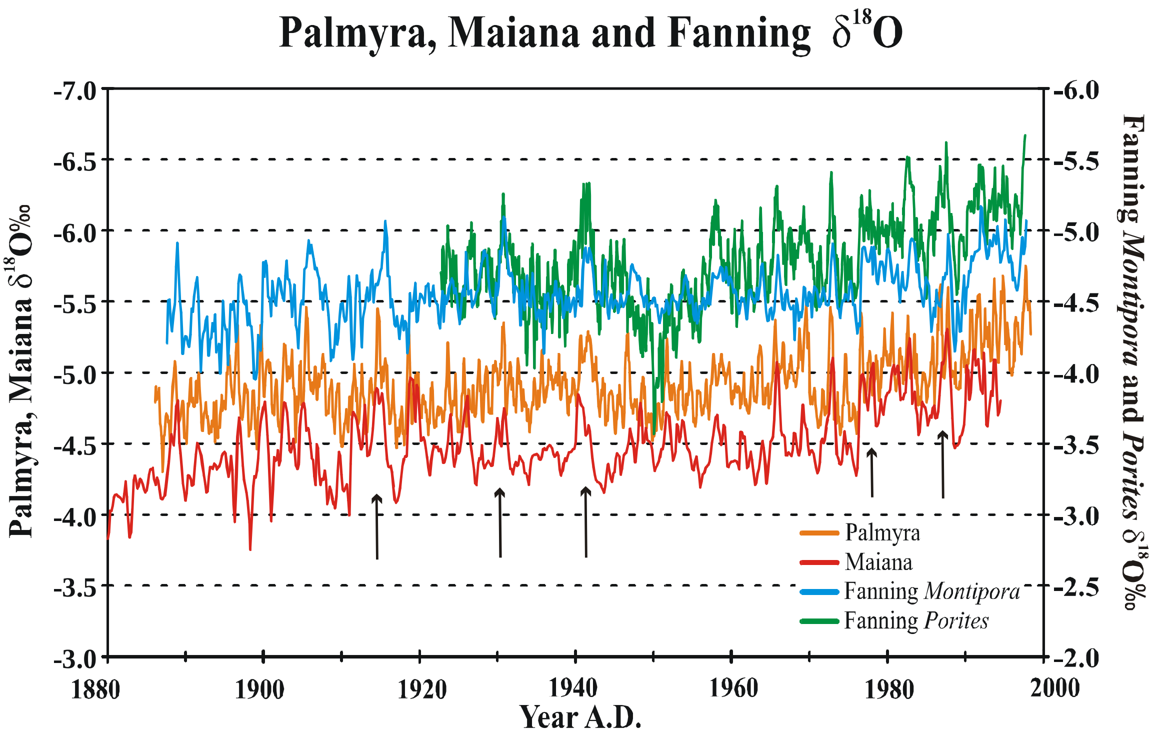

Figure 23. Plot of FI4 $\delta^{18}O$ *Montipora venosa* with nearby islands Palmyra (5º52'N, 162ºW) and Maiana (1ºN, 173ºE) $\delta^{18}O$ *Porites* records showing that similarities in the three time series prove the usefulness of *Montipora venosa* as a paleoclimatic indicator. Arrows indicate ENSO events recorded by all three corals. Palmyra data from Cobb et al. (2001) and Maiana data from Urban et al. (2000).

4. Singular Spectrum Analysis (SSA)

The results of the singular spectrum analysis of FI4 *M. venosa* $\delta^{18}O$ can be found in the tables presented below. SSA was run multiple times with different window lengths (m) to evaluate the stable eigenset of RCs. Results for SSA with m=61 (10.17yr) and m=81 (13.5yr) are presented below (Tables 3 and 4). The components repeated in both tables are the most prominent periods in the time series.

Table III. Singular spectrum analysis of unfiltered FI4 *Montipora venosa* $\delta^{18}O$, m=61 (10.17yr)

Eigenvector	Period (Years)	Variance (%)	Cumulative Variance (%)
12, 11	1.9*	4.3	80.7
10	2.1*	3.1	76.4
9	2.4	3.5	73.3
8	2.6*	3.7	69.8
7, 6, 5, 4, ENSO Band	3.0, 3.6*, 5.1*, 5.1*	21.2%	66.1
3	8.8	7.4	44.9
2	16.7*	13.6	37.5
1	trend*	23.8	23.8

* denotes components that are repeated when m=81

Table IV. Singular spectrum analysis of unfiltered FI4 *Montipora venosa* $\delta^{18}O$, m=81 (13.5yr)

Eigenvector	Period (Years)	Variance (%)	Cumulative Variance (%)
16, 15, 14	1.9*	4.8	81.0
13	2.1	2.4	76.1
12	2.2*	2.4	73.7
11, 10	2.6*	5.5	71.2
9 ,8, 5, 4, 7 ENSO Band	3.6*, 3.5, 4.6, 5.1, 6.7	21.0%	65.7
6	8.3	4.2	56.4
3	12.8	8.8	40.6
2	16.7*	12.1	31.8
1	trend*	19.7	19.7

Discussion

1. *FI4 $\delta^{18}O$ compared to central tropical Pacific Porites records*

FI4 $\delta^{18}O$ shows a gradual trend towards lower $\delta^{18}O$, which occurs in 3 main phases (Figures 11 and 24A). The first is a trend towards more negative $\delta^{18}O$ values from 1887-1933 of approximately 0.27‰. If interpreted exclusively as temperature, this change in $\delta^{18}O$ would translate to a warming of 1.6-2.5ºC over a period of 46 years, using the range of calibrated SST-$\delta^{18}O$ relationships shown in Table 1 [(-0.11) to (-0.17)‰ per 1ºC]. However, this is simply theoretical, since SST accounts for only 56%-75% of the variance seen in FI4 $\delta^{18}O$ (Table 1). The next phase is a quiet period with virtually no trend at all from 1934-1975. Then, in 1976 there is the first of a pronounced two-part decrease in mean $\delta^{18}O$ values that continues in 1991, resulting in an overall trend of 0.13‰ - a theoretical warming of 0.77-1.2ºC over a period of 21 years. The 1976 shift towards warmer conditions recorded in *M. venosa* at Fanning Island is also observed in the NCEP OI SST data set (Figure 14) and has previously been documented in coral $\Delta^{14}C$ in the eastern Pacific (Guilderson and Schrag, 1998). There is a warming from 1976-1997 (time period corresponding to the FI4 $\delta^{18}O$ data set) of 0.81ºC, which actually falls within the predicted range of temperature change according to *M. venosa* $\delta^{18}O$. This 1976 shift is also observed in the FI5 *Porites* $\delta^{18}O$ record (Figure 22). Since the overall range of $\delta^{18}O$ values (-5.67‰ to -3.57‰) in FI5 *Porites* is significantly larger than $\delta^{18}O$ values (-5.17‰ to -3.95‰ of FI4 *M. venosa* (2.10‰ vs. 1.22‰, respectively), it is not surprising that the shift seen in 1976 is slightly greater in FI5 (-0.71‰ within 1976) than in FI4 (-0.61‰ within 1976).

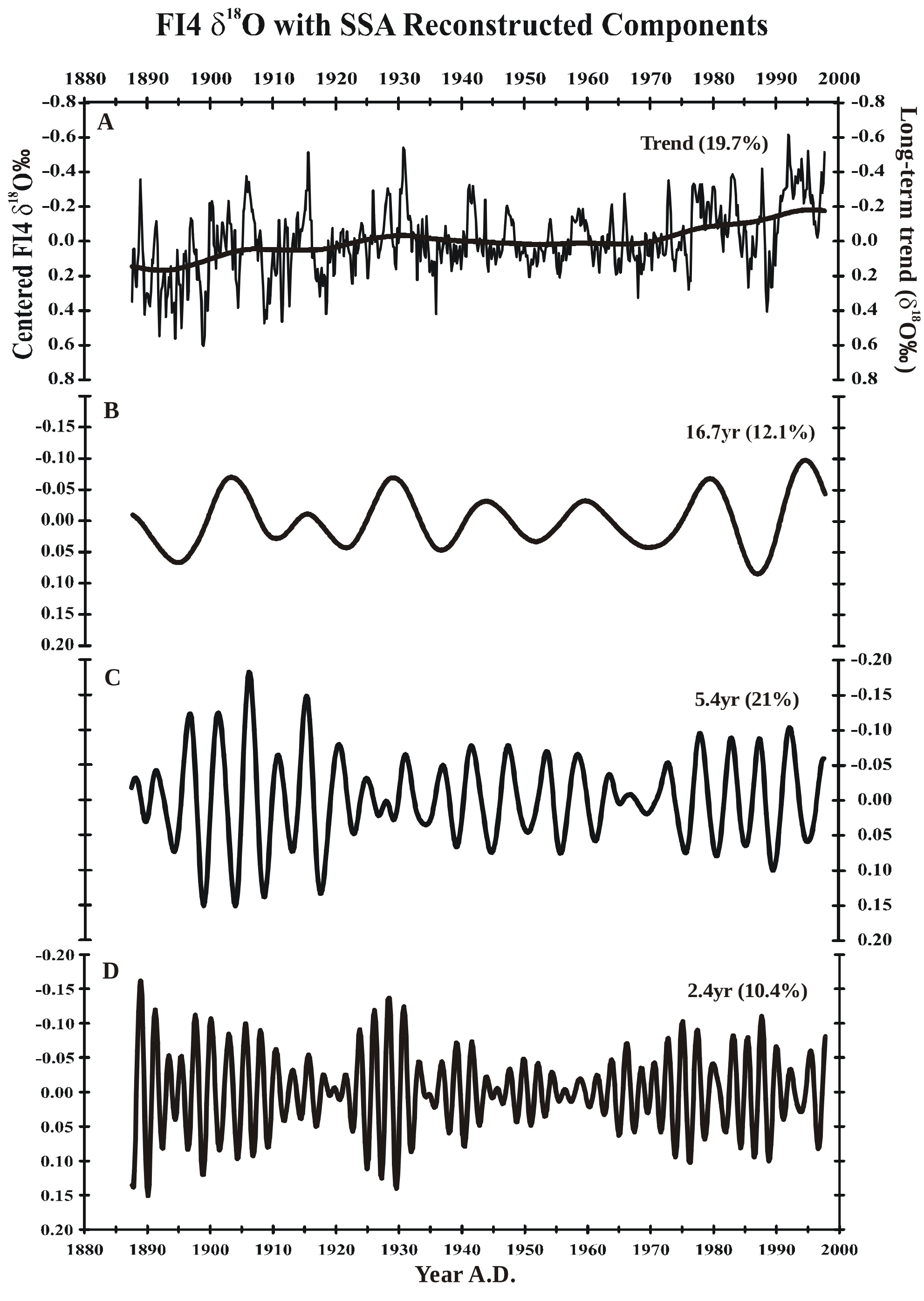

Figure 24. (A) FI4 $\delta^{18}O$ time series with the long-term trend superimposed. (B) 16 year component of FI4 $\delta^{18}O$, showing the decadal variability, which accounts for 12% of the total variability. (C) Interannual (4.6-6.7yrs) component of FI4 $\delta^{18}O$. It is the sum of 3 modes, totaling 15% of the total variability. (D) Quasi-biennial (2.1-2.6yrs) component of FI4 $\delta^{18}O$. It is the sum of 4 modes, totaling 10.4% of the total variability.

However, although the unexplained deviation in the FI5 $\delta^{18}O$ record in 1950 and 1951 contributes significantly to the difference in overall range of $\delta^{18}O$ values, other factors, such as differences in coral genus, growth rate, and sampling resolution may be important. Therefore, the greater range in $\delta^{18}O$ does not necessarily imply that *Porites* was recording a larger SST range than *M. venosa* at Fanning Island. The *Porites* $\delta^{18}O$ time series also has a much larger overall trend than does the *M. venosa* $\delta^{18}O$ time series. This trend in *Porites* records seems to be characteristic of central and western tropical Pacific records, as observed, for example, in *Porites* $\delta^{18}O$ records from Palmyra (Cobb et al., 2001, 2003), Kiritimati (Evans et al., 1998), and Nauru (Guilderson and Schrag, 1999). However, this trend is controversial since it is not seen at the same magnitude in all coral records, regardless of location. There are several possible causes for this discrepancy, including changes in the disequilibrium offset, vital effects, genus/species differences, or analytical artifacts. These remain questions as to whether this trend is a real environmental signal or just an artifact of coral growth, etc.

Not only is the 1976 shift seen at Fanning Island, it is observed in the *Porites* $\delta^{18}O$ records just north of Fanning Island at Palmyra (5º52'N, 162ºW) (Cobb et al., 2001, 2003) and even farther west at the easternmost edge of the WPWP at Maiana Atoll (1ºN, 173ºE) (Fig. 23) (Urban et al., 2000). The fact that this shift is found in several coral records as well as instrumental records over a fairly large region of the Pacific supports the fidelity of corals to record subtle changes in oceanographic conditions, such as SST and PPT. It also substantiates the replication strategy, because by studying several genera of coral from multiple locations a more complete evaluation of errors and more complete picture of the nature of large climatic events may be developed.

The decrease in $\delta^{18}O$ values observed over the long term trend in the Maiana record is less pronounced than that seen in the FI4 *Montipora* at Fanning Island (0.06‰ vs. 0.13‰, respectively), suggesting a possible east to west trend in warming across the Pacific basin. There has been some speculation about the trends toward a warmer climate seen throughout the 20th century. Cane et al. (1997) suggest that the pattern of SST changes across the Pacific Ocean is due to an increase in the temperature gradient from west to east. The gradient increase could be due to vigorous upwelling of colder water in the eastern Pacific, which offsets the exogenous warming in the east, especially since the thermocline is much shallower than in the west, and the SST warming is enhanced in the western Pacific. As a consequence of this new, larger temperature gradient, the trade winds would become stronger, which in turn would create a positive feedback on the thermal gradient (Cane et al., 1997). However, the $\delta^{18}O$ isotopic difference between Maiana and Fanning presented in figure 25 do not support this hypothesis. For the first (1887-1933) of the three phases of the FI4 time series Maiana's trend towards lower $\delta^{18}O$ values is only half as much as the Fanning *Montipora* (0.14‰ vs. 0.27‰, respectively). During the second phase (1934-1975), Fanning *Montipora* has no $\delta^{18}O$ trend at all, while Maiana's trend towards lower $\delta^{18}O$ values is 0.12‰. Finally, in the third phase (1976-1994; Maiana time series ends in 1994) Maiana's trend towards lower $\delta^{18}O$ values is again half as much as Fanning *Montipora* (0.06‰ vs. 0.11‰). In the end, the trend between the two islands only differs by a few hundredths of a per mil (‰), suggesting that there really has been no difference in temperature gradient across the Pacific basin during this time period. The relationship between Fanning Island and an incomplete Urvina Bay $\delta^{18}O$ time series from the eastern Pacific (Dunbar et al., 1994), further supports this idea. Figure 25 also demonstrates the timing of El Niño events across the Pacific from west to east, and as one would expect Maiana tends to experience El Niño events before Fanning Island.

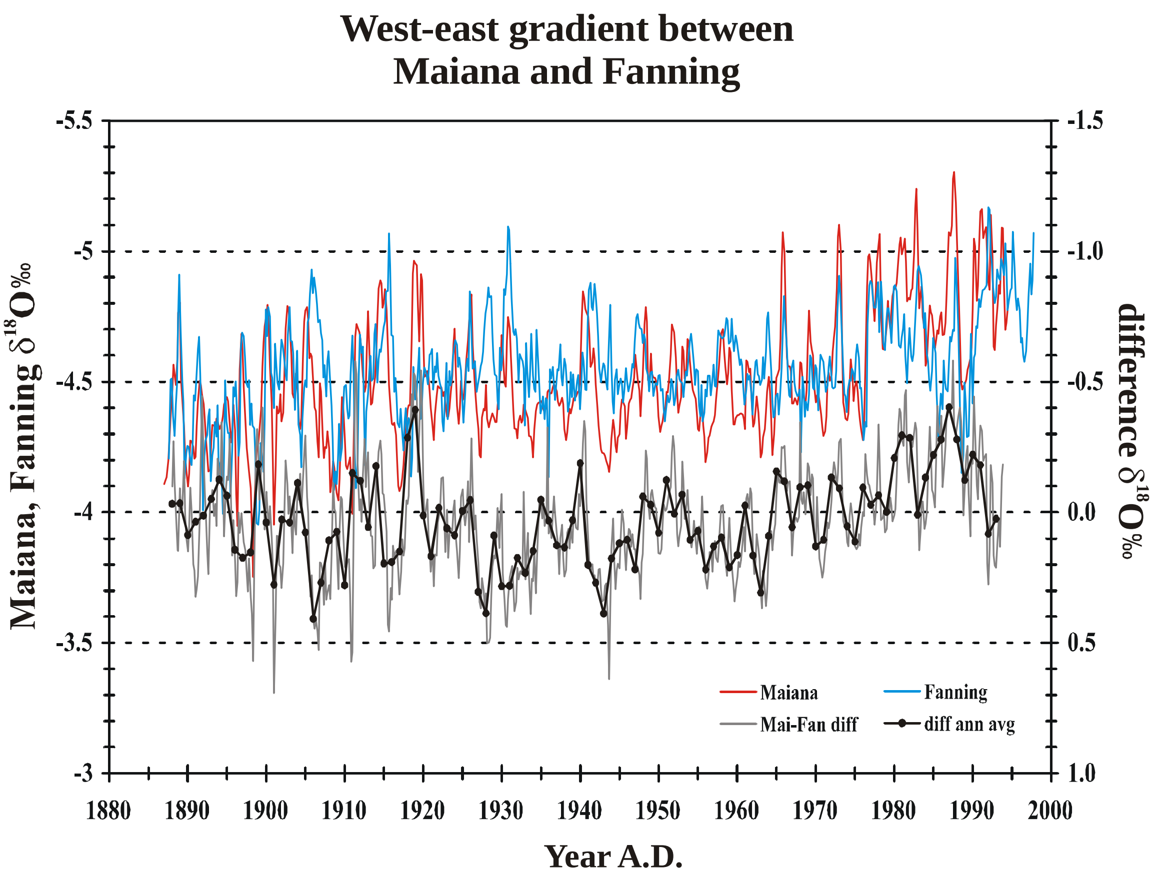

Figure 25. Plot of Maiana *Porites* and Fanning Island *Montipora* $\delta^{18}O$ to highlight the timing of ENSO events as they occur across the Pacific Ocean from west to east.

In addition to the effect of SST, $\delta^{18}O$ of coral is also known to be influenced by isotopic changes in the surrounding seawater ($\delta^{18}O_{sw}$) (Shen et al., 1992), which is linearly related to changes in SSS in the central equatorial Pacific (Fairbanks et al., 1997). Due to the fact that SST only accounts for only 56%-75% of the total variance in the FI4 $\delta^{18}O$ time series, there must be another climatic parameter besides SST influencing $\delta^{18}O$ in *M. venosa* at Fanning Island .

Variability of $\delta^{18}O_{sw}$ and SSS at Fanning Island are influenced by precipitation patterns due to its geographic location within the ITCZ (McPhaden and Picaut, 1990; Picaut and Delcroix, 1995; Picaut et al., 1996; Picaut et al., 1997; Picaut et al., 2001). Latitudinally, Fanning Island lies on the edge of the maximum precipitation zone. Meridionally, Fanning lies on the edge of the salinity front at easternmost edge of the WPWP, as described earlier. Zonal salinity gradients affected by the migration of EWPCZ, which is in phase with interannual ENSO variability, are mainly a result of horizontal advection processes (meridional Ekman salt transport) and variation in precipitation/evaporation budgets (Delcroix and Hénin, 1991; McPhaden and Picaut, 1990; Picaut and Delcroix, 1995; Picaut et al., 1996; Picaut et al., 1997; Picaut et al., 2001; Gouriou and Delcroix, 2002). It is most likely that the other main factor influencing coral $\delta^{18}O$ variability at Fanning Island is a result of rainfall regimes and the coinciding SSS variability at this location.

2. *FI4 $\delta^{18}O$ and regional indices (Niño 3.4, SOI, and PPT)*

The Niño 3.4 region is known to have the largest ENSO-related SST anomalies (Figures 2, 9, 17) (Barnston et al., 1997). Fanning Island lies on the western edge of this region, and therefore the FI4 *M. venosa* $\delta^{18}O$ record was predicted to record the same El Niño and La Niña events with similar amplitude and timing as the Niño 3.4 index.

Interestingly, two of the major El Niño events, 1918-1920 and 1968-1969, are not recorded in the Fanning Island *M. venosa* $\delta^{18}O$ record, but are recorded in the Niño 3.4 index, and in the Maiana and Palmyra *Porites* $\delta^{18}O$ records. However, FI4 $\delta^{18}O$ does correlate with the SOI during these events (Figures 17 and 18). Also, the 1931-1932 El Niño is recorded in both the FI4 $\delta^{18}O$ record and the Niño 3.4 index, but not by the SOI. This is somewhat puzzling due to the fact that the SOI is basin-wide, and not local to Fanning Island. Also, the fact that the SOI spans a much larger area may contribute to the lower correlation (29%; Table 2) between the SOI and FI4 $\delta^{18}O$. The SO is closely connected to interannual tropical Pacific SST variation associated with El Niño events, which in turn is closely linked to trade wind variability. The SO is also related to major changes in rainfall patterns over the tropical Pacific (Trenberth and Shea, 1987; Philander, 1990; Diaz and Kiladis, 1992).

The impact of rainfall variability on the ability of FI4 *Montipora venosa* to record the 1918-1920 ENSO event cannot be assessed since PPT data do not start until 1922. However, during both 1931-1932 and 1968-1969 significant amounts of rainfall occurred between June and August (Figures 4 and 20). PPT, Niño 3.4, and FI4 $\delta^{18}O$ all record the 1931-1932 event, but in 1968-1969, only PPT and Niño 3.4 record the event. In the absence of a salinity record, PPT might be the best indicator of SSS changes, since salinity minimums (maximums) coincide with PPT maximums (minimums) in this area (Delcroix and Hénin, 1991). Although linear extension or growth rate has not been shown to be highly correlated with $\delta^{18}O$ (Land et al., 1975; McConnaughey, 1989; Leder et al., 1996), it may be noteworthy that the linear extension rate of core FI4 decreased during the 1968-1969 ENSO event (Figure 8), hitting a minimum in 1971. Perhaps the coral was growing so slowly during this time that the sampling regime of 6 samples per year did not allow for a record of this event to be evidenced in the time series. The unusually slow growth during this time may possibly be a sign of bleaching. However, the coral slab and x-ray positive do not show signs of bleaching, nor do the SST data give any indication of thermal stress since later temperatures increase by at least 2ºC and the linear extension of the coral is not affected.

3. *Singular Spectrum Analysis*

3a. *Reconstructed modes of variability in core FI4*

The RCs that explain the largest amount of variance in the FI4 δ^{18}O time series are shown in Figure 24. The 5.4yr component (panel C) is the sum of RCs 4 and 5 (Table 4) and is representative of the interannual component of ENSO. The 2.4yr component (panel D) is the sum of RCs 10, 11, 12, and 13 (Table 4) and represents the quasi-biennial component of the FI4 δ^{18}O time series data. The amplitude of all three components shown reflect the "quiet period" of the mid-20th century (Linsley et al., 2000 and references therein), suggesting that ENSO variability as recorded in core FI4 *Montipora venosa* δ^{18}O was also subdued during this time. The Pacific Decadal Oscillation (PDO) (Mantua and Hare, 2002, among others), a lower frequency El Niño-like pattern, is weakly negatively correlated to the FI4 16yr interdecadal component, as seen in Figure 26. FI4 *M. venosa* δ^{18}O 16yr component seems to be out of phase with the PDO between ~1887 and 1928 A.D., in and out of phase until ~1976, and then out of phase again until

~1995. These three phases roughly correspond to the three phases of FI4 *Montipora venosa* as discussed earlier in section one (Figure 24). During the time FI4 and PDO are both in and out of phase (1928-1976), the PDO is in a cool, or negative phase, which generally corresponds to times of less frequent El Niño events. This observation is in agreement with the ENSO quiet period seen in FI4 *Montipora venosa* (Figure 25, C and D). The weak relationship between the PDO and FI4 $\delta^{18}O$ *M. venosa* suggests that there is an mildly active decadal component to the oceanographic climatology at Fanning Island. The weak correlation of the FI4 $\delta^{18}O$ *M. venosa* 16yr component with the PDO is expected due to the location of Fanning Island. Palmyra Island, also in the central tropical Pacific (6ºN, 162ºW), displays a relatively prominent decadal component (Cobb et al., 2001), supporting the suggestion that this region of the Pacific Ocean is dominated by both ENSO and lower frequency interdecadal variability. The lower/longer frequency changes observed in core FI4 substantiate the use of the coral *Montipora venosa* due to its ability to record centennial-scale climate variability.

3b. *The Quasi-biennial Oscillation and FI4 $\delta^{18}O$ 2yr mode of variability*

The Quasi-biennial Oscillation (QBO) is a near-biennial (22-34 months, avg. of 28 months) circulation of surface winds across the tropics and is a prominent factor in interannual global stratospheric variability (Naujokat, 1986; Rasmusson, 1990; Baldwin et al., 2001). The QBO consists of alternating easterly and westerly wind regimes, which have been shown to be linked to warm and cold phases of the SO and to be an interactive component in the timing of ENSO events (Naujokat, 1986; Rasmusson, 1990; Gray et al., 1992; Labitzke and van Loon, 1999; Baldwin et al, 2001).

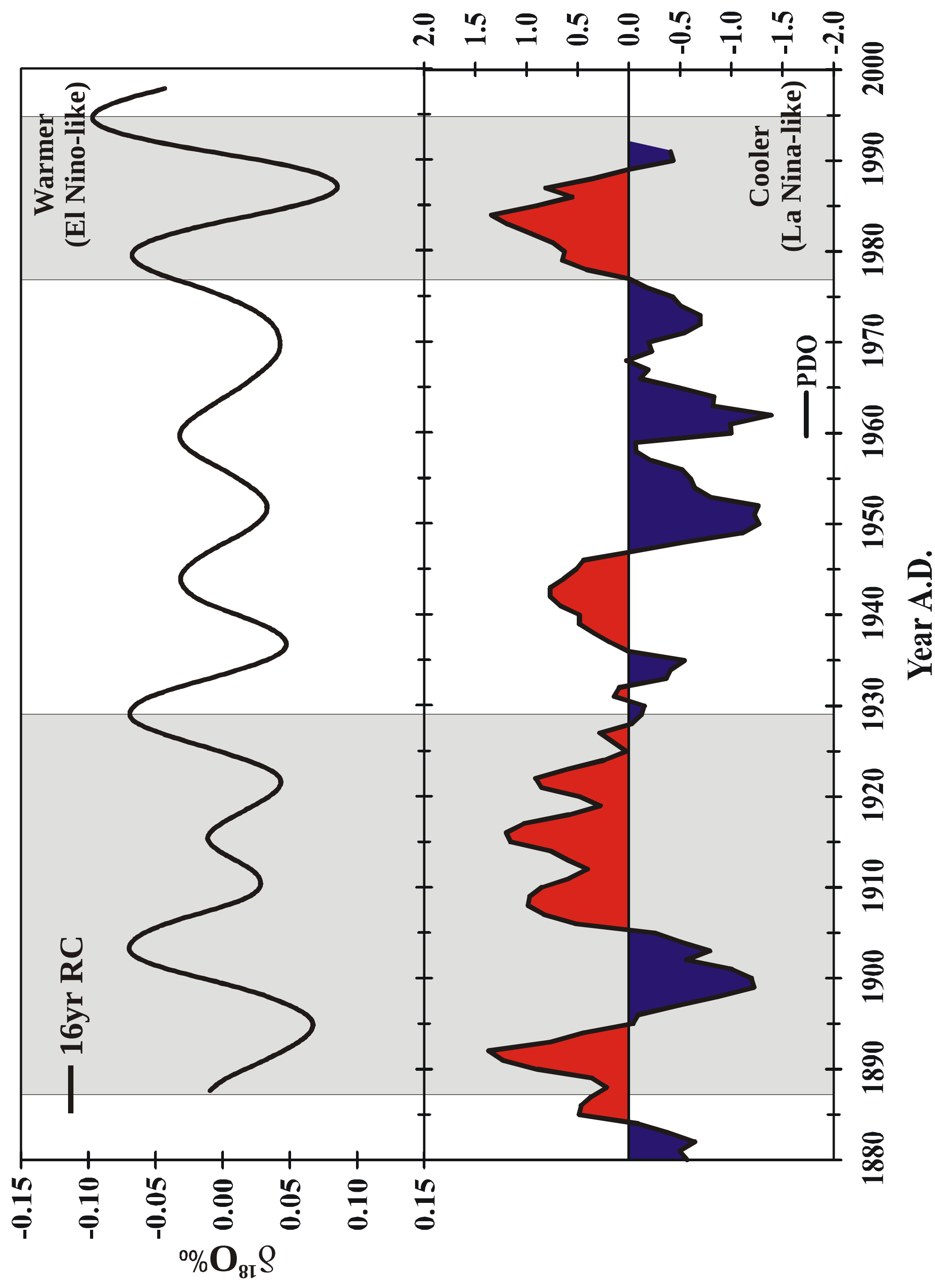

Figure 26. FI4 $\delta^{18}O$ 16yr component is plotted with the PDO (Mantua and Hare, 2002) to highlight decadal-scale shifts in the nature of ENSO. It is interesting to note that the FI4 $\delta^{18}O$ data is mostly out-of-phase with the PDO.

The QBO appears to capture the interannual features of ENSO, including the associated SST fluctuations (Rasmusson et al., 1990; Gray et al., 1992; Baldwin et al., 2001). The easterly (negative) phase of the QBO tends to be of higher intensity and longer duration than the westerly (positive) phase. The easterly phase has been shown to be linked to the warm phases of ENSO (El Niño) due to Pacific atmospheric circulation and pressure anomalies that are a result of QBO forcings on tropical deep convection about the equator (Gray et al., 1992; Baldwin et al., 2001). El Niño events usually begin between January and July, intensify during the Northern Hemisphere fall, and reach maximum anomaly values during the following Northern Hemisphere winter. Researchers have found a similar seasonal bias in QBO phase reversals – wind anomalies tend to turn easterly from April to July. During the beginning of an El Niño, if the onset of an easterly QBO phase coincides with a negative phase SO (high surface pressure at Darwin, low surface pressure at Tahiti), there is the potential for an ENSO warm event. However, the heat energy in the WPWP must be sufficient in order for eastward propagation of equatorial deep convection to begin. If all these factors coincide, it will be followed by an El Niño (Gray et al., 1992).

Figure 27 shows the relationship between the QBO and FI4 *Montipora venosa* $\delta^{18}O$ 2yr component as well as the CAC SST 2yr component. The climatic characteristics seen during an El Niño event, such as an increase of SST and PPT over the central and eastern tropical Pacific, are characteristic of an easterly phase of the QBO. Temperature, wind, and thus rain are closely related in a rotating atmosphere such as Earth's, and this can be clearly seen in the FI4 time series as well as in instrumental records.

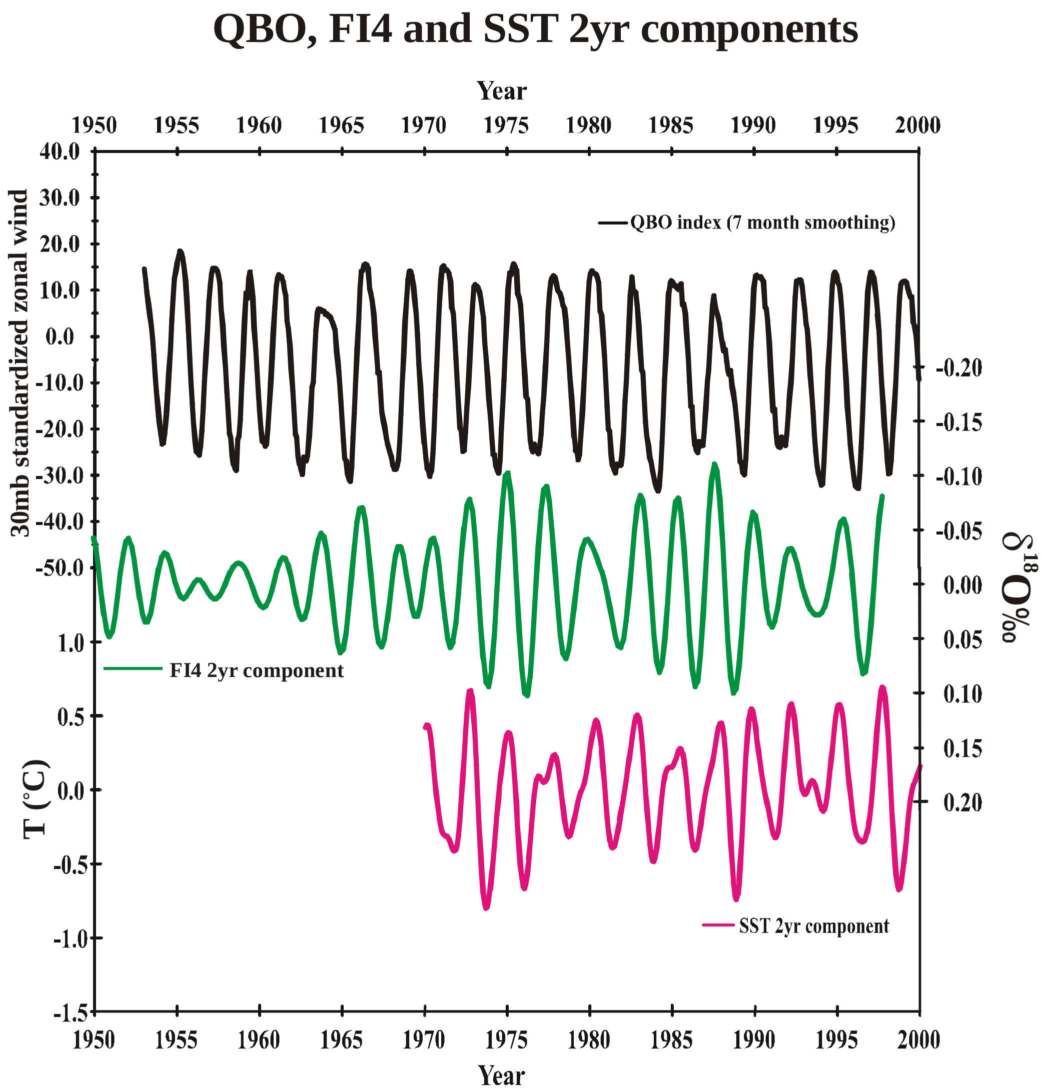

Figure 27. The QBO Index is combination of 30 hPa zonal wind (m/s) data from Canton Island (3ºS, 172ºW; Jan. 1953-Aug. 1967), Maldives (1ºS, 73ºE; Sept. 1967-Dec. 1975), and Singapore (1ºN, 104ºE; Jan. 1976-Sept. 2001) (Naujokat, 1987; http://tao.atmos.washington.edu/data_sets/qbo/). It is presented here with 7 month smoothing to filter out the seasonal noise. The correlation of the QBO with the 2yr component of both FI4 $\delta^{18}O$ and SST are accentuated here.

Conclusions

The best way to understand and predict future climate change is to fully comprehend past climate variability. As global warming becomes a more prominent societal issue, the knowledge of paleoclimates becomes critical.

Corals have been proven to be reliable and consistent recorders of tropical climate during their lifetime (Cole and Fairbanks, 1990; Cole et al., 1992; Druffel, 1997; Evans et al., 1999; Urban et al., 2000; Cobb et al., 2001, 2003; Grottoli et al., 2003 among others). To date, the coral genus *Porites* has been the coral most commonly utilized to reconstruct tropical climates (e.g., Gagan et al., 1994; Boiseau et al., 1998; Cole et al., 2000; Linsley et al., 2000; Charles et al., 2003). Presented here is evidence that the previously unstudied coral *Montipora venosa* from Fanning Island in the central equatorial Pacific provides accurate and reproducible climate reconstructions. Despite the slower growth rate and difference in sampling regime, the FI4 *Montipora venosa* $\delta^{18}O$ time series correlates well with that of nearby core FI5 *Porites,* as well as with other *Porites* time series data from Maiana and Palmyra Islands. The *Montipora venosa* core also upholds the hypothesis that the central equatorial Pacific is the key location for studying ENSO events.

The trend towards lower $\delta^{18}O$ values (warmer water) seen in many tropical coral records (Evans et al., 1998; Guilderson and Schrag, 1998; Guilderson and Schrag, 1999; Urban et al., 2000; Cobb et al., 2001, 2003) is still controversial and needs to be further studied. The Cane et al. (1997) hypothesis of an increase in temperature gradient across the Pacific is not supported by comparison of the *Montipora venosa* data with cotal sites farther west (Maiana; Urban et al., 2000) or east (Galapagos; Dunbar et al., 1994). In fact, the FI4 $\delta^{18}O$ time series studied in conjunction with other equatorial Pacific corals suggests there has been no change in temperature gradient at all.

In order to fully appreciate the trend phenomenon seen after 1976, more corals of several different genera from across the equatorial Pacific need to be studied and a more complete picture of tropical paleoclimate put together.

References Cited

Alexander, M.A., Bladé, I., Newman, M., Lanzante, J.R., Lau, N.C., Scott, J.D., 2002, The atmospheric bridge: the influence of ENSO teleconnections on air-sea interaction over the global oceans, *Journal of Climate*, vol. 15, pp. 2205-2231.

Allison, N., Finch, A.F., Newville, M., Sutton, S.R., 2005, Strontium in coral aragonite: 3. Sr coordination and geochemistry in relation to skeletal architecture, *Geochimica et Cosmochimica Acta*, vol. 69, 10.1016/j.gca.2005.01.026.

Archer, D., Barber, D. Dunne, J., Flament, P., Gardner, W., Garside, C., Goyet C., Johnson, E., Kirchman, D., McPhaden, M., Newton, J., Peltzer, E., Welling, L., White, J., Yoder, J., Aiken, J., Balch, W., 1997, A meeting place of great ocean currents: Shipboard observations of a convergent front at 2ºN in the Pacific, *Deep-Sea Research Part II: Topical Studies in Oceanography*, vol. 44, pp. 1827-1849.

Bagnato, S., Linsley, B.K., Howe, S.S., 2004, Evaluating the use of the massive coral *Diploastrea heliopora* for paleoclimate reconstruction, *Paleoceanography*, vol. 19, pp. 1-12.

Baldwin, M.P., Gray, L.J., Dunkerton, T.J., Hamilton, K., Haynes, P.H., Randel, W.J., Holton, J.R., Alexander, M.J., Hirota, I., Horinouchi, T., Jones, D.B.A., Kinnersley, J.S., Marquardt, C., Sato, K., Takahashi, M., 2001, The Quasi-Biennial Oscillation, *Reviews of Geophysics*, vol. 39, no. 2, pp. 179-229.

Barnston, A.G., Chelliah, M., 1997, Documentation of a highly ENSO-related SST region in the equatorial Pacific, *Atmosphere-Ocean*, vol. 35, pp. 367-383.

Battisti, D.S., 1988, Dynamics and thermodynamics of a warming event in a coupled tropical atmosphere-ocean model, *Journal of the Atmospheric Sciences*, vol. 45, pp. 2889-2919.

Battisti, D.S., Hirst, A.C., Interannual variability in a tropical atmosphere-ocean model: influence of the basic state, ocean geometry, and non-linearity, *Journal of the Atmospheric Sciences*, vol. 46, pp. 1687-1712.

Beck, J.W., Edwards, R.L., Ito, E., Taylor, F.W., Recy, J., Rougerie, F., Joannot, P., Henin, C., 1992, Sea-surface temperature from coral skeletal strontium/calcium ratios, *Science*, vol. 257, pp. 644-647.

Boiseau, M., Juillet-Leclerc, A., Yiou, P., Salvat, B., Isdale, P., Guillame, M., 1998, Atmospheric and oceanic evidences of El Nino-Southern Oscillation events in the south central Pacific Ocean from coral stable isotopic records over the last 137 years, *Paleoceanography*, vol. 13, pp. 671-685.

Cane, M.A., Pozdnyakov, D., Seager, R., Zebiack, S.E., Murtugudde, R., Clement, A.C., Kaplan, A., Kushnir, Y., 1997, Twentieth-century sea surface temperature trends, *Science*, vol. 275, pp. 957-960.

Chave, K.E., Gallagher, B.S., Gonzalez, Jr., F.I., Gordon, Jr., D.C., Krasnick, G.J., Maragos, J.E., Roy, K.J., Schiesser, H.G., Shepherd, G.L., Shimada, K.M., Smith, S.V., Stroup, E.D., DeWreede, R., Doty, M.S., Fournier, R.O., Chave, E.H., Gosline, W.A., Guinther, E.B., Wass, R.C., Kay, E.A., Banner, D.M., Randall, H.A., 1970, Fanning Island expedition, *Hawaii Institute of Geophysics*, report for the National Science Foundation, pp. 201.

Chiswell, S.M., Donahue, K.A., Wimbush, M., 1995, Variability in the central equatorial Pacific 1985-1989, *Journal of Geophysical Research*, vol. 100, pp. 15,849-15,863.

Cobb, K.M., Charles, C.D., Hunter, D.E., 2001, A central tropical Pacific coral demonstrates Pacific, Indian, and Atlantic decadal climate connections, *Geophysical Research Letters*, vol. 28, pp. 2209-2212.

Cobb, K.M., Charles, C.D., Cheng, H., Edwards, R.L., 2003, El Nino/Southern Oscillation and tropical Pacific climate during the last millennium, *Nature*, vol. 424, pp. 271-276.

Cohen, A.L., Layne, G.D., Hart, S.R., Lobel, P.S., 2001, Kinetic control of skeletal Sr/Ca in a symbiotic coral: implications for the paleotemperature proxy, *Paleoceanography*, vol. 16, pp. 20-26.

Cole, J.E., Fairbanks, R.G., 1990, The Southern Oscillation recorded in the $\delta^{18}O$ of corals from Tarawa Atoll, *Paleoceanography*, vol. 5, pp. 669-683.

Cole, J.E., Shen, G.T., Fairbanks, R.G., Moore, M., 1992, Coral monitors of El Nino/Southern Oscillation dynamics across the equatorial Pacific, in *El Nino: Historical and Paleoclimate Aspects of the Southern Oscillation*, Diaz, H., Markgraf, V., Cambridge University Press: UK, 1992, pp.349.

Cole, J.E., Fairbanks, R.G., Shen, G.T., 1993, Recent variability in the Southern Oscillation: Isotopic results from a Tarawa Atoll coral, *Science*, vol. 260, pp. 1790-1793.

Cole, J.E., Dunbar, R.B., McClanahan, T.R., Muthiga, N.A., 2000, Tropical Pacific forcing of decadal SST variability in the western Indian Ocean over the past two centuries, *Science*, vol. 287, pp. 617-619.

Delcroix, T., Hénin, C., 1991, Seasonal and interannual variations of sea surface salinity in the tropical Pacific Ocean, *Journal of Geophysical Research*, vol. 96, pp. 22,135-22,150.

Delcroix, T., Picaut, J., 1998, Zonal displacement of the western equatorial Pacific "fresh pool", *Journal of Geophysical Research*, vol. 103, C1, pp. 1087-1098

Diaz, H.F., Kiladis, G.N., 1992, Atmospheric teleconnections associated with the extreme phases of the Southern Oscillation, in *El Nino: Historical and Paleoclimate Aspects of the Southern Oscillation*, Diaz, H., Markgraf, V., Cambridge University Press: UK, 1992, pp. 349.

Diaz, H.F., Pulwarty, R.S., 1992, A comparison of Southern Oscillation and El Nino signals in the tropics, in *El Nino: Historical and Paleoclimate Aspects of the Southern Oscillation*, Diaz, H., Markgraf, V., Cambridge University Press: UK, 1992, pp. 349.

Draschba, S., Pätzold, J., Wefer, G., 2000, North Atlantic climate variability since AD 1350 recorded in $\delta^{18}O$ and skeletal density of Bermuda corals, *International Journal of Earth Sciences*, vol. 88, pp. 733-741.

Druffel, E.R.M., 1997, Geochemistry of corals: Proxies of past ocean chemistry, ocean circulation, and climate, *Proceedings of the National Academy of Sciences*, vol. 94, pp. 8354-8361.

Dunbar, R.B., Wellington, G.M., Colgan, M.W., Glynn, P.W., 1994, Eastern Pacific sea surface temperatures since 1600 A.D.: the $\delta^{18}O$ record of climate variability in Galapagos corals, *Paleoceanography*, vol. 9, pp. 291-315.

Enfield, D.B., 1992, Historical and prehistorical overview of El Nino/Southern Oscillation, in *El Nino: Historical and Paleoclimate Aspects of the Southern Oscillation*, Diaz, H., Markgraf, V., Cambridge University Press: UK, 1992, pp. 349.

Epstein, S.R., Buchsbaum, R., Lowenstam, H.A., Urey, H.C., 1953, Revised carbonate-water isotopic temperature scale, *Bulletin of the Geological Society of America*, vol. 64, pp. 1315-1326.

Evans, M.N., Fairbanks, R.G., Rubenstone, J.L., 1999, The thermal oceanographic signal of El Niño reconstructed from a Kiritimati Island coral, *Journal of Geophysical Research*, vol. 104, C6, pp. 13,409-13,421.

Fairbanks, R.G., Evans, M.N., Rubenstone, J.L., Mortlock, R.A., Broad, K., Moore, M.D., Charles, C.D., 1997, Evaluating climate indices and their geochemical proxies measured in corals, *Coral Reefs*, pp. 93-100.

Fu, C., Diaz, H.F., Fletcher, J.O., 1986, Characteristics of the response of sea surface temperature in the central Pacific associated with warm episodes of the Southern Oscillation, *Monthly Weather Review*, vol. 114, pp. 1716-1738.

Gagan, M.K., Chivas, A.R., Isdale, P.J., 1994, High-resolution isotopic records from corals using ocean temperature and mass-spawning chronometers, *Earth and Planetary Science Letters*, vol. 121, pp. 549-558.

Gagan, M.K., Ayliffe, L.K., Beck, J.W., Druffel, E.R.M., Dunbar, R.B., Schrag, D.P., 2000, New views of tropical paleoclimates from corals, *Quaternary Science Reviews*, vol. 19, pp. 45-64.

Gouriou, Y., Delcroix, T., 2002, Seasonal and ENSO variations of sea surface salinity and temperature in the South Pacific Convergence Zone during 1976-2000, *Journal of Geophysical Research*, vol. 107, C12, 8011, doi:10.1029/2001JC000830.

Graham, N.E., Barnett, T.P., 1995, ENSO and ENSO-related predictability. Part II: Northern hemisphere 700-mb height predictions based on a hybrid coupled ENSO model, *Journal of Climate*, vol. 8, pp. 544-549.

Gray, W.M., Sheaffer, J.D., Knaff, J.A., 1992, Hypothesized mechanism for stratospheric QBO influence on ENSO variability, *Geophysical Research Letters*, vol. 19, pp. 107-110.

Gray, W.M., Sheaffer, J.D., Knaff, J.A., 1992, Influence of the stratospheric QBO on ENSO variability, *Journal of the Meteorological Society of Japan*, vol. 70, pp. 975-995.

Grottoli, A.G., 2000, Stable carbon isotopes ($\delta^{13}C$) in coral skeletons, *Oceanography*, vol. 13, pp. 93-97.

Grottoli, A.G., Gille, S.T., Druffel, E.R.M., Dunbar, R.D.B., 2003, Decadal timescale shift in a central equatorial Pacific coral radiocarbon record, *Radiocarbon*, vol. 45, no. 1, pp. 91-99.

Guilderson, T.P., Schrag, D.P., 1998, Abrupt shift in subsurface temperatures in the tropical Pacific associated with changes in El Niño, *Science*, vol. 281, pp. 240-243.

Guilderson, T.P., Schrag, D.P., 1999, Reliability of coral isotope records from the western Pacific warm pool: a comparison using age-optimized records, *Paleoceanography*, vol. 14, pp. 457-464.

Haug, G.H., Hughen, K.A., Sigman, D.M., Peterson, L.C., Rohl, U., 2001, Southward migration of the Intertropical Convergence Zone though the Holocene, *Science*, vol. 293, pp. 1304-1308.

Heikoop, J.M., Dunn, J.J., Risk, M.J., Schwarcz, H.P., McConnaughey, T.A., Sandeman, I.M., 2000, Separation of kinetic and metabolic isotope effects in carbon-13 records preserved in reef coral skeletons, *Geochimica et Cosmochimica Acta*, vol. 64, pp. 975-987.

Highsmith, R.C., 1979, Coral growth rates and environmental control of density banding, *Journal of Experimental Marine Biology and Ecology*, vol. 37, pp. 105-125.

Hönisch, B., Hemming, N.G., Grottoli, A.G., Amat, A., Hanson, G.N., Bijma, J., 2004, Assessing scleractinian corals as recorders for paleo-pH: empirical calibration and vital effects, *Geochimica et Cosmochimica Acta*, vol. 68, 10.1016/j.gca.2004.03.002.

Horii, T., Hanawa, K., 2004, A relationship between timing of El Niño onset and subsequent evolution, *Geophysical Research Letters*, vol. 31, 10.1029/2003GL019239.

Kaplan, A., Cane, M.A., Kushnir, Y., Clement, A.C., Blumenthal, M.B., Rajagopalan, B., 1998, Analyses of global sea surface temperature 1856-1991, *Journal of Geophysical Research*, vol. 103, pp. 18,567-18,589.

Knutson, D.W., Buddemeier, R.W., Smith, S.V., 1972, Coral chronometers: seasonal growth bands in reef corals, *Science*, vol. 177, pp. 270-272.

Labitzke, K., Van Loon, H., 1995, *The stratosphere: phenomena, history, and relevance*, Springer, pp. 179.

Land, S., Lang, J.C., Barnes, D.J., 1975, Extension rate: A primary control on the isotopic composition of West Indian (Jamaican) scleractinian reef coral skeletons, *Marine Biology*, vol. 33, pp. 221-233.

Leder, J.J., Swart, P.K., Szmant, A.M., Dodge, R.E., 1996, The origins of variations in the isotopic record of scleractinian corals: I. Oxygen, *Geochimica et Cosmochimica Acta*, vol. 60, pp. 2857-2870.

Linsley, B.K., Dunbar, R.B., Wellington, G.M., Mucciarone, D.A., 1994, A coral-based reconstruction of Intertropical Convergence Zone variability over Central America since 1707, *Journal of Geophysical Review*, vol. 99, pp. 9977-9994.

Linsley, B.K., Messier, R.G., Dunbar, R.B., 1999, Assessing between-colony oxygen isotope variability in the coral *Porites lobata* at Clipperton Atoll, *Coral Reefs*, vol. 18, pp. 13-27.

Linsley, B.K., Ren, L., Dunbar, R.B., Howe, S.S., 2000, El Nino Southern Oscillation (ENSO) and decadal-scale climate variability at 10ºN in the eastern Pacific from 1893-1994: A coral-based reconstruction from Clipperton Atoll, *Paleoceanography*, vol. 15, pp. 322-335.

Linsley, B.K., Wellington, G.M., Schrag, D.P., 2000, Decadal sea surface temperature variability in the subtropical south Pacific from 1726-1997 A.D., *Science*, vol. 290, pp. 1145-1148.

Lough, J.M., Barnes, D.J., 1997, Several centuries of variation in skeletal extension, density and calcification in massive *Porites* colonies from the Great Barrier Reef: a proxy for seawater temperature and a background of variability against which to identify unnatural change, *Journal of Experimental Marine Biology and Ecology*, vol. 211, pp. 29-67.

Lough, J.M., Barnes, D.J., 2000, Environmental controls on the growth of the massive coral *Porites*, *Journal of Experimental Marine Biology and Ecology*, vol. 245, pp. 225-243.

Lough, J.M., 2004, A strategy to improve the contribution of coral data to high-resolution paleoclimatology, *Palaeogeography, Palaeoclimatology, Palaeoecology*, vol. 204, pp. 115-143.

Mantua, N.J., Hare, S.R., 2002, The Pacific Decadal Oscillation, *Journal of Oceanography*, vol. 58, pp. 35-44.

Marshall, J.F., McCulloch, M.T., 2002, An assessment of the Sr/Ca ratio in shallow water hermatypic corals as a proxy for sea surface temperature, *Geochimica et Cosmochimica Acta*, vol. 66, pp. 3263-3280.

McConnaughey, T., 1989, ^{13}C and ^{18}O isotopic disequilibrium in biological carbonates: I. Patterns, *Geochimica et Cosmochimica Acta*, vol. 53, pp. 151-162.

McConnaughey, T., 1989, ^{13}C and ^{18}O isotopic disequilibrium in biological carbonates: II. *In vitro* simulation of kinetic isotope effects, *Geochimica et Cosmochimica Acta*, vol. 53, pp. 163-171.

McGauley, M., Zhang, C., Bond, N.A., 2004, Large-scale characteristics of the atmospheric boundary layer in the eastern Pacific cold tongue-ITCZ region, *Journal of Climate*, vol. 17, pp. 3907-3920.

McPhaden, M.J., Picuat, J., 1990, El Niño-Southern Oscillation displacements of the western equatorial Pacific warm pool, *Science*, vol. 250, pp. 1385-1388.

Muller, A., Gagan, M.K., McCulloch, M.T., 2001, Early marine diagenesis in corals and geochemical consequences for paleoceanographic reconstructions, *Geophysical Research Letters*, vol., 28, pp., 4471-4474.

Müller, A., Gaga, M.K., Lough, J.M., 2004, Effect of early marine diagenesis on coral reconstructions of surface-ocean $^{13}C/^{12}C$ and carbonate saturation state, *Global Biogeochemical Cycles*, vol. 18, GB1033, doi: 10.1029/2003GB002112.

Naujokat, Barbara, 1986, An update of the observed quasi-biennial oscillation of the stratospheric winds over the tropics, *Journal of the Atmospheric Sciences*, vol. 43, no. 17, pp. 1873-1877.

Picaut, J., Delcroix, T., 1995, Equatorial wave sequence associated with warm pool displacements during the 1986-1989 El Niño-La Niña, *Journal of Geophysical Research*, vol. 100, C9, pp. 18,393-18,408.

Picaut, J., Ioualalen, M., Menkes, C., Delcroix, T., McPhaden, M.J., 1996, Mechanism of the zonal displacements of the Pacific warm pool: Implications for ENSO, *Science*, vol. 274, pp. 1486-1489.

Picaut, J., Masia, F., du Penhoat, Y., 1997, An advective-reflective conceptual model for the oscillatory nature of the ENSO, *Science*, vol. 277, pp. 663-666.

Picaut, J., Ioualalen, M., Delcroix, T., Masia, F., Murtugudde, R., Vialard, J., The oceanic zone of convergence on the eastern edge of the Pacific warm pool: A synthesis of results and implications for El Niño-Southern Oscillation and biogeochemical phenomena, *Journal of Geophysical Research*, vol. 106, C2, pp. 2363-2386.

Philander, G.S., 1990, *El Niño, La Niña, and the Southern Oscillation*, Academic Press, Inc., pp. 291.

Reynolds, R.W., Smith, T.M., 1994, A high resolution global sea surface temperature climatology, *Journal of Climate*, vol. 7

Rimbu, N., Lohmann, G., Felis, T., Pätzold, J., 2003, Shift in ENSO teleconnections recorded by a Northern Red Sea coral, *Journal of Climate*, vol. 16, pp. 1414-1422.

Serra, Y.L., Houze Jr., R.A., 2002, Observations of variability on synoptic timescales in the east Pacific ITCZ, *Journal of the Atmospheric Sciences*, vol. 59, pp. 1723-1743.

Shen, G.T., Cole, J.E., Lea, D.W., Linn, L.J., McConnaughey, T.A., Fairbanks, R.G., 1992, Surface ocean variability at Galapagos from 1936-1982: Calibration of geochemical tracers in corals, *Paleoceanography*, vol. 7, pp. 563-588.

Suarez, M.J., Schopf, P.S., 1988, A delayed action oscillator for ENSO, *Journal of the Atmospheric Sciences*, vol. 45, pp. 3283-3287.

Sun, Y., Sun, M., Lee, T., Nie, B., 2005, Influence of seawater Sr content on coral Sr/Ca and Sr thermometry, *Coral Reefs*, vol. 24, pp. 23-29.

Taft, B.A., Kessler, W.S., 1991, Variations of zonal currents in the central tropical Pacific during 1970 to 1987: sea level and dynamic height measurements, *Journal of Geophysical Research*, vol. 96, pp. 12,599-12,618.

Trenberth, K.E., Shea, D.J., 1987, On the evolution of the Southern Oscillation, *Monthly Weather Review*, vol. 115, pp. 3078-3096.

Urban, F.E., Cole, J.E., Overpeck, J.T., 2000, Influence of mean climate change on climate variability from a 155-year tropical Pacific coral record, *Nature*, vol. 407, pp. 989-993.

Van Loon, H., Labitzke, K., 1987, The Southern Oscillation. Part V: the anomalies in the lower stratosphere of the northern hemisphere in winter and a comparison with the Quasi-biennial Oscillation, *Monthly Weather Review*, vol. 115, pp. 357-369.

Vautard, R., Ghil, M., 1989, Singular spectrum analysis in nonlinear dymanics, with applications to paleoclimatic time series, *Physica D*, vol. 35, pp. 395-424.

Vautard, R., Yiou, P., Ghil, M., 1992, Singular-spectrum analysis: a toolkit for short, noisy chaotic signals, *Physica D*, vol. 58, pp. 95-126.

Wallace, J.M., Chang, F-C., 1982, Interannual variability of the wintertime polar vortex in the northern hemisphere middle stratosphere, *Journal of the Meteorological Society of Japan*, vol. 60, pp. 149-155.

Watanabe, T., Gagan, M.K., Correge, T., Scott-Gagan, H., Cowley, J., Hantoro, W.S., 2003, Oxygen isotope systematics in *Diploastrea heliopora*: New coral archive of tropical paleoclimate, *Geochimica et Cosmochimica Acta*, vol. 67, pp. 1349-1358.

Weber, J.N., Woodhead, P.M.J., 1970, C and O isotope fractionation in the skeletal carbonate of reef-building corals, *Chemical Geology*, vol. 6, pp. 93-117.

Weber, J.N., Woodhead, P.M.J., 1972, Temperature dependence of oxygen-18 concentration in reef coral carbonates, *Journal of Geophysical Research*, vol. 77, pp. 463-473.

Weber, J.N., 1973, Incorporation of strontium into reef coral skeletal carbonate, *Geochimica et Cosmochimica Acta*, vol. 37, pp. 2173-2190.

APPENDIX

Depth (mm)	Year A.D.	$\delta^{13}C$ (‰)	$\delta^{18}O$ (‰)	Rep. δ13C	Rep. Diff.	Rep. δ18O	Rep. Diff.
1	1997.79	-1.170	-5.065				
2	1997.64	-0.836	-4.995				
3	1997.59	-0.505	-4.788	-0.530, '-0.480	0.050	-4.817, '-4.759	0.058
4	1997.54	-0.402	-4.760				
5	1997.29	-0.926	-4.964				
6	1997.04	-0.935	-4.769				
7	1996.79	-0.610	-4.620				
8	1996.54	-0.469	-4.560				
9	1996.40	-0.562	-4.623				
10	1996.26	-0.819	-4.683				
11	1996.11	-1.070	-4.650	-1.224, '-0.915	0.309	-4.584, '-4.715	0.131
12	1995.97	-1.161	-4.756				
13	1995.83	-1.048	-4.852				
14	1995.68	-0.603	-4.761				
15	1995.54	-0.502	-4.786				
16	1995.34	-0.515	-4.861				
17	1995.14	-1.191	-5.105				
18	1994.94	-0.806	-4.849				
19	1994.74	-0.592	-4.853	-0.638, '-0.545	0.093	-4.909, '-4.797	0.112
20	1994.54	-0.404	-4.778				
21	1994.37	-0.737	-4.769				
22	1994.21	-1.055	-5.069				
23	1994.04	-1.012	-5.001				
24	1993.87	-1.032	-4.829				
25	1993.71	-1.184	-5.046				
26	1993.54	-0.930	-4.909				
27	1993.40	-0.975	-4.882	-1.109, '-0.840	0.269	-4.977, '-4.787	0.190
28	1993.26	-0.942	-4.901				
29	1993.11	-0.881	-4.933				
30	1992.97	-0.903	-4.825				
31	1992.83	-0.741	-4.797				
32	1992.68	-0.786	-4.799				
33	1992.54	-0.626	-4.936	-0.638, '-0.613	0.025	-4.930, '-4.942	0.012
34	1992.37	-0.765	-4.969				
35	1992.21	-1.182	-5.014				
36	1992.04	-1.635	-5.273				
37	1991.92	-1.132	-5.135				
38	1991.79	-0.912	-4.873				
39	1991.67	-0.731	-4.859				
40	1991.54	-0.621	-4.862				
41	1991.40	-0.845	-4.848	-0.908, '-0.781	0.127	-4.844, '-4.851	0.007
42	1991.26	-0.847	-4.848				
43	1991.11	-1.132	-4.820				
44	1990.97	-0.853	-4.755				
45	1990.83	-0.979	-4.915				
46	1990.68	-0.870	-4.606				
47	1990.54	-0.713	-4.805				
48	1990.34	-0.968	-4.596				

49	1990.14	-0.869	-4.622	-0.857, '-0.880	0.023	-4.610, '-4.634	0.024
50	1989.94	-0.908	-4.407				
51	1989.74	-0.301	-4.754				
52	1989.54	0.138	-4.338				
53	1989.34	-0.048	-4.236				
54	1989.14	-0.569	-4.400				
55	1988.94	-0.654	-4.500				
56	1988.74	-0.256	-4.145				
57	1988.54	0.071	-4.153	0.207, '-0.066	0.141	-4.134, '-4.171	0.037
58	1988.26	-0.438	-4.540				
59	1987.99	-0.663	-4.871				
60	1987.71	-0.758	-5.010				
61	1987.62	-0.427	-4.689				
62	1987.54	-0.262	-4.750				
63	1987.34	-0.607	-4.635	-0.547, '-0.667	0.120	-4.604, '-4.665	0.061
64	1987.14	-0.591	-4.689				
65	1986.94	-0.201	-4.556				
66	1986.74	-0.258	-4.439				
67	1986.54	-0.004	-4.492				
68	1986.40	-0.500	-4.510				
69	1986.26	-0.697	-4.597				
70	1986.11	-0.604	-4.388				
71	1985.97	-0.445	-4.464	-0.417, '-0.473	0.056	-4.431, '-4.496	0.065
72	1985.83	-0.256	-4.430				
73	1985.68	0.088	-4.264				
74	1985.54	0.318	-4.324				
75	1985.34	-0.732	-4.602				
76	1985.14	-0.681	-4.630				
77	1984.94	-0.720	-4.668				
78	1984.74	-0.195	-4.513				
79	1984.54	0.036	-4.439	0.114, '-0.042	0.156	-4.417, '-4.461	0.044
80	1984.34	-0.422	-4.581				
81	1984.14	-0.653	-4.583				
82	1983.94	-0.360	-4.768				
83	1983.74	-0.277	-4.693				
84	1983.54	-0.023	-4.901				
85	1983.04	-0.690	-4.945				
86	1982.87	-0.861	-4.897				
87	1982.71	-0.339	-4.758	-0.360, '-0.318	0.042	-4.841, '-4.674	0.167
88	1982.54	0.129	-4.625				
89	1982.34	-0.373	-4.581				
90	1982.14	-0.745	-4.576				
91	1981.94	-0.565	-4.713				
92	1981.74	-0.462	-4.591				
93	1981.54	-0.143	-4.442	-0.137, '-0.149	0.012	-4.505, '-4.378	0.127
94	1981.34	-0.574	-4.779				
95	1981.14	-0.711	-4.707				
96	1980.94	-0.789	-4.673				
97	1980.74	-0.398	-4.623				
98	1980.54	-0.078	-4.650				

99	1980.40	-0.198	-4.793				
100	1980.26	-0.631	-4.864				
101	1980.11	-0.731	-4.874	-0.600, '-0.862	0.262	-4.827, '-4.920	0.093
102	1979.97	-0.929	-4.873				
103	1979.83	-0.825	-4.827				
104	1979.68	-0.264	-4.581				
105	1979.54	0.038	-4.721				
106	1979.29	-0.653	-4.780				
107	1979.04	-0.568	-4.782				
108	1978.79	-0.214	-4.616				
109	1978.54	0.193	-4.657	0.251, 0.135	0.116	-4.605, '-4.708	0.103
110	1978.34	-0.510	-4.977				
111	1978.14	-0.724	-4.659				
112	1977.94	-0.568	-4.885				
113	1977.74	-0.069	-4.818				
114	1977.54	0.071	-4.762				
115	1977.29	-0.297	-4.821				
116	1977.04	-0.517	-4.896				
117	1976.79	-0.765	-4.859	-0.723, '-0.806	0.083	-4.845, '-4.872	0.027
118	1976.71	-0.609	-4.934				
119	1976.62	-0.417	-4.762				
120	1976.54	-0.148	-4.275				
121	1976.34	-0.388	-4.375				
122	1976.14	-0.163	-4.255				
123	1975.94	-0.328	-4.382	-0.267, '-0.388	0.121	-4.408, '-4.356	0.052
124	1975.74	-0.174	-4.504				
125	1975.54	0.071	-4.461				
126	1975.37	-0.702	-4.696				
127	1975.21	-0.818	-4.599				
128	1975.04	-0.789	-4.606				
129	1974.87	-0.387	-4.418				
130	1974.71	-0.595	-4.634				
131	1974.54	-0.244	-4.494	-0.244, '-0.243	0.001	-4.554, '-4.434	0.120
132	1974.34	-0.465	-4.523				
133	1974.14	-0.553	-4.480				
134	1973.94	-0.539	-4.376				
135	1973.74	-0.223	-4.457				
136	1973.54	0.059	-4.453				
137	1973.21	0.085	-4.789				
138	1972.88	-0.406	-4.940				
139	1972.71	-0.019	-4.618	0.053, '-0.090	0.037	-4.580, '-4.656	0.076
140	1972.54	-0.067	-4.478				
141	1972.14	-0.474	-4.467				
142	1971.74	-0.441	-4.613				
143	1971.34	0.113	-4.437				
144	1970.94	0.364	-4.577				
145	1970.54	0.503	-4.609				
146	1970.29	0.122	-4.380				
147	1970.04	-0.112	-4.622	-0.110, '-0.113	0.003	-4.605, '-4.639	0.034
148	1969.79	0.371	-4.471				

149	1969.54	0.420	-4.476				
150	1969.37	-0.142	-4.684				
151	1969.21	-0.288	-4.538				
152	1969.04	-0.025	-4.380				
153	1968.87	0.269	-4.397	0.234, 0.303	0.069	-4.366, '-4.427	0.061
154	1968.71	0.288	-4.443				
155	1968.54	0.452	-4.306				
156	1968.34	0.073	-4.663				
157	1968.14	-0.104	-4.189				
158	1967.94	0.005	-4.484				
159	1967.74	0.282	-4.444				
160	1967.54	0.581	-4.452				
161	1967.29	0.034	-4.493	0.059, 0.008	0.051	-4.431, '-4.555	0.124
162	1967.04	-0.124	-4.622				
163	1966.79	0.125	-4.438				
164	1966.54	0.405	-4.452				
165	1965.96	-0.173	-4.841				
166	1965.82	-0.282	-4.711				
167	1965.68	-0.079	-4.625				
168	1965.54	0.230	-4.474				
169	1965.29	-0.057	-4.367	-0.169, 0.056	0.113	-4.348, '-4.385	0.037
170	1965.04	-0.098	-4.493				
171	1964.79	0.079	-4.370				
172	1964.54	0.158	-4.359				
173	1964.04	-0.046	-4.705				
174	1963.94	-0.312	-4.770				
175	1963.84	-0.469	-4.760				
176	1963.74	-0.286	-4.731				
177	1963.64	-0.179	-4.674	-0.207, '-0.151	0.056	-4.598, '-4.749	0.151
178	1963.54	0.000	-4.458				
179	1963.29	-0.306	-4.597				
180	1963.04	-0.352	-4.472				
181	1962.79	-0.167	-4.517				
182	1962.54	0.209	-4.530				
183	1962.40	-0.070	-4.613	-0.051, '-0.088	0.037	-4.526, '-4.699	0.173
184	1962.26	-0.360	-4.569				
185	1962.11	-0.381	-4.485				
186	1961.97	0.132	-4.365				
187	1961.83	0.294	-4.399				
188	1961.68	0.395	-4.570				
189	1961.54	0.524	-4.465				
190	1961.34	-0.004	-4.549				
191	1961.14	-0.032	-4.484	0.006, '-0.069	0.063	-4.481, '-4.487	0.006
192	1960.94	-0.046	-4.411				
193	1960.74	0.283	-4.504				
194	1960.54	0.529	-4.600				
195	1960.29	0.266	-4.557				
196	1960.04	-0.160	-4.639				
197	1959.79	-0.022	-4.675				
198	1959.54	0.113	-4.587				

199	1959.37	0.079	-4.726	0.123, 0.035	0.088	-4.628, '-4.824	0.196
200	1959.21	-0.092	-4.745				
201	1959.04	-0.210	-4.576				
202	1958.87	-0.321	-4.699				
203	1958.71	-0.213	-4.764				
204	1958.54	0.177	-4.729				
205	1958.37	0.063	-4.684				
206	1958.21	-0.511	-4.673				
207	1958.04	-0.935	-4.657	-1.072, '-0.798	0.274	-4.645, '-4.669	0.024
208	1957.87	-0.446	-4.679				
209	1957.71	-0.094	-4.681				
210	1957.54	-0.166	-4.706				
211	1957.37	0.040	-4.516				
212	1957.21	-0.274	-4.454				
213	1957.04	-0.221	-4.510	-0.116, '-0.325	0.209	-4.521, '-4.498	0.023
214	1956.87	-0.365	-4.607				
215	1956.71	-0.052	-4.391				
216	1956.54	0.346	-4.489				
217	1956.34	0.192	-4.556				
218	1956.14	-0.049	-4.439				
219	1955.94	-0.491	-4.474				
220	1955.74	-0.584	-4.364				
221	1955.54	0.334	-4.337	0.259, 0.409	0.150	-4.252, '-4.421	0.169
222	1955.40	-0.093	-4.559				
223	1955.26	0.054	-4.319				
224	1955.11	0.206	-4.413				
225	1954.97	0.141	-4.534				
226	1954.83	0.134	-4.585				
227	1954.68	0.159	-4.460				
228	1954.54	0.314	-4.522				
229	1954.29	-0.077	-4.641	-0.054, '-0.099	0.045	-4.725, '-4.557	0.168
230	1954.04	0.124	-4.695				
231	1953.79	0.392	-4.581				
232	1953.54	0.494	-4.504				
233	1953.37	-0.202	-4.574				
234	1953.21	-0.339	-4.442				
235	1953.04	-0.033	-4.444				
236	1952.87	-0.039	-4.536				
237	1952.71	0.265	-4.473	0.250, 0.280	0.030	-4.486, '-4.460	0.026
238	1952.54	0.359	-4.538				
239	1952.34	0.085	-4.552				
240	1952.14	-0.025	-4.440				
241	1951.94	0.183	-4.412				
242	1951.74	0.271	-4.507				
243	1951.54	0.385	-4.511	0.396, 0.374	0.022	-4.463, '-4.559	0.096
244	1951.37	0.236	-4.370				
245	1951.21	-0.443	-4.455				
246	1951.04	-0.312	-4.438				
247	1950.87	-0.027	-4.359				
248	1950.71	0.095	-4.342				

249	1950.54	0.113	-4.435				
250	1950.37	0.035	-4.495				
251	1950.21	-0.461	-4.437	-0.417, '-0.505	0.088	-4.393, '-4.481	0.088
252	1950.04	-0.476	-4.590				
253	1949.87	-0.238	-4.468				
254	1949.71	0.183	-4.497				
255	1949.54	0.607	-4.492				
256	1949.29	-0.058	-4.439				
257	1949.04	-0.269	-4.583				
258	1948.79	-0.202	-4.455				
259	1948.54	0.244	-4.550	0.269, 0.219	0.050	-4.499, '-4.600	0.101
260	1948.40	0.197	-4.549				
261	1948.26	0.172	-4.694				
262	1948.11	0.045	-4.676				
263	1947.97	-0.204	-4.638				
264	1947.83	-0.011	-4.689				
265	1947.68	-0.070	-4.722				
266	1947.54	0.327	-4.685				
267	1947.34	0.198	-4.757	0.245, 0.151	0.094	-4.741, '-4.772	0.031
268	1947.14	-0.078	-4.759				
269	1946.94	-0.035	-4.654				
270	1946.74	0.453	-4.527				
271	1946.54	0.552	-4.589				
272	1946.37	0.208	-4.425				
273	1946.21	-0.439	-4.519	-0.465, '-0.409	0.056	-4.553, '-4.484	0.069
274	1946.04	-0.112	-4.419				
275	1945.87	-0.130	-4.572				
276	1945.71	0.162	-4.536				
277	1945.54	0.273	-4.396				
278	1945.37	-0.188	-4.441				
279	1945.21	-0.228	-4.532				
280	1945.04	-0.358	-4.499				
281	1944.87	-0.118	-4.466	-0.130, '-0.106	0.024	-4.493, '-4.438	0.055
282	1944.71	-0.096	-4.442				
283	1944.54	0.367	-4.633				
284	1944.34	0.202	-4.366				
285	1944.14	0.035	-4.396				
286	1943.94	0.032	-4.572				
287	1943.74	0.185	-4.848				
288	1943.54	0.576	-4.473				
289	1943.34	0.462	-4.474	0.514, 0.409	0.105	-4.412, '-4.535	0.123
290	1943.14	-0.093	-4.563				
291	1942.94	-0.156	-4.566				
292	1942.74	0.012	-4.526				
293	1942.54	0.347	-4.481				
294	1942.29	0.357	-4.665				
295	1942.04	0.433	-4.800				
296	1941.79	0.195	-4.876				
297	1941.54	0.304	-4.733	0.279, 0.328	0.049	-4.716, '-4.749	0.033
298	1941.29	0.054	-4.879				

299	1941.04	-0.321	-4.844				
300	1940.92	-0.114	-4.689				
301	1940.79	0.071	-4.470				
302	1940.67	0.327	-4.443				
303	1940.54	0.403	-4.513	0.360, 0.446	0.086	-4.471, -4.555	0.084
304	1940.34	0.039	-4.663				
305	1940.14	-0.116	-4.504				
306	1939.94	0.076	-4.385				
307	1939.74	-0.121	-4.558				
308	1939.54	0.296	-4.473				
309	1939.40	0.277	-4.457				
310	1939.26	0.213	-4.417				
311	1939.11	-0.267	-4.532	-0.321, '-0.213	0.108	-4.615, '-4.448	0.167
312	1938.97	-0.002	-4.424				
313	1938.83	-0.142	-4.538				
314	1938.68	-0.074	-4.526				
315	1938.54	0.188	-4.307				
316	1938.34	0.163	-4.465				
317	1938.14	-0.114	-4.556				
318	1937.94	-0.354	-4.591				
319	1937.74	-0.024	-4.464	-0.009, '-0.038	0.029	-4.483, '-4.445	0.038
320	1937.54	0.090	-4.553				
321	1937.42	-0.155	-4.681				
322	1937.29	-0.253	-4.541				
323	1937.17	-0.069	-4.591				
324	1937.04	-0.189	-4.484				
325	1936.92	-0.160	-4.488				
326	1936.79	-0.226	-4.417				
327	1936.67	-0.354	-4.546	-0.272, '-0.436	0.164	-4.529, '-4.563	0.034
328	1936.54	0.192	-4.386				
329	1936.40	-0.117	-4.639				
330	1936.26	-0.077	-4.475				
331	1936.11	-0.020	-4.553				
332	1935.97	0.027	-4.080				
333	1935.83	-0.129	-4.406	-0.190, '-0.067	0.123	-4.438, '-4.374	0.064
334	1935.68	-0.369	-4.465				
335	1935.54	0.076	-4.397				
336	1935.43	-0.128	-4.348				
337	1935.32	0.255	-4.418				
338	1935.21	0.260	-4.479				
339	1935.10	-0.127	-4.392				
340	1934.99	-0.243	-4.457				
341	1934.87	-0.073	-4.185	-0.090, '-0.055	0.035	-4.190, '-4.179	0.011
342	1934.76	-0.080	-4.540				
343	1934.65	-0.012	-4.588				
344	1934.54	0.071	-4.523				
345	1934.42	-0.262	-4.766				
346	1934.29	-0.304	-4.457				
347	1934.17	-0.245	-4.483				
348	1934.04	-0.227	-4.464				

349	1933.92	-0.309	-4.549	-0.333, '-0.285	0.048	-4.530, '-4.568	0.038
350	1933.79	-0.224	-4.689				
351	1933.67	0.329	-4.591				
352	1933.54	0.519	-4.461				
353	1933.40	0.294	-4.428				
354	1933.26	-0.247	-4.567				
355	1933.11	-0.260	-4.650				
356	1932.97	-0.033	-4.286				
357	1932.83	-0.010	-4.541	-0.061, 0.041	0.020	-4.578, '-4.504	0.074
358	1932.68	0.343	-4.571				
359	1932.54	0.435	-4.588				
360	1932.21	0.152	-4.608				
361	1932.10	-0.018	-4.475				
362	1931.99	-0.308	-4.749				
363	1931.87	-0.135	-4.468	-0.218, '-0.052	0.166	-4.607, '-4.328	0.279
364	1931.79	-0.021	-4.696				
365	1931.65	0.320	-4.709				
366	1931.54	0.529	-4.618				
367	1930.88	-0.540	-5.141				
368	1930.71	-0.261	-5.056				
369	1930.54	-0.222	-4.795				
370	1930.45	-0.264	-4.833				
371	1930.36	-0.411	-4.894	-0.437, '-0.384	0.053	-4.827, '-4.960	0.133
372	1930.27	-0.362	-4.848				
373	1930.18	-0.527	-4.722				
374	1930.09	-0.571	-4.569				
375	1930.00	-0.597	-4.400				
376	1929.90	-0.461	-4.697				
377	1929.81	-0.229	-4.712				
378	1929.72	-0.270	-4.466				
379	1929.63	-0.010	-4.399	-0.028, 0.008	0.020	-4.397, '-4.401	0.004
380	1929.54	0.281	-4.374				
381	1929.29	0.111	-4.524				
382	1929.04	-0.106	-4.529				
383	1928.79	-0.128	-4.679				
384	1928.54	-0.376	-4.885				
385	1928.37	-0.118	-4.768				
386	1928.21	-0.218	-4.932				
387	1928.04	0.078	-4.698	0.010, 0.145	0.135	-4.746, '-4.649	0.097
388	1927.87	0.102	-4.806				
389	1927.71	-0.101	-4.606				
390	1927.54	-0.386	-4.622				
391	1927.42	-0.290	-4.563				
392	1927.29	-0.282	-4.560				
393	1927.17	-0.225	-4.578	-0.291, '-0.159	0.132	-4.643, '-4.513	0.130
394	1927.04	-0.033	-4.414				
395	1926.92	0.044	-4.518				
396	1926.79	-0.010	-4.445				
397	1926.67	0.144	-4.591				
398	1926.54	0.391	-4.557				

399	1926.25	0.303	-4.545				
400	1925.96	-0.226	-4.866				
401	1925.85	-0.277	-4.679	-0.335, '-0.218	0.117	-4.712, '-4.646	0.066
402	1925.75	-0.067	-4.478				
403	1925.65	-0.009	-4.576				
404	1925.54	0.139	-4.608				
405	1925.42	-0.088	-4.541				
406	1925.29	-0.189	-4.458				
407	1925.17	0.137	-4.349				
408	1925.04	-0.139	-4.332				
409	1924.92	-0.230	-4.490	-0.288, '-0.171	0.117	-4.438, '-4.541	0.103
410	1924.79	-0.044	-4.534				
411	1924.67	-0.020	-4.704				
412	1924.54	0.243	-4.416				
413	1924.37	0.039	-4.673				
414	1924.21	-0.395	-4.621				
415	1924.04	-0.482	-4.689				
416	1923.87	-0.042	-4.576				
417	1923.71	0.004	-4.597	0.022, '-0.014	0.008	-4.553, '-4.640	0.087
418	1923.54	0.064	-4.451				
419	1923.42	-0.500	-4.503				
420	1923.29	-0.317	-4.563				
421	1923.17	-0.302	-4.331				
422	1923.04	-0.309	-4.399				
423	1922.92	-0.708	-4.641	-0.694, '-0.721	0.027	-4.660, '-4.621	0.039
424	1922.79	-0.416	-4.468				
425	1922.67	-0.182	-4.353				
426	1922.54	-0.135	-4.252				
427	1922.37	-0.226	-4.429				
428	1922.21	-0.220	-4.508				
429	1922.04	0.031	-4.479				
430	1921.87	0.103	-4.561				
431	1921.71	-0.005	-4.645	0.053, '-0.063	0.010	-4.606, '-4.684	0.078
432	1921.54	0.119	-4.452				
433	1921.43	-0.183	-4.584				
434	1921.32	0.005	-4.436				
435	1921.21	0.168	-4.515				
436	1921.10	0.311	-4.639				
437	1920.99	0.316	-4.620				
438	1920.87	0.308	-4.577				
439	1920.76	-0.045	-4.611	-0.018, '-0.071	0.053	-4.640, '-4.581	0.059
440	1920.65	0.152	-4.479				
441	1920.54	0.240	-4.514				
442	1920.29	-0.076	-4.543				
443	1920.04	0.009	-4.556				
444	1919.79	0.372	-4.372				
445	1919.54	0.529	-4.351				
446	1919.42	0.029	-4.735				
447	1919.29	0.140	-4.521	0.128, 0.151	0.023	-4.554, '-4.487	0.067
448	1919.17	0.250	-4.430				

449	1919.04	0.133	-4.443				
450	1918.92	-0.168	-4.432				
451	1918.79	-0.299	-4.567				
452	1918.67	-0.046	-4.401				
453	1918.54	0.610	-3.913	0.608, 0.612	0.004	-3.925, '-3.901	0.024
454	1918.40	-0.016	-4.253				
455	1918.26	-0.506	-4.365				
456	1918.11	-0.332	-4.357				
457	1917.97	-0.119	-4.290				
458	1917.83	-0.070	-4.335				
459	1917.68	-0.198	-4.524				
460	1917.54	0.196	-4.157				
461	1917.37	-0.112	-4.297	-0.106, '-0.117	0.011	-4.290, '-4.304	0.014
462	1917.21	-0.280	-4.350				
463	1917.04	-0.167	-4.430				
464	1916.87	0.147	-4.241				
465	1916.71	0.194	-4.424				
466	1916.54	0.394	-4.458				
467	1916.40	0.099	-4.544				
468	1916.26	-0.004	-4.438				
469	1916.11	-0.434	-4.681	-0.513, '-0.354	0.159	-4.739, '-4.623	0.116
470	1915.97	-0.347	-4.669				
471	1915.83	-0.479	-4.724				
472	1915.68	-0.479	-5.403				
473	1915.54	0.400	-4.698				
474	1915.37	-0.517	-4.973				
475	1915.21	-0.262	-4.746				
476	1915.04	-0.248	-4.721				
477	1914.87	-0.128	-4.703	-0.075, '-0.180	0.105	-4.654, '-4.752	0.098
478	1914.71	0.080	-4.619				
479	1914.54	0.124	-4.605				
480	1914.34	0.038	-4.635				
481	1914.14	-0.076	-4.462				
482	1913.94	-0.213	-4.730				
483	1913.74	-0.466	-4.666	-0.435, '-0.496	0.061	-4.679, '-4.653	0.026
484	1913.54	0.034	-4.423				
485	1913.37	-0.265	-4.567				
486	1913.21	-0.181	-4.621				
487	1913.04	-0.008	-4.476				
488	1912.87	0.203	-4.430				
489	1912.71	0.411	-4.352				
490	1912.54	0.854	-4.049				
491	1912.44	0.518	-4.404	0.497, 0.539	0.042	-4.489, -4.318	0.171
492	1912.34	-0.171	-4.611				
493	1912.24	-0.137	-4.654				
494	1912.14	0.023	-4.573				
495	1912.04	-0.088	-4.716				
496	1911.87	0.079	-4.650				
497	1911.71	0.179	-4.418				
498	1911.54	0.437	-4.023				

499	1911.42	0.394	-4.123	0.441, 0.347	0.094	-4.046, '-4.200	0.154
500	1911.29	0.184	-4.214				
501	1911.17	-0.028	-4.409				
502	1911.04	-0.246	-4.720				
503	1910.92	-0.343	-4.655				
504	1910.79	-0.117	-4.537				
505	1910.67	0.024	-4.385				
506	1910.54	0.192	-4.339				
507	1910.29	0.037	-4.394	-0.006, 0.079	0.073	-4.465, '-4.323	0.142
508	1910.04	0.027	-4.534				
509	1909.79	0.237	-4.399				
510	1909.54	0.554	-4.181				
511	1909.37	0.451	-4.214				
512	1909.21	0.354	-4.441				
513	1909.04	0.474	-4.016	0.541, 0.406	0.135	-3.945, '-4.086	0.141
514	1908.87	0.068	-4.177				
515	1908.71	0.354	-4.143				
516	1908.54	0.696	-4.041				
517	1908.37	0.330	-4.484				
518	1908.21	0.831	-4.353				
519	1908.04	0.404	-4.656				
520	1907.87	0.058	-4.581				
521	1907.71	-0.031	-4.579	-0.033, '-0.028	0.005	-4.533, '-4.624	0.091
522	1907.54	0.251	-4.336				
523	1907.42	-0.031	-4.650				
524	1907.29	-0.098	-4.508				
525	1907.17	-0.127	-4.600				
526	1907.04	-0.557	-4.745				
527	1906.92	-0.611	-4.662				
528	1906.79	-0.327	-4.736				
529	1906.67	0.061	-4.699	0.000, -0.122	0.122	-4.646, '-4.751	0.105
530	1906.54	0.193	-4.768				
531	1906.33	-0.151	-4.831				
532	1906.12	-0.152	-4.899				
533	1905.92	-0.061	-4.828				
534	1905.71	-0.364	-4.976				
535	1905.54	0.068	-4.733				
536	1905.42	-0.178	-4.747				
537	1905.29	-0.345	-4.743	-0.329, '-0.361	0.032	-4.722, '-4.764	0.042
538	1905.17	-0.176	-4.580				
539	1905.04	-0.072	-4.318				
540	1904.92	-0.151	-4.577				
541	1904.79	-0.293	-4.474				
542	1904.67	-0.408	-4.554				
543	1904.54	0.501	-4.062	0.521, 0.481	0.040	-4.003, '-4.121	0.118
544	1904.34	0.136	-4.295				
545	1904.14	-0.383	-4.287				
546	1903.94	-0.640	-4.626				
547	1903.74	-0.190	-4.500				
548	1903.54	0.154	-4.331				

549	1903.37	-0.289	-4.840				
550	1903.21	-0.016	-4.509				
551	1903.04	-0.073	-4.769	-0.096, '-0.050	0.046	-4.731, '-4.806	0.075
552	1902.87	0.020	-4.803				
553	1902.71	0.313	-4.586				
554	1902.54	0.517	-4.440				
555	1902.37	0.107	-4.599				
556	1902.21	0.051	-4.560				
557	1902.04	-0.242	-4.698				
558	1901.87	-0.195	-4.633				
559	1901.71	-0.044	-4.551	-0.118, 0.030	0.088	-4.612, '-4.490	0.122
560	1901.54	0.142	-4.409				
561	1901.42	-0.179	-4.525				
562	1901.29	0.095	-4.546				
563	1901.17	-0.248	-4.658				
564	1901.04	-0.405	-4.615				
565	1900.92	0.150	-4.313				
566	1900.79	-0.040	-4.518				
567	1900.67	-0.244	-4.454	-0.357, '-0.131	0.226	-4.434, '-4.473	0.039
568	1900.54	0.217	-4.671				
569	1900.34	-0.140	-4.840				
570	1900.14	0.399	-4.655				
571	1899.94	-0.103	-4.783				
572	1899.74	0.516	-4.248				
573	1899.54	0.683	-4.099	0.784, 0.581	0.203	-4.121, '-4.076	0.045
574	1899.34	-0.269	-4.371				
575	1899.14	0.242	-4.022				
576	1898.94	0.816	-3.949				
577	1898.74	0.756	-3.960				
578	1898.54	0.081	-4.354				
579	1898.34	0.121	-4.285				
580	1898.14	0.144	-4.434				
581	1897.94	0.238	-4.325	0.168, 0.308	0.140	-4.359, '-4.290	0.069
582	1897.74	0.203	-4.547				
583	1897.54	0.368	-4.440				
584	1897.29	0.080	-4.590				
585	1897.04	0.027	-4.708				
586	1896.79	0.166	-4.646				
587	1896.54	0.709	-4.108				
588	1896.34	0.173	-4.335				
589	1896.14	-0.171	-4.512	-0.187, '-0.155	0.032	-4.485, '-4.539	0.054
590	1895.94	-0.192	-4.443				
591	1895.74	-0.259	-4.489				
592	1895.54	0.447	-4.086				
593	1895.42	0.130	-4.039				
594	1895.29	-0.521	-4.312				
595	1895.17	-0.479	-4.231				
596	1895.04	-0.512	-4.417				
597	1894.92	-0.321	-4.315	-0.332, '-0.309	0.023	-4.317, '-4.313	0.004
598	1894.79	-0.365	-4.515				

599	1894.67	-0.209	-4.323				
600	1894.54	0.224	-4.055				
601	1894.40	0.148	-3.955				
602	1894.26	-0.357	-4.262				
603	1894.11	-0.241	-4.176	-0.205, '-0.276	0.071	-4.128, '-4.223	0.095
604	1893.97	-0.060	-4.092				
605	1893.83	-0.374	-4.405				
606	1893.68	-0.311	-4.407				
607	1893.54	-0.009	-4.158				
608	1893.40	-0.690	-4.435				
609	1893.26	-0.513	-4.200				
610	1893.11	-0.467	-4.219				
611	1892.97	-0.187	-4.074	-0.174, '-0.200	0.026	-4.016, '-4.132	0.116
612	1892.83	-0.603	-4.359				
613	1892.68	-0.375	-4.458				
614	1892.54	0.260	-4.257				
615	1892.42	-0.093	-4.309				
616	1892.29	0.034	-4.272				
617	1892.17	0.072	-4.323				
618	1892.04	0.398	-4.054				
619	1891.92	0.382	-3.986	0.428, 0.335	0.093	-3.963, '-4.008	0.045
620	1891.79	-0.013	-4.239				
621	1891.67	-0.564	-4.519				
622	1891.54	-0.433	-4.554				
623	1891.44	-0.583	-4.676				
624	1891.34	-0.819	-4.769				
625	1891.24	-0.747	-4.529				
626	1891.14	-0.798	-4.533				
627	1891.04	-0.895	-4.545	-0.936, '-0.853	0.083	-4.512, '-4.578	0.066
628	1890.94	-0.843	-4.423				
629	1890.84	-0.769	-4.581				
630	1890.74	-0.708	-4.358				
631	1890.64	-0.401	-4.303				
632	1890.54	-0.228	-4.165				
633	1890.29	-0.431	-4.201	-0.496, '-0.366	0.130	-4.232, '-4.169	0.063
634	1890.04	-0.783	-4.265				
635	1889.79	-0.554	-4.225				
636	1889.54	-0.350	-4.092				
637	1889.42	-0.981	-4.552				
638	1889.29	-0.678	-4.489				
639	1889.17	-0.795	-4.680				
640	1889.04	-0.877	-4.756				
641	1888.92	-0.962	-4.967	-0.883, '-1.040	0.157	-4.912, '-5.022	0.110
642	1888.79	-0.687	-4.757				
643	1888.67	-0.506	-4.601				
644	1888.54	-0.259	-4.310				
645	1888.37	-0.485	-4.496				
646	1888.21	-0.406	-4.129				
647	1888.04	-1.183	-4.546				
648	1887.87	-0.623	-4.481				

649	1887.71	-0.172	-4.528	-0.203, '-0.140	0.063	-4.500, '-4.555	0.055
650	1887.54	0.620	-3.959				
651		0.291	-4.287				
652		0.476	-4.016				
653		0.146	-4.405				
654		-0.185	-4.657				
655		-0.268	-4.581				
656		-0.390	-4.792				
657		0.301	-4.178	0.302, 0.299	0.003	-4.186, -4.170	0.016
658		-0.117	-4.535				
659		0.203	-4.379				
660		0.554	-4.150				
661		0.311	-3.790				
662		-0.070	-4.447				
663		-1.031	-4.873	-1.008, '-1.054	0.046	-4.851, '-4.894	0.043
664		-0.871	-4.592				
665		-0.070	-4.321				
666		0.053	-4.484				
667		-0.358	-4.527				
668		0.088	-4.413				
669		-0.130	-4.479				
670		0.446	-4.167				
671		-0.144	-4.494	-0.128, '-0.159	0.031	-4.476, '-4.512	0.036
672		0.086	-4.243				
673		-0.090	-4.513				
674		-0.117	-4.067				
675		0.061	-4.229				
676		0.355	-4.113				
677		0.094	-4.200				
678		-0.398	-4.494				
679		-0.304	-4.406	-0.233, '-0.375	0.142	-4.342, '-4.469	0.127
680		-0.211	-4.443				
681		-0.114	-4.406				
682		-0.025	-4.355				
683		-0.124	-4.493				
684		-0.111	-4.366				
685		0.347	-4.085				
686		0.042	-4.388				
687		0.397	-4.194	0.447, 0.374	0.073	-4.181, '-4.207	0.026
688		-0.094	-4.429				
689		-0.282	-4.579				
690		-0.465	-4.754				
691		-0.298	-4.661				
692		0.124	-4.300				
693		-0.257	-4.683	-0.194, '-0.319	0.125	-4.710, '-4.656	0.054
694		-0.140	-4.560				
695		0.147	-4.382				
696		-0.240	-4.651				
697		-0.297	-4.754				
698		-0.362	-4.763				

699		-0.396	-4.604				
700		-0.014	-4.460				
701		-0.047	-4.504	-0.077, '-0.016	0.061	-4.560, '-4.447	0.113
702		-0.231	-4.588				
703		-0.055	-4.582				
704		0.246	-4.272				
705		-0.567	-4.803				
706		-0.328	-4.501				
707		0.053	-4.337				
708		-0.457	-4.771				
709		0.482	-4.144	0.404, 0.560	0.156	-4.168, '-4.120	0.048
710		0.407	-4.225				
711		-0.292	-4.613				
712		-0.426	-4.679				
713		-0.627	-4.723				
714		-0.264	-4.798				
715		-0.271	-4.669				
716		-0.050	-4.649				
717		0.412	-4.376	0.438, 0.386	0.052	-4.392, '-4.360	0.032
718		0.510	-4.131				
719		0.248	-4.384				
720		0.814	-3.987				
721		0.258	-4.495				
722		0.191	-4.496				
723		0.460	-4.187	0.484, 0.435	0.049	-4.177, '-4.197	0.02
724		-0.014	-4.536				
725		-1.112	-5.093				
726		-1.135	-4.900				
727		-1.049	-4.818				
728		-1.246	-4.927				
729		-0.615	-4.274				
730		-0.503	-4.404				
731		-1.096	-4.618	-1.189, '-1.003	0.186	-4.619, '-4.617	0.002
732		-1.583	-5.374				
733		-1.667	-5.181				
734		-1.543	-4.951				
735		-1.048	-4.721				
736		-0.006	-4.328				
737		-0.296	-4.418				
738		-1.348	-5.113				
739		-1.031	-4.855	-1.060, '-1.002	0.058	-4.886, '-4.824	0.062
740		-0.743	-4.729				
741		-0.517	-4.470				
742		-0.774	-4.604				
743		-0.794	-4.828				
744		0.025	-3.963	0.061, '-0.011	0.072	-4.032, '-3.894	0.138
745		-1.451	-4.843				
746		-1.376	-4.831				
747		-0.920	-4.519	-0.989, '-0.851	0.138	-4.588, '-4.450	0.138
748		-0.518	-4.392				

749		-0.154	-4.176				
750		-0.812	-4.472				
751		0.266	-3.593				
752		-0.240	-3.938				
753		-0.878	-4.334	-0.856, '-0.900	0.044	-4.258, '-4.409	0.151
754		-1.260	-4.415				
755		-1.281	-4.416				
756		-1.234	-4.401				
757		-0.747	-4.060				
758		-1.063	-4.241				
759		-1.062	-4.082				
760		-1.518	-4.633				
761		-1.441	-4.596	-1.514, '-1.367	0.147	-4.522, '-4.670	0.148
762		-1.040	-4.799				
763		-0.879	-4.702				
764		-0.259	-4.510				
765		0.057	-4.621				

Standard	δ13C	δ18O
NBS-19-1	1.924	-2.213
NBS-19-2	1.960	-2.217
NBS-19-3	1.961	-2.187
NBS-19-4	1.939	-2.244
NBS-19-5	1.936	-2.269
NBS-19-6	1.930	-2.220
NBS-19-7	1.980	-2.190
NBS-19-8	1.958	-2.191
NBS-19-9	1.957	-2.173
NBS-19-10	1.952	-2.187
NBS-19-11	1.940	-2.219
NBS-19-12	1.951	-2.200
NBS-19-13	1.945	-2.163
NBS-19-14	1.965	-2.175
NBS-19-15	1.950	-2.185
NBS-19-16	1.962	-2.184
NBS-19-17	1.963	-2.173
NBS-19-18	1.971	-2.185
NBS-19-19	1.951	-2.202
NBS-19-20	1.947	-2.239
NBS-19-21	1.948	-2.224
NBS-19-22	1.942	-2.208
NBS-19-23	1.954	-2.194
NBS-19-24	1.943	-2.189
NBS-19-25	1.958	-2.213
NBS-19-26	1.959	-2.180
NBS-19-27	1.984	-2.169
NBS-19-28	1.952	-2.202
NBS-19-29	1.961	-2.177
NBS-19-30	1.960	-2.199
NBS-19-31	1.972	-2.157
NBS-19-32	1.946	-2.188
NBS-19-33	1.957	-2.162
NBS-19-34	1.939	-2.231
NBS-19-35	1.962	-2.221
NBS-19-36	1.945	-2.216
NBS-19-37	1.977	-2.180
NBS-19-38	1.988	-2.216
NBS-19-39	1.961	-2.201
NBS-19-40	1.958	-2.192
NBS-19-41	1.966	-2.220
NBS-19-42	1.942	-2.197
NBS-19-43	1.981	-2.178
NBS-19-44	1.959	-2.173
NBS-19-45	1.974	-2.196
NBS-19-46	1.942	-2.212
NBS-19-47	1.935	-2.209

NBS-19-48	1.927	-2.217
NBS-19-49	1.963	-2.176
NBS-19-50	1.951	-2.166
NBS-19-51	1.970	-2.190
NBS-19-52	1.932	-2.213
NBS-19-53	1.939	-2.210
NBS-19-54	1.938	-2.231
NBS-19-55	1.961	-2.169
NBS-19-56	1.975	-2.169
NBS-19-57	1.948	-2.215
NBS-19-58	1.931	-2.189
NBS-19-59	1.947	-2.155
NBS-19-60	1.963	-2.159
NBS-19-61	1.959	-2.203
NBS-19-62	1.965	-2.162
NBS-19-63	1.964	-2.176
NBS-19-64	1.906	-2.230
NBS-19-65	1.934	-2.235
NBS-19-66	1.958	-2.161
NBS-19-67	1.961	-2.229
NBS-19-68	1.935	-2.214
NBS-19-69	1.934	-2.233
NBS-19-70	1.960	-2.179
NBS-19-71	1.971	-2.183
NBS-19-72	1.951	-2.176
NBS-19-73	1.956	-2.165
NBS-19-74	1.959	-2.204
NBS-19-75	1.945	-2.197
NBS-19-76	1.973	-2.175
NBS-19-77	1.975	-2.176
NBS-19-78	1.954	-2.205
NBS-19-79	1.924	-2.273
NBS-19-80	1.925	-2.239
NBS-19-81	1.955	-2.215
NBS-19-82	1.968	-2.223
NBS-19-83	1.956	-2.213
NBS-19-84	1.982	-2.198
NBS-19-85	1.987	-2.206
NBS-19-86	1.989	-2.223
NBS-19-87	1.919	-2.221
NBS-19-88	1.929	-2.222
NBS-19-89	1.920	-2.254
NBS-19-90	1.908	-2.251
NBS-19-91	1.901	-2.258
NBS-19-92	1.916	-2.248
NBS-19-93	1.921	-2.224
NBS-19-94	1.930	-2.205
NBS-19-95	1.923	-2.239

NBS-19-96	1.936	-2.215
NBS-19-97	1.921	-2.228
NBS-19-98	1.949	-2.221
NBS-19-99	1.918	-2.223
NBS-19-100	1.958	-2.234
NBS-19-101	1.971	-2.249
NBS-19-102	1.971	-2.168
NBS-19-103	1.966	-2.209
NBS-19-104	1.964	-2.222
NBS-19-105	1.944	-2.236
NBS-19-106	1.979	-2.224
NBS-19-107	1.955	-2.219
NBS-19-108	1.955	-2.208
NBS-19-109	1.959	-2.173
NBS-19-110	1.952	-2.192
NBS-19-111	1.961	-2.161
NBS-19-112	1.952	-2.207
NBS-19-113	1.952	-2.214
NBS-19-114	1.969	-2.185
NBS-19-115	1.940	-2.220
NBS-19-116	1.949	-2.221
NBS-19-117	1.943	-2.203
NBS-19-118	1.960	-2.199
NBS-19-119	1.979	-2.218
NBS-19-120	1.986	-2.135
NBS-19-121	1.969	-2.134
NBS-19-122	1.986	-2.189
NBS-19-123	1.978	-2.201
NBS-19-124	1.946	-2.144
NBS-19-125	1.939	-2.174
NBS-19-126	1.940	-2.216
NBS-19-127	1.945	-2.210
NBS-19-128	1.958	-2.136
NBS-19-129	1.945	-2.176
NBS-19-130	1.945	-2.180
NBS-19-131	1.927	-2.174
NBS-19-132	1.927	-2.215
NBS-19-133	1.933	-2.207
NBS-19-134	1.943	-2.231
NBS-19-135	1.967	-2.220
NBS-19-136	1.947	-2.251
NBS-19-137	1.939	-2.244
NBS-19-138	1.954	-2.255
NBS-19-139	1.965	-2.213
NBS-19-140	1.947	-2.226
NBS-19-141	1.965	-2.198
NBS-19-142	1.975	-2.189
NBS-19-143	1.946	-2.198

NBS-19-144	1.964	-2.176

Depth (mm)	Year A.D.	Sr/Ca (mmol/mol)
1	1997.79	9.03
2	1997.64	9.07
3	1997.59	9.12
4	1997.54	9.13
5	1997.29	9.13
6	1997.04	9.06
7	1996.79	9.14
8	1996.54	9.18
9	1996.40	9.19
10	1996.26	9.20
11	1996.11	9.16
12	1995.97	9.15
13	1995.83	9.10
14	1995.68	9.09
15	1995.54	9.12
16	1995.34	9.17
17	1995.14	9.15
18	1994.94	9.12
19	1994.74	9.07
20	1994.54	9.12
21	1994.37	9.09
22	1994.21	9.32
23	1994.04	9.23
24	1993.87	9.13
25	1993.71	9.10
26	1993.54	9.06
27	1993.40	9.10
28	1993.26	9.14
29	1993.11	9.16
30	1992.97	9.13
31	1992.83	9.06
32	1992.68	9.13
33	1992.54	9.12
34	1992.37	9.09
35	1992.21	9.15
36	1992.04	9.08
37	1991.92	9.10
38	1991.79	9.15
39	1991.67	9.04
40	1991.54	9.19
41	1991.40	9.15
42	1991.26	9.11
43	1991.11	9.08
44	1990.97	9.13
45	1990.83	9.15
46	1990.68	9.13

47	1990.54	9.12
48	1990.34	9.10
49	1990.14	9.11
50	1989.94	9.12
51	1989.74	9.05
52	1989.54	9.12
53	1989.34	9.17
54	1989.14	9.24
55	1988.94	9.22
56	1988.74	9.16
57	1988.54	9.22
58	1988.26	9.21
59	1987.99	9.24
60	1987.71	9.29
61	1987.62	9.22
62	1987.54	9.33
63	1987.34	9.21
64	1987.14	9.17
65	1986.94	9.14
66	1986.74	9.09
67	1986.54	9.17
68	1986.40	9.22
69	1986.26	9.12
70	1986.11	9.16
71	1985.97	9.18
72	1985.83	9.19
73	1985.68	9.18
74	1985.54	9.22
75	1985.34	9.11
76	1985.14	9.17
77	1984.94	9.22
78	1984.74	9.21
79	1984.54	9.27
80	1984.34	9.14
81	1984.14	9.23
82	1983.94	9.19
83	1983.74	9.25
84	1983.54	9.29
85	1983.04	9.26
86	1982.87	9.23
87	1982.71	9.13
88	1982.54	9.13
89	1982.34	9.13
90	1982.14	9.17
91	1981.94	9.07
92	1981.74	9.17
93	1981.54	9.16
94	1981.34	9.27

95	1981.14	9.23
96	1980.94	9.18
97	1980.74	9.09
98	1980.54	9.14
99	1980.40	9.18
100	1980.26	9.24
101	1980.11	9.18
102	1979.97	9.11
103	1979.83	9.14
104	1979.68	9.25
105	1979.54	9.30
106	1979.29	9.18
107	1979.04	9.09
108	1978.79	9.16
109	1978.54	9.10
110	1978.34	9.11
111	1978.14	9.21
112	1977.94	9.21
113	1977.74	9.17
114	1977.54	9.18
115	1977.29	9.15
116	1977.04	9.18
117	1976.79	9.19
118	1976.71	9.16
119	1976.62	9.23
120	1976.54	9.16
121	1976.34	9.22
122	1976.14	9.18
123	1975.94	9.18
124	1975.74	9.29
125	1975.54	9.15
126	1975.37	9.17
127	1975.21	9.18
128	1975.04	9.17
129	1974.87	9.32
130	1974.71	9.20
131	1974.54	9.22
132	1974.34	9.26
133	1974.14	9.27
134	1973.94	9.33
135	1973.74	9.27
136	1973.54	9.25
137	1973.21	9.28
138	1972.88	9.23
139	1972.71	9.24
140	1972.54	9.25
141	1972.14	9.36
142	1971.74	9.24

143	1971.34	9.28
144	1970.94	9.24
145	1970.54	9.19
146	1970.29	9.22
147	1970.04	9.24
148-152	1969	9.25
153-157	1968	9.16
158-162	1967	9.19
163-164	1966	9.28
165-170	1965	9.29
171-173	1964	9.35
174-180	1963	9.29
181-185	1962	9.28
186-191	1961	9.20
192-196	1960	9.22
197-201	1959	9.20
202-207	1958	9.23
208-213	1957	9.31
214-218	1956	9.24
219-224	1955	9.34
225-230	1954	9.21
231-235	1953	9.27
236-240	1952	9.20
241-246	1951	9.19
247-252	1950	9.23
253-257	1949	9.25
258-262	1948	9.25
263-268	1947	9.22
269-274	1946	9.17
275-280	1945	9.18
281-285	1944	9.23
286-290	1943	9.22
291-295	1942	9.24
296-299	1941	9.25
300-305	1940	9.12
306-311	1939	9.34
312-317	1938	9.27
318-324	1937	9.31
325-331	1936	9.30
332-339	1935	9.34
340-348	1934	9.21
349-355	1933	9.27
356-361	1932	9.25
362-366	1931	9.30
367-374	1930	9.30
375-382	1929	9.27
383-387	1928	9.21
388-394	1927	9.25

395-399	1926	9.21
400-408	1925	9.28
409-415	1924	9.31
416-422	1923	9.28
423-429	1922	9.32
430-436	1921	9.30
437-443	1920	9.25
444-449	1919	9.31
450-456	1918	9.26
457-463	1917	9.27
464-469	1916	9.24
470-476	1915	9.29
477-481	1914	9.31
482-487	1913	9.28
488-495	1912	9.27
496-502	1911	9.31
503-508	1910	9.37
509-513	1909	9.25
514-519	1908	9.41
520-526	1907	9.37
527-532	1906	9.30
533-539	1905	9.30
540-545	1904	9.26
546-551	1903	9.40
552-557	1902	9.44
558-564	1901	9.36
565-570	1900	9.34
571-575	1899	9.26
576-580	1898	9.28
581-585	1897	9.26
586-589	1896	9.28
590-596	1895	9.43
597-603	1894	9.31
604-610	1893	9.32
611-618	1892	9.46
619-627	1891	9.42
628-634	1890	9.38
635-640	1889	9.26
641-647	1888	9.29
648-650	1887	9.37